The historic quay walls of Amsterdam

A study into the hidden structural capacity of masonry quay walls under the condition of a partly failing foundation

R. Voortman

TU Delft

Movares
adviseurs & ingenieurs

The historic quay walls of Amsterdam

A study into the hidden structural capacity of masonry quay walls under the condition of a partly failing foundation

by

R. Voortman

to obtain the degree of Master of Science
at the Delft University of Technology,
to be defended publicly on Monday January 25, 2021 at 10:00 AM.

Student number:	4514998	
Project duration:	September, 2019 – January, 2021	
Thesis committee:	Prof. dr. ir. J. G. Rots,	TU Delft
	Dr. ir. J. G. de Gijt,	TU Delft
	Ir. P. A. Korswagen,	TU Delft
	Ir. M.G.A. van den Elzen,	Movares

An electronic version of this thesis is available at http://repository.tudelft.nl/.
Cover image by Overview, source imagery Maxar Technologies

TU Delft

Movares
adviseurs & ingenieurs

Preface

This thesis is written to conclude my Master Structural Engineering at the faculty of Civil Engineering and Geosciences at the Delft University of Technology. The research was performed under the supervision of my graduation committee and in cooperation with consultancy and engineering firm Movares Nederland B.V.

My interest in the quay walls of Amsterdam started about two and a half years ago at a lunch lecture by the municipality of Amsterdam about the problems in the city related to the bridges and quay walls. The scale of the problems fascinated me the most, how to renovate and rebuild kilometres of quay wall in the historic old city centre. After brainstorming for thesis topics with friends, I found that Movares was working on emergency measures to secure the stability of the structures. At Movares, I spoke with Martijn van den Elzen and Thom Olsthoorn, and together we formed the base of my research, how does a quay wall behave when the pile foundation is failing? I will forever be grateful for their endless enthusiasm in my research on quay walls and all the mental support they have given me in this hectic process and challenging year. To the colleagues of Movares I worked with, thank you for the fun time we spend and the insights you provided me with!

This thesis could not have written without the support of my other supervisors; I would like to thank Paul Korswagen for his flexibility and the countless meetings we had. Your scientific approach lifted the quality of my work to a better level. Secondly, I very much appreciate Jarit de Gijt for the knowledge about quay walls he could share with me from his experience. Also, his take to simplify problems and go to the basics of engineering when possible were helpful. Finally, I would like to thank Jan Rots for help shaping the research and overseeing the process, and ultimately, his experience in masonry structures.

By finalising this thesis, my student days come to an end as well, I would like to thank my friends for their support in times of need and the fun times we shared while studying. I came to Delft to obtain my master's degree in Structural Engineering, and I had the best time accomplishing this! Also, I am very grateful for the support of my family, and my parents in particular, thanks for being there for me and providing me with the opportunities to develop myself in education and life. Finally, I would like to thank Manuela for encouraging me to go the university, this would not have been possible without all of your support!

Rick Voortman
Amsterdam, January 2021

Summary

The city of Amsterdam contains about 1600 bridges and 600 kilometres of quay walls. Of these walls, about 200 kilometres are of masonry walls placed on a timber floor and founded on timber piles. These quay walls are sometimes over 100 years old. Due to the increasing loads in the past century and the degrading of material properties in the masonry wall and timber elements, the quay walls are in bad shape. When designing a quay wall, a cross-sectional analysis is used to calculate the desired dimensions to withstand the loads. When this calculation is performed on a quay wall over a 100 years old, containing a failing pile foundation, the quay wall should fail. However, many of the quay walls under the condition of a partly failing foundation, are deforming, but still standing. During recent years, at 16 locations in Amsterdam, the risk of collapse appeared imminent, and emergency structures are put into place. Possible practical measures are removing trees on the quay walls, traffic limitations in the city centre and placing temporary struts and sheet piles to provide stability.

Since the scale of the problem in Amsterdam is large, the time to renovate all the quay walls is lengthy. Therefore there is a need for knowledge on the state of quay walls at the end of their life phase when partly failing. Different failure mechanisms occur, and various measures are developed to control those and provide (temporary) stability. This research answers the question: How can 2D analyses of quay walls, in multiple directions, under the condition of a partly failing foundation, provide insight into the hidden structural capacity within the masonry work?

The study focuses on the severeness and scale of the foundation defects in the quay wall's cross-sectional and longitudinal direction. For the longitudinal models, the effects of the masonry material qualities are studied by using different material properties. Also examined is the effect of the failing foundation pile's post-peak behaviour, modelled as brittle and checked for plastic behaviour. Finally, the relevancy of the timber floor is studied for a stiff continuous floor and most notable, the full removal of the floor.

To study this, two 2D regular plane stress, nonlinear elastic, finite element models are created in Diana FEA. The foundation piles are modelled as nonlinear elastic springs via a force-displacement diagram. The foundation piles' defects are modelled by assuming a smaller pile diameter, resulting in a weaker force-displacement diagram and larger displacements in the quay wall system. The foundation defects can be scaled over a small or big area by adapting multiple foundation piles over the length of the quay wall. The masonry's behaviour is researched by using a macro material model using smeared material properties for the brick and mortar, resulting in a continuous material. The material model used is the Total Strain Rotating Crack Model, which can be used in a 3D analysis of the quay wall system in future research. Finally, the interface between the timber floor and masonry is modelled using a coulomb friction interface criterion. This simulates the effects of the mortar layer connecting the timber floor and masonry work in a quay wall.

The results conclude that analysing a foundation defect in the cross-sectional direction of the quay wall results in instability of the wall without further horizontal and vertical constraints to keep the quay wall in place. Modelling the pile foundation defects using a reduced pile diameter and consequently, a decreased force-displacement diagram as spring input provides the model with temporary stability. Ultimately, the cross-sectional analyses contribute little knowledge on residual strength and hidden structural capacity.

Separately, the longitudinal model implements a vertical constraint in the masonry by using the bending capacities of the material. The results present an expected correlation between the scale of the foundation defects and the vertical displacements. Similar to the cross-sectional analyses, the reduced pile capacity of the foundation piles provides the model residual strength compared to the situation where the total failure of a timber pile is used.

The timber foundation pile's failure mechanism needs to be researched in-depth since the results present a notable difference for crack patterns and force-displacement curvatures when modelled brittle or plasti-

cally. For brittle failure, a horizontal crack forms at the tip of the central, vertical crack, due to the abrupt enlargement in vertical displacement of the quay wall.

The functionality of the timber floor in the longitudinal analyses presents itself when the crack patterns are analysed. The presence of the timber floor results in multiple smaller cracks instead of a single large crack when foundation defects of the quay wall system are analysed without a timber floor.

It can be concluded that the masonry quality, most notably the tensile strength, affect the results significantly in terms of maximum values in the force-displacement diagrams and crack development. The material properties are based on Groningen masonry experiments, and it is recommended to perform experiments to the masonry quality of Amsterdam quay walls.

Finally, the observed displacements related to the intervention points of the municipality conclude that foundation defects result in cracks for displacements below the marking points of 20 and 25 millimetres. For weaker masonry, the quay wall fails before the indication values. It is recommended to perform more measurements to the quay walls in Amsterdam and study the reliability of the intervention points.

Symbols and abbreviations

Sign	Description	Unit
E	Young's modulus	N/mm^2
E_x	Young's modulus parallel to bed-joints	N/mm^2
E_y	Young's modulus perpendicular to bed-joints	N/mm^2
G_{xy}	shear modulus	N/mm^2
f_t	tensile strength	N/mm^2
f_c	compressive strength	N/mm^2
G_f^I	tensile fracture energy	J/m
G_c	compressive fracture energy	J/m
G_f^{II}	shear energy	J/m
c	cohesion	N/mm^2
ϕ	friction angle	degrees
μ	friction coefficient	-
ν	Poissoin's ratio	-
ρ	mass density	kg/m^3
k_s	shear stiffness	N/mm^3
k_n	normal stiffness	N/mm^3
h_w	height of the wall	m
t_w	thickness of the wall	m
h_f	height of the floor	m
L_f	length of the floor	m
L_p	length of the piles	m
$d_{p1,2,3}$	diameter of pile 1,2,3	m
$h.o.h._{1,2}$	pile distance 1-2,2-3	m
h_s	pile length in soil	m
γ_{dry}	dry volumetric soil weight	kN/m^3
γ_{wet}	saturated volumetric soil weight	kN/m^3
γ_w	volumetric soil weight water	kN/m^3
φ	internal friction coefficient	degrees
q	distributed load	kN/m^2
σ_v	vertical soil stress	kN/m^2
$\sigma_v^{'}$	effective soil stress	kN/m^2
σ_w	hydraulic stress soil side	kN/m^2
σ_h	horizontal soil stress	kN/m^2
F_h	horizontal force at 1/3 h	kN/m

Abbreviation	Definition
FEM	finite element method
GEO	geotechnical
STR	structural
HYD	hydraulic
EQU	equilibrium
UPL	uplift
URM	unreinforced masonry
FEA	finite element analysis
LE	linear elastic
NLE	nonlinear elastic
NAP	reference level (normaal Amsterdams peil)
TSCM	total strain crack model
TSRCM	total strain rotating crack model
EMM	engineering masonry model

Contents

1 Introduction

1.1. Motive

Just like many other cities in the Netherlands, the city of Amsterdam contains many canals and waterways. These canals come in combination with about 1600 bridges and 600 kilometres of quay walls. Of these walls, about 200 kilometres are masonry walls placed on a timber floor and founded on timber piles. At least 10 kilometres are in such a bad state that there is a high risk of collapse. (Kruyswijk, 2019) In recent years, on multiple areas in the city, quay walls have (partially) collapsed. For example, in December 2017, over a length of 25 meters the quay wall at the Entrepotkade in Amsterdam collapsed. Sheet piles were then placed to stabilise the wall and provide a temporary solution (Cobouw, 2017). Another recent example, which shows the importance of knowledge on the behaviour of the Amsterdam quay walls, is the blockade of streets during the 2019 Amsterdam canal pride. About 700 meters of the most vulnerable quay wall sections were blocked because the municipality wanted to limit the risks for the collapsing of the structures and endangering the safety of the hundreds of thousands of visitors going to the event (AT5, 2019). For the upcoming years, it is likely to assume the blockades will occur at other events as well. Additionally, at 16 locations in Amsterdam, emergency measures are put into place to avoid the collapse of the quay walls (Gemeente Amsterdam, 2019a). Possible practical measures are the removal of trees on the quay walls, limitations of traffic in the city centre and placing temporary struts and sheet piles to provide stability (Gemeente Amsterdam, 2019a).

In the upcoming years, the city of Amsterdam needs approximately two billion euros to do: inspections to the state of the bridges and walls in the city, repair and/or renew bridges, and quay walls and maintenance (Couzy and Koops, 2019). There is about 200 kilometres of quay wall, these are designed for a service lifetime of 100 years, so ideally two kilometres of quay wall need to be renewed every year. For now, this is not feasible, as in the last years only about 500 metres of quay wall renewed. The program to replace or repair all the damaged quay walls and bridges is expected to take at least 20 years. In this program, it is important to spread the peak of the maintenance work, while afterwards the work will focus on the 2 kilometres a year (Gemeente Amsterdam, 2019a). For now, the extent of the problems is too large and there is little knowledge about the state of the bridges and quay walls and little technical knowledge about the mechanism of the construction, to make the right assumptions about the load bearing capacity of the quay walls. (Gemeente Amsterdam, 2019a)

The Innovatiepartnerschap is a strategy to develop new solutions. It is a special type of tender from the municipality of Amsterdam to replace about one kilometre of quay wall in the city. In April 2019 six combinations are chosen to develop their innovative ideas to a final plan. In 2021, three winning combinations can execute their design in a pilot project. When finished successfully, an agreement for four to eight years for the building of multiple kilometres of quay wall can be agreed upon. (Gemeente Amsterdam, 2018)

To conclude, in the city of Amsterdam quay walls are collapsing due to multiple reasons and in different magnitudes. Temporary solutions are placed to provide stability. A large scale program to monitor and inspect the state of quay walls and bridges is in progress and a tender should result in innovative ideas for the future. For now there is need on technical knowledge of the behaviour of retaining walls and occurring failure

mechanisms. How much structural capacity is left in the quay walls when fail they partially? Are the emergency structures that are placed in the city necessary or can the structure provide enough strength for itself? When this is the case, not all the temporary solutions are necessary. This would spread the workload and the peak of the maintenance. Additionally it would result in more time to plan and built a long term solution.

1.2. Problem statement

The motive for this research is stated, there is need of knowledge on the state of quay walls at the end of their life phase when partly failing. Different failure mechanisms occur and different measures are developed to control those and provide (temporary) stability. But how much redistribution of forces happens in the masonry work of the gravity wall itself?

For this research, structural failure of foundation piles is taken into account. It might be possible for a single foundation pile to have a rotten, or no connection, to the supporting floor, the structural capacity of the foundation pile decreased to zero. The other parts of the structure (timber floor, horizontal support, masonry work) are fine. By analysing this in multiple directions, the failure mechanism would lead to displacements and possible instability of the masonry wall. This displacement would continue to develop into instability within the quay wall system when analysing the problem in the cross sectional direction. When the failure mechanism is observed in the longitudinal direction or the top view, it results in displacements, but no direct instability, see figure 1.1. In the top part, a situation is sketched where the quay wall system if fully functioning (left cross section, middle longitudinal direction and right the top view); middle part, the failure mechanism occurs; bottom sketch, expected displacement field of the quay wall.

1.3. Research question

The main objective of the research is obtaining more insight in the structural behaviour of quay walls by looking at the redistribution of forces in multiple analyses of the quay wall system when it is partly failing.

The problem statement and objective of the research results in the following main research question:

How can 2D analyses of quay walls, in multiple directions, under the condition of a partly failing foundation, provide insight into the hidden structural capacity within the masonry?

To answer this main research question and fulfil the objective some sub-questions are formulated:

1. How to model the failure mechanism of a (partly) failing pile foundation of a quay wall?
2. How do forces distribute in the masonry work of a quay wall in failing condition?
3. Which input parameters have the most influence on the behaviour of the masonry work of the quay wall?
4. How do the combined results of the cross sectional and longitudinal directions provide insight in hidden structural capacity?

1.4. Scope and limitations

The research will focus on a typical Amsterdam quay wall, as specified in **??**. The Groenburgwal will be used as a reference case for the research, for this case study in Amsterdam there is already data available .

Since the goal of the research is to obtain more knowledge on the structural behaviour, the acting loads, dimensions of the quay wall and surrounding soil parameters are fixed once determined. Making the material properties variables to determine the influence on the failure mechanism. The literature research focuses on determining the boundary conditions for the input parameters in the model. The structural models will focus on the differences in structural behaviour when analysing multiple 2D models.

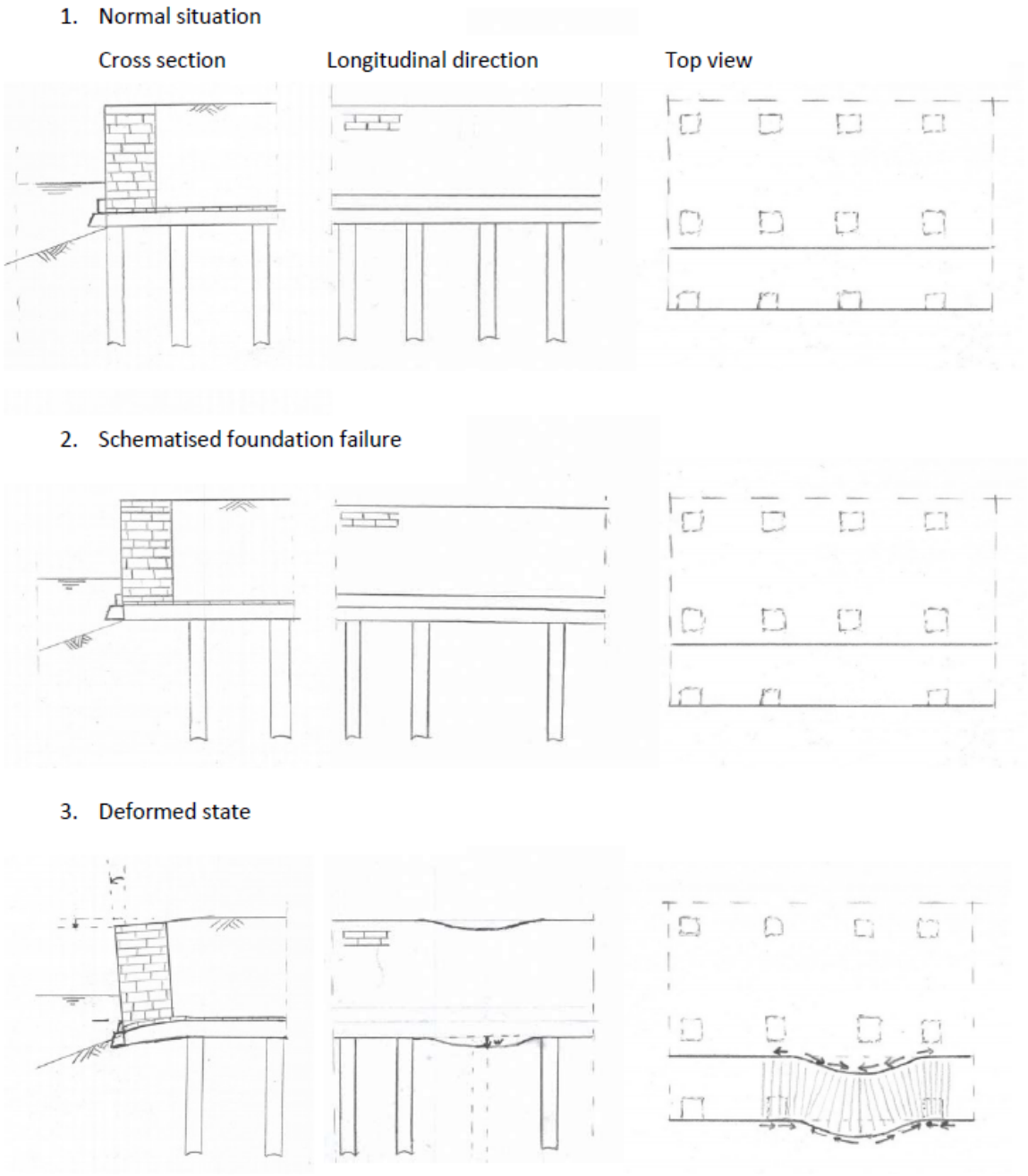

Figure 1.1: Different cross sections and stages of a quay wall partly failing

Due to the restriction in time, the research will focus on a single failure mechanism: the structural failure of a foundation pile. Future research on quay walls would have the possibility to focus on the remaining failure mechanisms or combinations.

1.5. Methodology and reading guide

To fulfil the objective and answer the research questions for the thesis, a research method is presented in this chapter. Different approaches are needed to provide an answer. The different approaches are specified in the following paragraphs.

Research methodology			
Phase		Question	Summary
1	Literature study	Q1	Research on material properties and failure mechanisms
2	2D Diana FEA models	Q2 & Q3	Analysis on the impact of different parameters to provide insight in structural response after failure in 2D.
4	Method comparison	Q4	Analyse results in different directions and compare models.

Table 1.1: Research methodology

The main report of the thesis will consist of three parts and eleven chapters.

Part one - Literature study: Before the work on a functioning model can start, research is to be performed, forming input data. Chapter two will look into the situation of quay walls in Amsterdam. The relevant failure mechanisms are researched further and the different elements of a quay wall are specified. Also, the current control measures and measurement methods are described.

To provide the research with some boundaries, the third chapter is devoted to the dimensions of the quay wall found at the Groenburgwal in Amsterdam.

Chapter four will focus on the properties of timber and soil. Boundaries have to be determined for the timber piles and floor. A second questions to analyse is how do the timber piles interact with the soil layers and how especially how this is degrading over time.

Continuing on material properties, chapter five provides masonry material values that represent the situation in Amsterdam. There will also be a theoretical part on the structural behaviour of masonry and the masonry and timber connection will be elaborated.
Hereafter, in the sixth chapter, the acting loads have to be determined and schematised before an analysis can start. For the acting loads, the reference case data can be used for dimensions and soil parameters.

The different materials have to be modelled, so background information about material models and the advantages or disadvantages of these are needed. Chapter seven will go further into numerical modelling of quay walls.

Part two - 2D Numerical analysis of quay walls: After the literature study, a model is created in Diana FEA. This phase focuses on 2D elements in the cross sectional and longitudinal directions. The impact of different parameters such as, pile capacity, masonry strength, timber floor setup and the number of foundation piles deflected are researched to determine which have the largest influence on deformations and strength.

Chapter eight will go into the 2D cross sectional analysis and chapter nine will elaborate on the model of the 2D longitudinal direction. Both chapters will follow the same structure; the model will be presented, input parameters and the analysis will be discussed after which the results will be presented and conclusions are drawn.

Part three - Final remarks: In chapter ten, simplifications and assumptions will be discussed. Thereafter in chapter eleven, the conclusions on the sub and main question will be formed and finally, recommendations to further research on the topic will be presented.

2

Quay walls in Amsterdam

This part focuses on the situation in Amsterdam and the first research question: Which failure mechanisms are likely to occur in Amsterdam and how to model these? Important factors to model the quay wall are the boundary conditions on loads, dimensions, material properties and soil conditions.

2.1. History of quay walls in the Netherlands

The first quay walls in cities in the Netherlands date from the 13th and 14th century. In the following centuries developments in materials and technical knowledge evolved the quay wall. From a wall using its weight (gravity) to keep it in place, to quay walls using anchors as retaining mechanism. From the use of brick walls, new materials such as reinforced concrete, steel sheet piles and pre-stressed concrete made their introduction. (de Gijt, 2010) Figure 2.1 shows a time lapse of the evolution in quay walls. Nowadays, quay walls can be classified into four classes of quay walls (CUR commissie 186, 2013).

1. Class 1: Shallow founded gravity wall
2. Class 2: Deep founded gravity wall
3. Class 3: Deep founded L-wall (retaining wall)
4. Class 4: Steel or concrete sheet pile wall

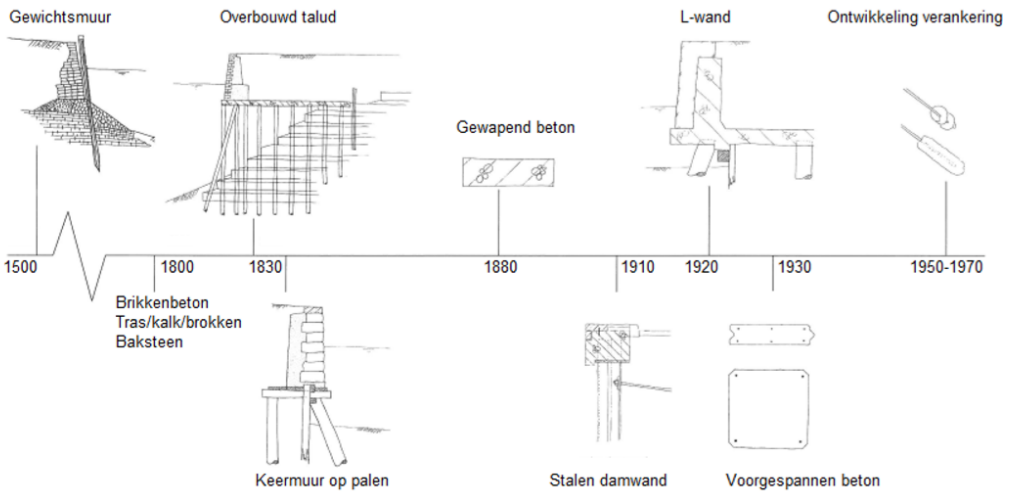

Figure 2.1: History of quay walls. (CUR commissie 186, 2013)

When analysing quay walls, not only the type of structure is important, but also its function. The CUR 186 describes six possible functions for a quay wall.

1. Retaining function, the structure should resist water and soil pressure, where the retaining height and design depth are an important factor.
2. Supporting function, the structure should transfer vertical forces (permanent and live loads from ground level to the soil beneath the wall.
3. Mooring function, during mooring of ships, a quay wall should need enough structural capacity to withstand a collision with a ship. Also additional forces as wind and waves play a role.
4. Traffic function, when roads are built directly next or on a quay wall, the wall needs sufficient capacity to transfer the dynamic loads to the soil beneath.
5. Storage function, when a quay wall is used for storage, typically in harbours, the wall needs sufficient capacity to transfer the vertical loads to the soil beneath.
6. Surrounding function, when the quay wall also plays a role in the surrounding area due to its monumental value, recreational use or changes in the functional purpose of the wall in the area.

The function and use of quay walls also developed over time. With a lot of the quay walls in Amsterdam being more than 100 years old, over the years, the use of the quay wall differs from its original use. When at first transport of goods was being carried out by horse and wagon, 100 years later it is possible that a 60-100 tons crane is located on the quay wall (Gemeente Amsterdam, 2019a).

(a) Heerengracht circa 1900 (Library of congress) (b) Heerengracht present (Urban Capture)

The second consequence of the quay walls being old, is material degradation. Rotting of the piles might be one of the largest problems. Especially because the piles are placed below water or ground level and hard to monitor. A program to investigate the foundation of all the bridges and quay walls will take about six years. The expectation is that there are many rotten piles. (Gemeente Amsterdam, 2019b) In chapter 4 more information can be found on material properties and degradation of timber piles. Figure 2.4 provides a good example where degradation of the material is visible.

2.2. Structure of a Amsterdam quay wall

The mentioned classes and functions of quay walls in **??** are not all relevant to the city of Amsterdam. Customary are masonry work gravity walls, on timber piles, with a deep foundation, within the boundaries of the defined class 2. The gravity wall (1) is placed on a timber floor (3) with a foundation of timber piles (5). In between the foundation piles and the floor are timber beams (kespen) (4) placed. For a horizontal support of the masonry wall, a timber beam (watersloof) (9) is placed at the front. It is also possible, but not in all situations, that in between the kespen the first foundation pile under an angle (schoorpaal) (8) an addition timber beam is placed (6) to distribute the forces. See picture 2.3 for a typical cross section of a historic quay wall in

Amsterdam. Furthermore, see the difference between 2.3 and 2.4, where in the latter there is no additional horizontal beam (6). In chapter 3, more information about the structural elements will be provided.

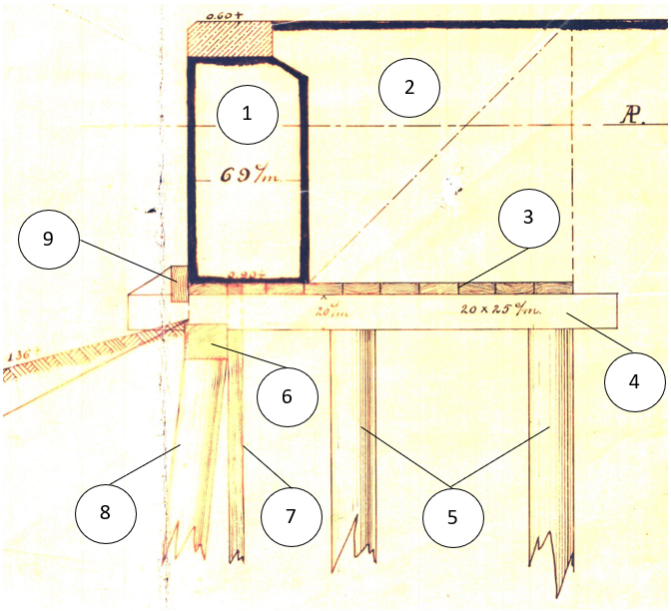

Figure 2.3: Typical quay wall in Amsterdam.(Movares, 2019)

Figure 2.4: Foundation of Amsterdam quay walls(Gemeente Amsterdam, 2019a)

2.3. Failure mechanisms

For defined class 2 and 3, quay walls in combination with deep foundations, the handbook quay walls distinguishes eight different failure mechanisms based on four categories of ultimate limit state of the Eurocode 7: Geotechnical (GEO), Structural (STR), Hydraulic (HYD), Equilibrium (EQU) and Uplift(UPL). Two more failure mechanisms specific for old masonry work quay walls are possible (9 and 10). To provide a better understanding of the failure mechanisms, in figure 2.6, the mechanisms are sketched.

1. Exceeding of geotechnical capacity compression pile (GEO)
2. Exceeding of geotechnical capacity tension pile (GEO/UPL)
3. Failure of the soil due to horizontal forces on pile foundation (GEO)
4. Exceeding of general stability (GEO)
5. Structural failure of retaining wall (STR)
6. Structural failure of foundation piles (STR)

7. Structural failure of construction due to displacement or failure of kesp (STR)
8. Failure due to internal erosion or piping (HYD)
9. Quay wall displaces across the foundation piles/floor (STR)
10. Structural failure of the timber floor causing material transport (STR)

In the Movares document, Beheersmaatregelen kademuren, several cases of quay walls, where control measures had to be placed, are coupled to these failure mechanisms on engineering judgment. It concludes that in recent years (2017-2018) the following mechanisms happened in Amsterdam: 3, 6, 7, 8, 9, 10 and mechanisms 2 and 4 won't occur in Amsterdam. These failure mechanisms would not occur because other mechanisms will start to develop sooner (Movares, 2019). This variety shows that with old quay walls it is not a single problem that results in failure, but geotechnical as well as structural problems related to the masonry work and timber parts of the structure. It also becomes clear that not all failure mechanisms occur at the same time.

As specified before, the scope of this research focuses on the failure of a foundation pile, failure mechanism six.

2.4. Control measures

The state of quay walls can be monitored and depending on observations of displacements, cracking of masonry and rotting or cracking parts of timber elements, the failure mechanisms can be coupled to cases in practise. Depended on the type of failure mechanisms, control measures can be implemented. These control measures can be placed at different parts of the structure:

1. Street side
2. Waterside
3. In the structure
4. Above the floor
5. Below the floor

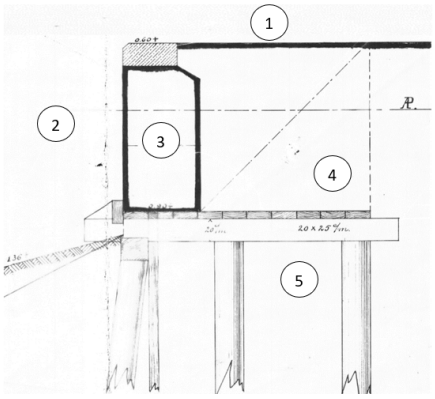

Figure 2.5: Possible locations of control measures

Measures differ in scale and time to implement. An reduction of traffic at the street side can be considered as an measure simple to implement with immediate effect. An option at the waterside would be a vertical sheet pile in front of the quay wall, filled with sand, this would take more than a week to built. A possibility for option 3, measure in the structure is to put steel piles through the masonry work. Placing geotextile over the timber floor would be a measure above the foundation floor to prevent failure mechanism 8, failure due to internal erosion or piping. Finally, below the floor, it is possible to place a ground retaining screen in longitudinal direction. For a complete overview of the possible control measures, see appendix A. (Movares, 2019)

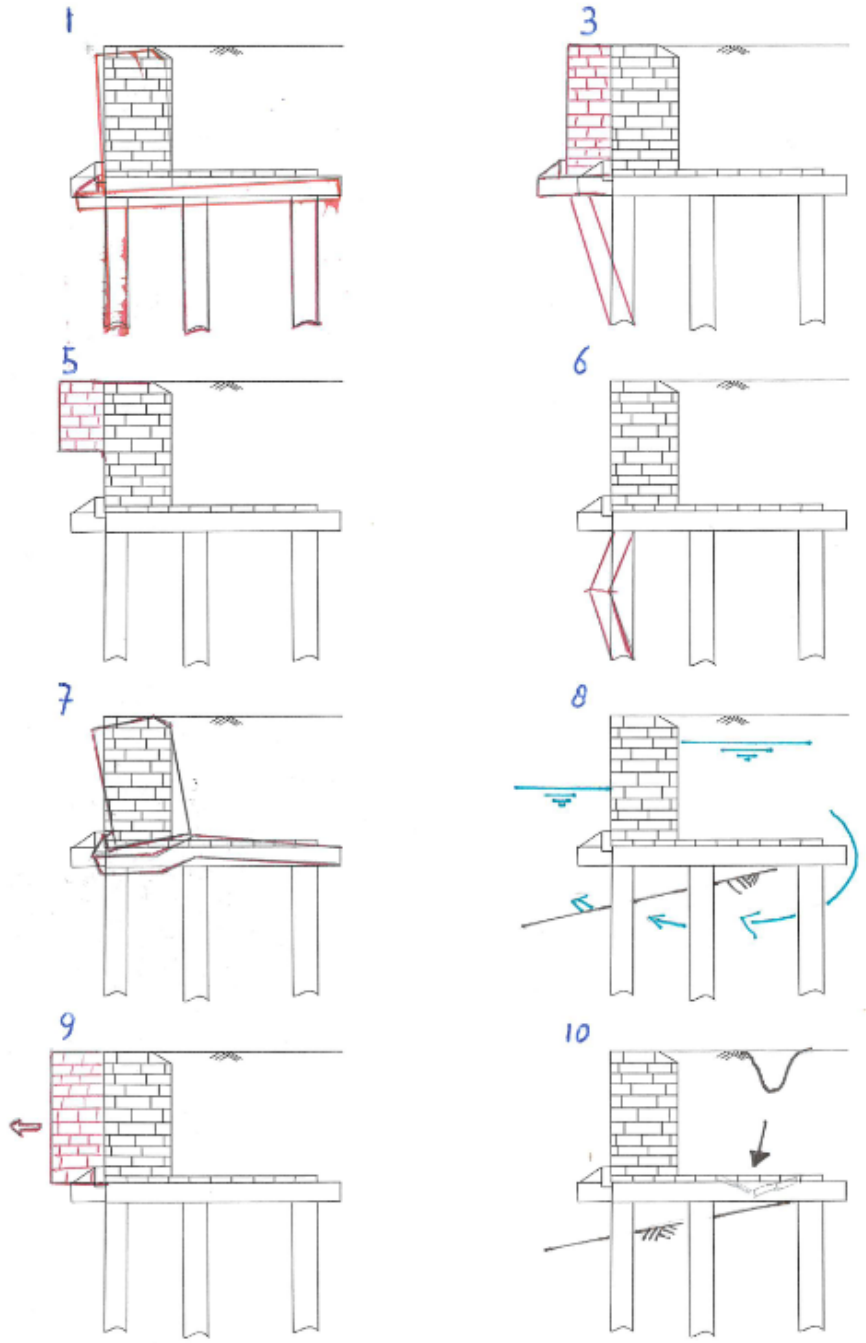

Figure 2.6: Failure mechanisms occurring in Amsterdam

2.5. Measurements in Amsterdam

In current research of literature there is not a specific method to determine the structural capacity of masonry in a quay wall when partly failing. The municipality of Amsterdam set up recommendations for control measures on quay walls when displacements are occurring. Based on insight in the construction, the lifetime, use and loads and deformations different measures are possible. When the horizontal or vertical deformation is more then 5 millimetres a month, the parking spots are removed on quay walls. When the total vertical or horizontal deformation is more than 20 millimetres, the traffic on the quay wall is stopped and trees are removed. When the total deformation of the quay wall is more than 25 millimetres, emergency measures need to be installed. Depending on the type of emergency structure, traffic is allowed again. (Gemeente Amsterdam, 2018)

When	Displacement	Measure
Immediately	-	Maximum axle load of 25 kN
Immediately	-	Maximum distributed load of 5kN/m^2
Displacement	>5 mm / month	Closure of parking spots
Displacement	>20 mm total	Closure of traffic
Displacement	>20 mm total	Removal of trees
Displacement	>25 mm total	Placing of emergency structure

Table 2.1: Intervention points of the municipalicy of Amsterdam

In November 2019 the municipality of Amsterdam decided for another ten quay walls that control measures have to be put into place. For eight of the locations it was decided that mainly the closure of parking spots would be sufficient for now, this would mean the displacements occurring are larger than 5 mm per month. For two locations, the Houtmankade and Prinsengracht, additional structures are built in January/February 2020. This would mean that the deformations at those two locations are more than 25 mm total.(Gemeente Amsterdam, 2019c)

Secondly, experts in hydraulic structures expect hidden structural capacity within failure mechanisms of quay walls. Identifying and activating them is not yet been fulfilled. A proposed method is analysing failure mechanisms and performing reliability based assessments. (Roubos, 2019)

3

Geometry of a quay wall

3.1. Elements of the quay wall

To provide the study with boundaries, it is necessary to determine parameters for the quay walls dimensions. Also, by simplifying the model, the elements to run into DIANA FEA are scaled-down. The assumptions made are stated down in this chapter and are further elaborated in chapter 4.

In this schematic, the critical structural elements, which are found in almost every old quay wall are: masonry wall and timber floor, kesp, piles and sloof as specified in chapter **??**. The main functions of these elements will be explained here. Also, when needed, assumptions will be made on the functions of these elements for thesis purposes.

1. Masonry: the masonry will carry most of its weight and transfers it via the floor and watersloof through the kesp and so on to the piles. From the point that bending occurs, the masonry will be the weakest link in the connection with the floor elements (Sas, 2007).

2. Floor: the main function of the floor is for construction purpose. On the floor, the first layer of masonry is built. A useful functioning floor element will spread the forces evenly through the kesp beneath it. Also, forces from the soil above and varying force conditions are spread over the floor elements.

3. Kesp: the kesp will provide stability during construction and ensures an even distribution of forces to the piles. There are multiple scenarios for the position of a kesp after a long service time. a) The piles are orientated next to the kesp, so only bending and shear forces arise. b) The piles are orientated underneath the kesp but under an angle, so compressive and tension forces occur. c) The piles are orientated directly underneath the kesp, so that the kesp has no additional structural function. In this situation, there is no need to do a calculation on the kesp. (Sas, 2007)

   Since the thesis's scope is not on the failure of the kesp but the foundation pile, an assumption is made that the piles are directly underneath the kesp and that the kesp has no additional structural value.

4. Piles: the piles have three main functions, support for the kesp, a structural function and a geotechnical function. The assumption made in the research is that a pile, due to any reason lost its structural capacity, so its structural function has degraded. It is important to keep in mind that due to the support of the soil, the pile can only deform. A new equilibrium situation will follow after the failure of a pile. So, for the model, it is important that even though the structural failure of a foundation pile is modelled, it will never decrease to zero. (Sas, 2007) For this reason, further research is performed on the non-linear behaviour of pile foundations and how to model these into Diana.

5. Sloof: The sloof functions as a horizontal constraint for the masonry wall. It can be placed at the front of the quay wall at the waterside but also in the middle of the quay wall processed in the masonry itself.

Most of the times it is slightly embedded into the kesp and it transfers its forces through the kesp, making the connecting point a weak spot on the kesp. For this reason (Sas, 2007) stated that the sloof is the element in the quay wall that can best be missed.

Due to timber rotting, it is found in practice that the sloof degrades a lot over time. In many occasions, the sloof is completely gone (Knuppe, 2019). Since it is assumed that the structural function of the pile foundation is affected (the most common reason is rotting) it is likely to assume that the sloof has no structural capacity left as well. For this reason and to simplify the FEM model, the sloof is not taken into account as an element into the analysis.

However, it is possible to analyse the effect of the sloof as a horizontal constraint into the model. In chapter 4, the interface between the timber floor and masonry wall is elaborated. This functions as a horizontal constraint due to friction between the elements. It is possible to take the sloof into account by increasing this friction value.

In quay walls in Amsterdam, cracks are occurring in the masonry work. The masonry might be restored multiple times. This is done from the water level upwards to the top. (CUR commissie 186, 2013) Therefore, below water level, material degradation might be worse than above, see figure 3.2. Secondly, because the restorations might be limited to certain depth, it is possible that over the thickness of the quay wall the strength differs. In this study the masonry is limited to a homogeneous material quality over the full depth and length of the quay wall, the possible difference in strength is not taken into account.

3.2. Dimensions of the elements

To model these elements and to determine the loads, it is necessary to start with some values for the dimensions of the elements. The Groenburgwal is inspected by Baars-CIPRO in April 2019. Based on the inspection report and drawings, the dimensions found in table 3.1 are used in the model. Values noted with an * are assumed since values are not provided in the inspection report.

The piles is assumed to rest in the first sand layer of Amsterdam, located at -8 till -10 meters below NAP. It is assumed that the pile is pushed half a metre into the sand layer, so the total length of the pile becomes 8.4 meters.

The thickness of the wall and the length of the floor are based on an old rule of thumb. The thickness of the wall is 0.4 times the retaining height and the length of the floor is the retaining height plus the thickness of the wall. So, in this case, for a retaining height of 2.0 meters, the thickness becomes 0.8 metre and the length of the floor 2.8 meters.

Sign	Description	Unit	Value
h_w	height of the wall	2.0	m
t_w	thickness of the wall	0.8*	m
h_f	height of the floor	0.1	m
L_f	length of the floor	2.8*	m
L_p	length of the piles	8.4*	m
d_{p1}	diameter of pile 1	0.25	m
d_{p2}	diameter of pile 2	0.24	m
d_{p3}	diameter of pile 3	0.24*	m
$h.o.h._1$	pile distance 1-2	1.1	m
$h.o.h._2$	pile distance 2-3	1.1*	m
$h.o.h._l$	pile distance longitudinal direction	1.1	m
h_s	pile length in soil	0.5*	m
L_w	water level from floor	0.4*	m

Table 3.1: Dimensions of a quay wall

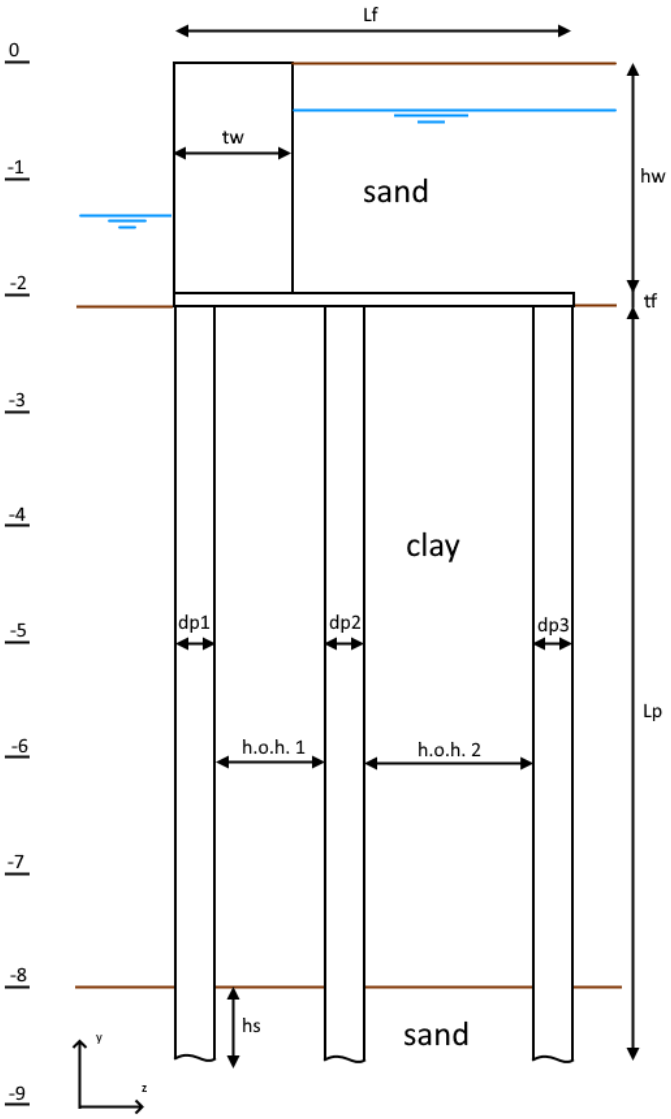

Figure 3.1: Dimensions of a quay wall

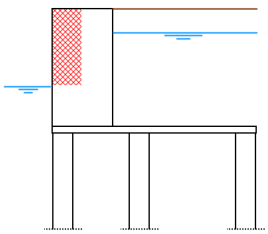

Figure 3.2: Different material qualities over the masonry wall after restoration

4

Timber and soil properties

4.1. Timber

Timber piles are used as a structural element in quay walls since 200 BC and are still being used today (de Gijt, 2010). An estimate 25 million timber foundation piles in the Netherlands have a bearing capacity and are still used. There is a widespread of species used, about 40. The type is an important factor in the degradation of the material. It is possible for a pile with a diameter of 200 millimetres, underwater, in 100 years, fully degraded by bacteria's with no structural capacity left. Where other species in the same circumstances have only a 5 mm affected region. (Klaassen et al., 2013) Other research shows that in Amsterdam, the species used are equally divided over pine and spruce wood. The quality of the material differs, since a wide variety of material age is used, piles of 40 years as well as over 150 years old. (Klaassen, 2013)

So, degradation is critical, the CUR 186 Handboek Binnenstedelijke Kademuren specifies three different degradations on foundation piles. Chemical, mechanical, biological degradation. The CUR 186 also provides a set of equations to determine the calculation values for stresses and strength.

The first degradation, chemical degradation isn't likely to occur, since timber is only vulnerable for high pH values which won't happen below water level.

Secondly, biological degradation for non-continuous damage due to contact with oxygen. When piles get in contact with oxygen due to lower water level, fungus activates and will affect the material quality. When fully covered with water, the process stops due to the lack of oxygen. The amount of degradation depends on the moisture content in the timber. When fully moist, the maximum degradation can be up to 10mm/year and when completely dried out, up to a maximum of 100mm/year.

Besides non-continuous biological degradation, there is continuous degradation. This form of biological degradation develops continuously over time and is mainly affected by contact with water. So, permeability is an essential factor when determining the continuous degradation of timber piles. The timber its permeability is determined by its type, as stated above, mostly pine and spruce are found. Spruce contains a denser structure and so less affected by continuous degradation than pine would be.

The third important mechanism is mechanical degradation. Due to a temporary change in the loading of the structure, it might be possible that a construction or foundation isn't capable of redistributing its forces. This can lead to failure. Without knowledge of the foundation its state, it is not possible to estimate mechanical degradation. So, for mechanical degradation, inspections are needed. (CUR commissie 186, 2013)

During a visual inspection from inside the canal, a team with divers collects samples from the timber piles, measure pile diameters and pile distances. Also, using technologies like sonar, scans can be made providing inside in the quality of the pile-masonry connections and indications of cracks in the masonry below water level. Apart from the visual inspection, it is possible to dive into the archives for information or do measurements outside the water.

The collected samples are taken to laboratories to perform tests. The strength capacities of the core as well as the structural relevant pile diameter, are needed to calculate the bearing capacity of the timber pile. More information about the bearing capacity of a timber pile and be found in chapter 4.3. The difference in measured pile diameter and structurally relevant pile diameter relates to the degradation of the pile. Most of the discussed types of degradation affected the outer part of the timber piles more than the centre.

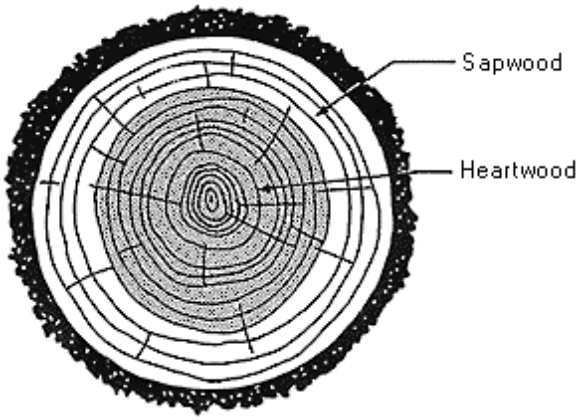

Figure 4.1: Heartwood and sapwood (Schmidt, 1990)

A typical pile cross-section, see figure 4.1, consists of heartwood and sapwood. Heartwood is the old and dark part that forms the centre, the structural base of the pile, opposite to sapwood it is denser and slow to absorb moisture. Sapwood is younger and functions to transport moisture to the roots and leaves of a tree, this makes it more porous and more vulnerable for decay than heartwood. (Schmidt, 1990) When conducting a test, the thickness of the sapwood layer is measured to get insight into the structurally relevant diameter of the timber pile.

Earlier research on the Groenburgwal in Amsterdam states that for the foundation piles spruce is used and as timber floor elements pine (Knuppe, 2019). Sawn timber elements have different properties then round piles. Therefore the elements used are placed into other strength classes. The NEN1912 - Timber for structural applications, specifies for sawn pine elements multiple classes depending on the quality of the pine used, ranging from C14 till C24. Since there is no data available from the quality of the pine used, the lowest quality class C14 is assumed. The un-sawned round spruce piles can be placed in strength class C30 (Swedish Wood).

In appendix C, material properties for the different strength classes can be found. These properties are used as input for further calculations on pile capacity and in Diana FEA, see table 4.1 for the Diana FEA input for the timber floor.

Sign	**Description**	**Value**	
	Unit		
E	Young's modulus	12000	N/mm^2
ν	Poisson's ratio	0.3	-
ρ	mass density	350	kg/m^3

Table 4.1: Material properties timber

4.2. Soil

The geology of the city of Amsterdam is governed by multiple layers of sand (zand), peat (veen) and clay (klei), see figure 4.2 for a typical cross-section of soil layers in Amsterdam. The first layers of peat and sea clay are

sediment transports from the river Amstel which was formed about 3000 years ago. The Amstel was running through a slightly clay environment and the area of Amsterdam consisted of a peat topsoil. In Amsterdam, the sand layers are known as the first and second sand layer (eerste en tweede zandlaand). These layers are formed during the Pleistoceen, an era that started 2.6 million years ago till 12.000 years ago which was known for cold (glacial) and warm periods (interglacial). During the glacial times, the water level was low, up to 100 meters lower than nowadays. In these dry times, you could have walked over the North Sea from Amsterdam to London. Due to the low vegetation and the lack of land ice in the last glacial era, strong winds made it possible to deposit large amounts of sand and so the first sand layer was formed. The layers of clay are formed during interglacial times where the sea level was higher. The in-between layer (tussenlaag) consists of sand but is not as strong as the sand layers. The second sand layer formed during a warm period and consist mainly of sand deposits from the sea. In Amsterdam, it was typical to drive the foundation piles of buildings and quay walls into the first sand layer, nowadays with larger buildings and quay wall renovations the second sand layer is the new standard.(de Gans, 2011)

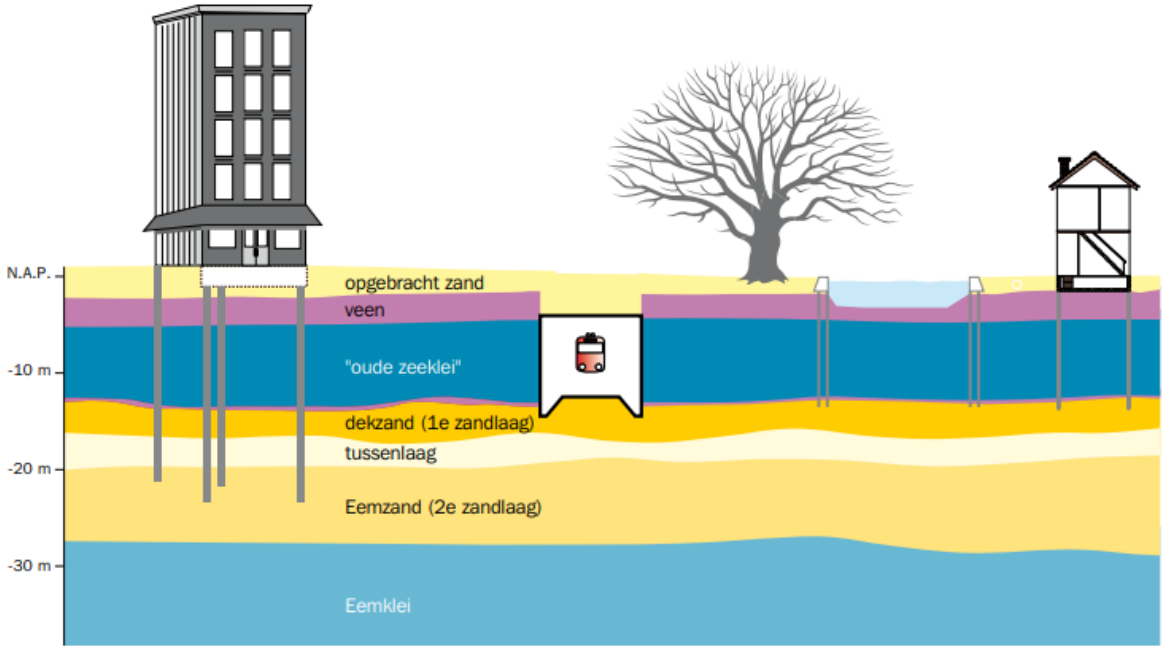

Figure 4.2: Soil layers in Amsterdam. (de Gans, 2011)

At the location of the reference case, there is data available from two different measurements retrieved from DINOLoket. The results of these measures are summarised in tables 4.3 and 4.4 and the full measurements can be found in appendix B. The depth parameters in tables 4.3 and 4.4 in meters are presented with respect to NAP. For S25G00127, the coordinates are put in AHN-viewer where the ground level is determined with respect to NAP, which is +0.5 metre.

Geotechnical measurements				
Number	Date	Identity	Coordinates	Type
1	02-05-2011	B25G2892	121612, 486771	Drilling
2	18-10-1999	S25G00127	121653, 486788	CPT

Table 4.2: Geotechnical measurements around Groenburgwal

Both measurements show similar results in combined clay and sand layers. Since measurement S25G00127 contains more layers, this data set will be used. The meters below -25.0 NAP will be assumed as the same sand layer till minus 50 meters below NAP. Also, the research assumes that no further data is needed below

Measurement B25G2892			
Start layer	End layer	Type	Other
+3.1	1.1	Sand	Moderate rough, slightly silty
1.1	-0.9	Peat	Slightly clay
-0.9	-9.9	Clay	Slightly sandy
-9.9	-51.9	Sand	Moderate rough, slightly silty
-51.9	-55.9	Clay	Moderate sandy
-55.9	-101.9	Sand	Rough, slightly silty

Table 4.3: Geotechnical measurement B25G2892

Measurement S25G00127			
Start layer	End layer	Type	Other
-1.5	-7.5	Clay	Weak
-7.5	-9.5	Sand	Slightly clay
-9.5	-12.5	Clay	Moderate
-12.5	-15.5	Sand	Moderate rough, slightly silty
-15.5	-18.5	Clay	Moderate sand, moderate
-18.5	-25.0	Sand	Moderate rough, slightly silty

Table 4.4: Geotechnical measurement S25G00127

this level. The first two meters from ground level are missing in S25G00127. Therefore, these are used from the top meters from B25G2892.

For calculations, characteristic soil properties are obtained from the NEN-EN 1997-1+C1:2012/NB:2012 table 2.b - Karakteristieke waarden van grondeigenschappen (NEN-EN-1997, 2012). The values needed are presented in table 4.5.

Characteristic soil properties						
Layer	From [m]	Till [m]	Type	γ_{dry} $[kN/m^3]$	γ_{wet} $[kN/m^3]$	φ [degrees]
1	0	-2	Sand, moderate rough, slightly silty,	18	20	27
2	-2	-8	Clay, weak	14	14	17.5
3	-8	-10	Sand, slightly clay	19	21	32.5
4	-10	-13	Clay, moderate	17	17	17.5
5	-13	-16	Sand, moderate rough, slightly silty,	18	20	27
6	-16	-19	Clay, moderate sandy,	18	18	27.5
6	-19	-25.5	Sand, moderate rough, slightly silty,	18	20	27
7	-25.5	-50	Sand, moderate rough, slightly silty,	18	20	27

Table 4.5: characteristic soil properties

4.3. Interface timber and soil

The quay wall connects with the soil layer via the timber floor and its timber pile foundation. Since it is not a given that the soil connects fully with the timber floor, for this research, it is assumed the quay wall rests fully on the timber piles and so, finds its horizontal and vertical stability from the pile foundation. To model a pile foundation, the bearing capacity of a timber pile has to be determined.

4.3.1. Geotechnical bearing capacity

The bearing capacity of a single foundation pile consists of two parts: base resistance and shaft friction. Note, the shaft friction can either work positive and negative. Using the Koppejan method and the soil measurements presented in B the base resistance can be found.

$$R_{b,cal,max} = A_b * q_{b,max} \tag{4.1}$$

with:

$$\begin{aligned} A_b &= \pi * \frac{D_{pile}^2}{4} \\ q_{b,max} &= \frac{1}{2} * \alpha_p * \beta * s * (\frac{q_{c,I,gem} + q_{c,II,gem}}{2} + q_{c,III,gem}) \end{aligned} \tag{4.2}$$

Where, A_b is the pile area and q_b is the averaged cone resistance. Input values can be found in table 4.6.

The shaft resistance of a timber pile can be calculated with:

$$R_{s,cal,max} = O_p * \int_L p_{max,shaft} * dz \tag{4.3}$$

with:

$$\begin{aligned} O_p &= \pi * D_{pile} \\ p_{max,shaft} &= q_{c,I,gem} * \alpha_s * l1 + q_{c,II,gem} * \alpha_s * l2 \end{aligned} \tag{4.4}$$

Where O_p is the circumference on the pile and $p_{max,shaft}$ the maximum shaft capacity. $q_{c,I,gem}$, $q_{c,II,gem}$ and $q_{c,III,gem}$ are cone resistances over specific depths along the pile as defined in figure 4.3 by the Koppejan method. Parameters that are set, are presented in table 4.6. Where $q_{c,I,gem}$ and $q_{c,II,gem}$ use the average cone resistance for 0.7 till 4 times the equivalent pile diameter under the pile tip and $q_{c,III,gem}$ the uses 8 times the length of the equivalent pile diameter above the pile tip to define the average cone resistance. The pile diameter is set as a variable parameter in the calculation. For these different diameters results can be found in table 4.7.

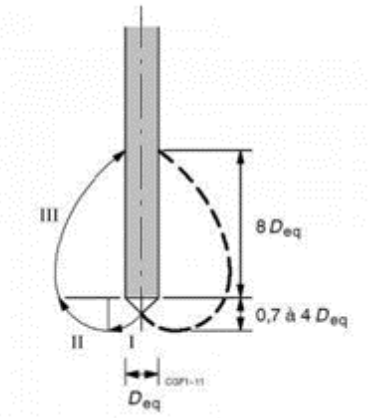

Figure 4.3: Koppejan method to determine cone resistance

Sign	Description	Value	Unit	Value from
α_p	pile tip factor	0.7	-	for timber pile (NEN 9997)
β	shape factor	1	-	for round shape (NEN 9997)
s	shape factor	1	-	for round shape (NEN 9997)
$q_{c,I,gem}$	cone resistance from tip to 0.7 - 4 D below tip	2.25	MPa	measurement
$q_{c,II,gem}$	cone resistance from tip to 0.7 - 4 D below tip	0	MPa	measurement
$q_{c,III,gem}$	cone resistance from tip to 8 D above tip	1	MPa	measurement
α_s	correction factor for friction between soil and shaft	0.02	-	for clay (NEN 9997)
α_s	correction factor for friction between soil and shaft	0.0125	-	for sandy clay (NEN 9997)
α_s	correction factor for friction between soil and shaft	0	-	for peat (NEN 9997)

Table 4.6: Input values for geotechnical bearing capacity

D_{pile}[m]	$A_b[m^2]$	$o_p[m^2]$	$q_{b,max}$[kN]	$R_{b,cal,max}$[kN]	$R_{s,cal,max}$[kN]
0.25	0.48	0.78	744	360	20
0.2	0.31	744	0.63	230	16
0.15	0.17	744	0.47	130	12
0.10	0.08	744	0.31	58	8

Table 4.7: Geotechnical capacity

4.3.2. Force-displacement diagram

Using the obtained values presented in table 4.7, for all pile types force-displacement diagram are created. To do this, there are multiple curvatures found for different pile types. The difference in the piles is the construction method, piles can be driven into the ground, which will push the soil aside, or the pile can be screwed into the ground where the soil is being removed. For the different curvatures see 4.4. This difference results in a different force-displacement diagram.

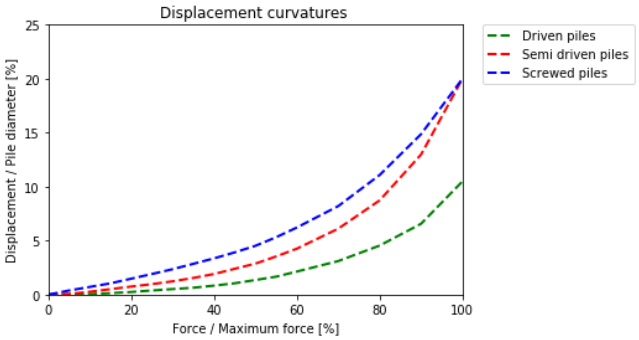

Figure 4.4: Displacement curvatures for different pile types

The piles used in Amsterdam are driven into the ground, so the green curvature of figure 4.4 is used. From this curvature to the force-displacement diagram works via the following method. Where the displacement is unknown and the pile diameter is known, and the percentage is obtained from the figure. As an example, the displacement at the maximum force of a 250 millimetres pile is calculated:

$$percentage = \frac{displacement}{pilediameter} = \frac{displacement}{250} = 10.5 percent \tag{4.5}$$

$$displacement = curvature * pilediameter = 250 * 0.105 = 26.25 millimeter \tag{4.6}$$

This progress can be repeated till the full displacement curvatures are obtained. The force-displacement diagrams for the shaft and base resistance are presented in figure 4.5.

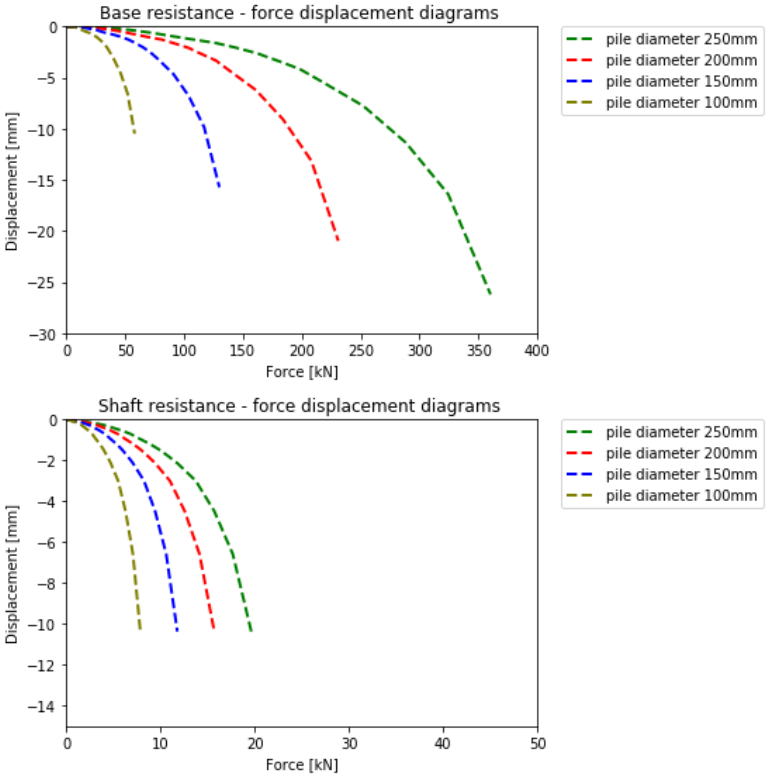

Figure 4.5: Force-displacement diagram for base and shaft resistance

From the figures in 4.5 as well as in table 4.6 it can be concluded that the base resistance is about 90-95 per cent of the total capacity. In a case study into pile foundations of Amsterdam, the base resistance capacity is about 80 per cent of the total resistance (van Daatselaar, 2019). In this study, the shaft resistance was higher, this difference is related to the difference in chosen subsoil layers. For further research in this thesis, this difference in neglected and the graphs in figure 4.5 are used. For detailed input into the curvatures, the exact force-displacement values can be found in appendix D.

5

Masonry properties

5.1. Masonry

Masonry is the building material that is still used on a large scale in the building industries since it is introduced thousands of years ago. Besides new methods of the last decades, techniques to assemble bricks remained the same. (Paulo B. Lourenço, 1995)

Masonry consists of multiple elements, brick and mortar. Figure 5.1a provides an example of the masonry components. Horizontal joints are referred to as bed joints and the vertical joints as head joints. Both materials are stone-like and show brittle behaviour. Different from, for example, a masonry wall in a building, quay walls are so-called multi wythe. A whyte is a continuous vertical layer of masonry with a one-unit thickness. A whyte can be independent and interlocked with other layers of wythe (Abbot).

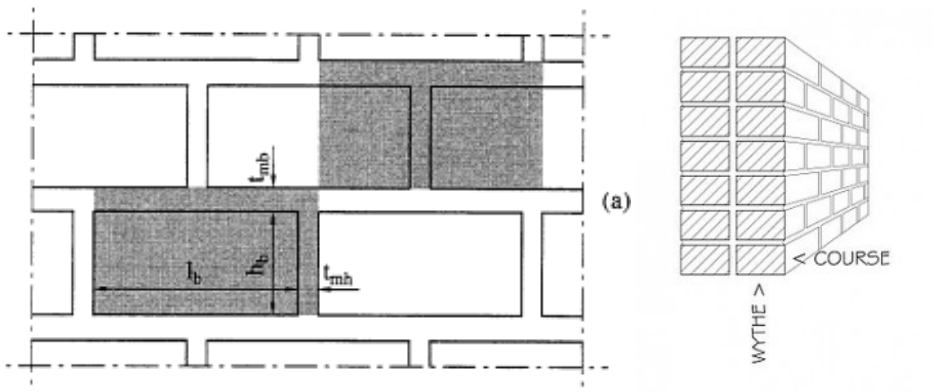

(a) Masonry terminology (Paulo B. Lourenço, 1995) (b) Masonry wythe (Abbot)

Masonry structures can be divided into three types: unreinforced, reinforced and confined structures, see figure 5.2. In the Netherlands and in the Amsterdam quay walls, mainly unreinforced masonry is used. Reinforced masonry with concrete or steel and confined systems are typical in regions with high seismic activity. For the scope of this research, only unreinforced masonry is taken into account.

As specified, masonry is an old building material, the first brick walls are from 2400 BC and made their introduction in the North of Europe around 1500 (de Gijt, 2010). In Amsterdam, after a city fire in 1452, the city municipality implemented a policy that all houses should consist of masonry walls instead of timber. From this year, the demand of brick was hard to supply. It is believed that most of the masonry used in Amsterdam is produced alongside the river Vecht. There, the clay contains iron, which results in red brick. The brick produced in Vecht has typical dimensions of 21 x 10 x 3,8 centimetre, sizes that are still used in present times. Till

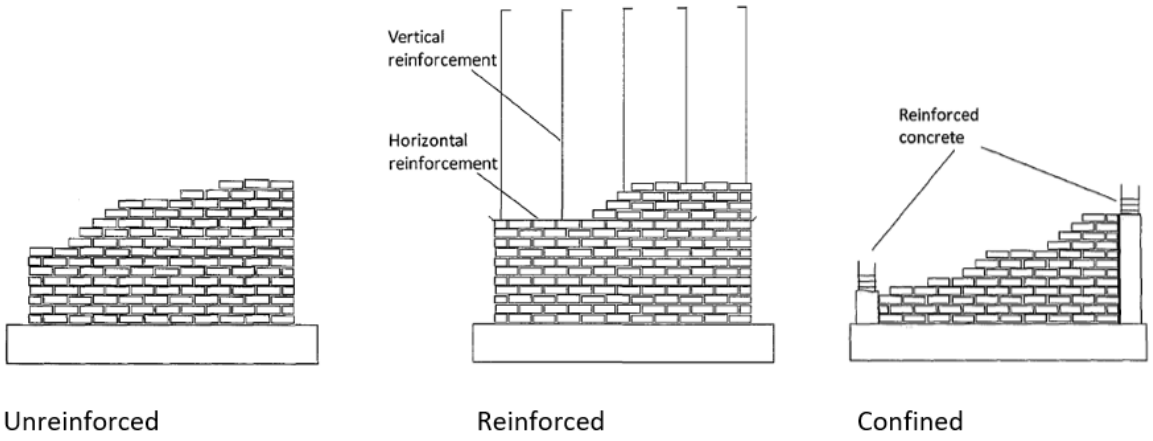

Figure 5.2: Different types of masonry (Andrés and Barraza, 2012)

the first half of the 17th century, the bricks were produced on low temperatures with a grainy clay resulting in a red to an orange glow. In the second half of the 17th century, brick makers used a coarser clay and higher temperatures; the result was a harder and a grizzled colour. From the 18th century onward, the colour was darker red again. As a mortar in Amsterdam, calcium from shells was used with a limited amount of sand. This is of importance since the results of this mixture is a flexible mortar which is useful to resist the soil deformations in Amsterdam. (Vermeer, 2003).

The properties of brick and mortar are important to analyse the structure. A recent study also concludes that for weaker materials, like older produced masonry, the anisotropic behaviour and difference is larger compared to modern-day masonry. (van Noort, 2012). However, this research is based on single wythe numerical experiments of masonry. If the same principles apply for multi wythe quay walls is debatable.

5.2. Structural behaviour of masonry

As specified before, masonry contains brick and mortar, both having different material properties. Since the model used is a macro model using one smeared material, the properties discussed in this chapter are based on the smeared capacity of masonry. The structural behaviour of masonry can be sorted into three categories, tension, compression and shear. To describe the behaviour in these categories, parameters as the Young's Modulus, compressive and tensile strength and fracture energy are used.

The Youngs Modulus describes the tensile behaviour of a material in its linear elastic stage. It is a relation between the stress and the strain of material. With masonry being an orthotropic material, meaning it has different material properties in different directions, the Youngs Modulus of the material is also different in the vertical and horizontal directions. Since the model used in this thesis contains the Total Strain Crack Model, which is not compatible with multiple Young's Moduli, the orthotropic behaviour of masonry is not taken into account.

In figure 5.3 the stress-strain diagrams in tension, compression and shear for quasi-brittle material like brick, mortar and masonry are presented. Note that these are drawn in different scales and are displayed for general behaviour. In general, the behaviour in compression is much stronger than in tension.

The displayed parameters Gf and Gc are the fracture energies. This is the energy needed to open an area for a crack. After a crack opens, softening takes place, where the stress gradually decreases under an increase in deformation until an ultimate strain, where the crack would be fully open.

The behaviour in tension and compression differs slightly. In compression, the material can continue to take on loads after is starts to crush and deform more rapidly, while in tension this transition is abrupt and

after a linear stage with a clear peak stress, a crack will occur, and then the material starts to soften.

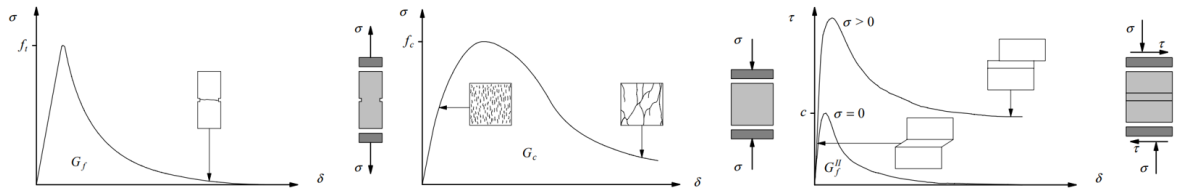

Figure 5.3: Behaviour of quasi brittle materials in tension compression and shear. (Lourenço, 1996)

For the behaviour in shear, there are two lines drawn. The top one contains the influence of compressive stress into account, which will result in higher resistance against sliding. The second line is the behaviour without a compressive force where the cohesion is the only resistance against sliding. It is important to know that for macro modelling of masonry the shear failing mechanisms as specified by (Lourenço, 1996) are not taking into account, since this focuses on the behaviour between brick and mortar, a micro model containing interfaces would be needed. The sliding phenomena would occur around the interface between masonry and the timber floor where cohesion is an important factor.

For the curvatures discussed based on the studies of Lourenço, cracking, crushing or sliding of the masonry will occur. In other research, (de Vent, 2011), starts to discuss cracking pattern in masonry and basic load situations for deformations and cracks.

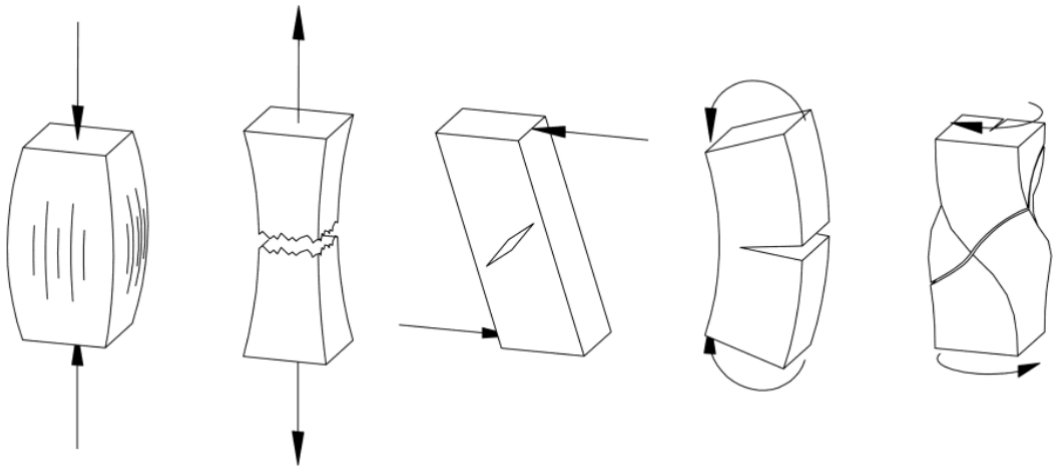

Figure 5.4: Five basic load situations for materials. (de Vent, 2011)

Besides, compression, tension and shear, (de Vent, 2011) discusses bending and torsion. For compression, it is more clearly visible that crack occurs parallel to the load and the material shortens, so again crushing behaviour. For tensile loads, the material elongates, and the crack occurs perpendicular to the load. A load combination in opposite working direction will result in shear forces, which will develop a diagonal crack in the material. As discussed, the tensile strength of masonry is lower than the compressive strength. This results that under bending conditions cracks occur where the tensile forces are at peak level. Finally, torsion occurs when out of place forces are applied to the structure.

De Vent also discusses the three main categories of structural failure, tilting, crack development and deformations, see figure 5.5 for tilting. The three types also imply different underlying reasons for failure, tilting due to the lack of external stability, deformations due to the lack of stiffness and crack development due to

the lack of strength.

While the setup of the model used in this thesis is not discussed yet, it is specified that the model would separately run in two directions. If the three structural failure mechanisms are considered, the assumption is that in a 2D cross-sectional model, the only occurring failure mechanism might be tilting due to external instability. For the 2D longitudinal model, the structural failure mechanisms would be crack development and deformations for bending or shearing due to the lack of stiffness or strength.

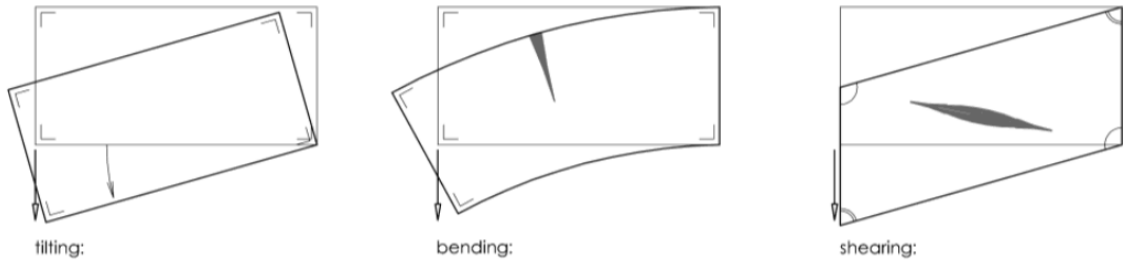

Figure 5.5: Tilting, bending and shearing of masonry.(de Vent, 2011)

5.3. Masonry in Amsterdam quay walls

For the masonry used in the Amsterdam quay walls, there have not been any tests performed to characterise the material properties. It is known that the bricks used are solid clay bricks. In the last decades, the province of Groningen in the Netherlands experienced over a 1000 human-induced shallow earthquakes due to the gas production. The houses and buildings in that area can be seen as unreinforced masonry load-bearing structures. (de Groot, 2019) For this new problem in the Netherlands, seismic loading on unreinforced masonry structures, lots of data was needed and so, on these masonry samples, research is available. The summary report for the material properties of original Groningen masonry (Jafari and Rots, 2016) contains an overview of performed tests by TU Delft, TU Eindhoven, and B|A|S. In this report, the characteristics of solid clay bricks from before the year 1945 can be found. For this research it is assumed that these characteristics are the closest to the bricks used in the Amsterdam quay wall. The data from this research can be found in appendix C, in table 5.1 these values are summarised, the values noted with a * are based on the research provided on numerical models in Diana FEA (van Noort, 2012). The work of van Noort had the goal to determine a procedure to formulate smeared material properties for masonry based on the properties of the mortar, brick and brick-mortar interface. It is concluded that the formulas from Pande, which are included in appendix E, are a good basis to formulate the Poisson's ratio and Young's moduli for masonry structures. However, to calculate these, there is a need for material parameters from the Amsterdam quay wall on brick and mortar. So, when this data comes available, during or after the research, the assumptions made in table 5.1 can be validated.

Sign	Description	Value	Unit
E	Young's modulus	6410	N/mm^2
ν	Poissoin's ratio	0.27*	-
f_c	compressive strength	12.65	N/mm^2
f_t	tensile strength	0.15*	N/mm^2
G_c	compressive fracture energy	26.07	N/mm
G_f	tensile fracture energy	0.035	N/mm
ρ	mass density	1773*	kg/m^3

Table 5.1: Material properties masonry

5.4. Masonry interface

As specified in chapter 3, a quay wall contains a connection between the timber floor elements and the masonry wall element. Although all the quay walls have a connection between those two parts, there is little information about the importance of this connection. It is found that shear friction coefficient μ of 0.5 or a friction angle of 26 °can be used between the elements (Naval Facilities Engineering Command, 1986). However, it is not specified if the elements here are dry or wet, and since it is a design manual, it is assumed that this friction coefficient is based on new brick and timber elements. In the Dutch code, NPR 9998 a friction coefficient of μ 0.75 is specified for timber and masonry elements. However, this code is based on the assessment of the structural safety of buildings. In here it is also not taken into account that the connection between the masonry and timber elements is underwater.

In thesis work of (Strikvoort, 2014) the behaviour of new as well as old bricks on timber are researched in dry and wet circumstances. Note, the test is performed on timber and brick elements, and not timber and masonry. In here two tests are performed, a tilting test and a horizontal shear test. The first results of the tilting test, where a loose piece of brick was slid over a timber element under an angle.

1. Dry new bricks: 30°, μ = 0.58
2. Dry old bricks: 21-22°, μ = 0.40
3. Wet old bricks: 16°, μ = 0.29

However, in these first tests, it was not taken into account that the weight of the quay wall rested on the first layer of bricks, providing extra friction. For the second tests, bricks were considered wet, and by pressing them for 1.5, 15, 150 or 1500 minutes (a logarithmic scale to approximate 140 years), the research takes into account the water content level. After 1500 minutes of pressing, the brick was dry again, resulting in lower friction coefficients.

Time [minutes]	**Angle of friction [degrees]**	**Friction coefficient [-]**
1.5	19	0.35
15	24.5	0.46
150	34.5	0.69
1500	33	0.65

Table 5.2: Angle of friction and friction coefficient between masonry and timber (Strikvoort, 2014)

The second experiment was the horizontal shear test. In this experiment the connection between timber and masonry could be kept wet. Also, there was no restriction in the extra load on the brick. The results presented show a top and residual value since stop and go tests were performed.

Time [minutes]	**Max. angle of friction [degrees]**	**Residual angle of friction [degrees]**	**Max. friction coefficient [-]**	**Residual friction coefficient [-]**
15	39.5	37.9	0.82	0.78
225	40.6	39.0	0.85	0.81
3375	40.8	37.3	0.86	0.76
5333	40.0	39.2	0.85	0.82
5580	42.9	39.2	0.91	0.82
11704	39.6	39.5	0.83	0.82

Table 5.3: Angle of friction and friction coefficient between masonry and timber stop and go tests (Strikvoort, 2014)

The results show a wide variety from μ = 0.35 - 0.91, wherein the code μ = 0.5 is used. In (Strikvoort, 2014) μ = 0.75 is set as a parameter, this value is compared to the value provided by the codes and was determined as an important factor in the deformations and safety values for programming in Plaxis. So, in Diana modelling,

the friction factor will be an important parameter to adjust, to see its significance on the deformation and redistribution in the quay walls.

As mentioned in chapter 3 the sloof is not taken into account as a single element into the model. However, it is possible that the watersloof has some capacity to function as a horizontal constraint. This can be incorporated into μ, so in the analysis, higher values of μ will be checked as well to see the importance of the parameter. To incorporate the sloof into the friction coefficient as an extra additional cohesion value. The increased value of the cohesion will only be used in the cross-sectional direction of the analyses since it is not present in the working direction of the longitudinal direction.

Element	**Cohesion** $[N/mm^2]$		**Condition**	**Angle of internal friction** $[degrees]$ $[coefficient[$
Masonry	0.2		dry	36.9, 0.75
Sloof	0.375		wet	42.0, 0.90
Total	0.575			

Table 5.4: Boundary conditions for interface condition

$$f_{s,k} * t_s = c1 \tag{5.1}$$

Shear strength of the timber (3 N/mm^2) times the thickness of the watersloof (100 mm).

$$c_{sloof} = c1/t_w \tag{5.2}$$

The additional cohesion is the calculated value divided by the thickness of the masonry wall (800 mm). Which results in an additional cohesion of 0.375 N/mm^2.

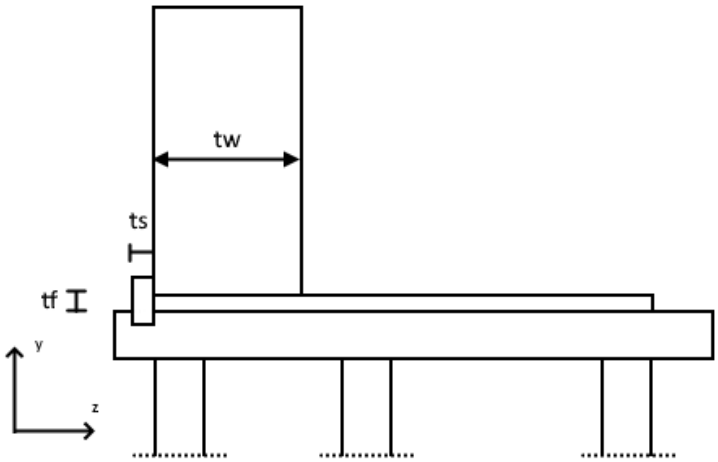

Figure 5.6: Dimensions of the sloof

6

Loads on quay walls

In the CUR166 references are made to CUR 211 and Eurocode 7 for multiple loads acting in quay walls, specified in three different categories, permanent loads, variable loads and accidental loads. Accidental loads are not likely to occur; examples of this are loads from collisions, earthquakes or extreme water level changes. The ones that do occur and of largest influence are:

1. Self-weight (permanent)
2. Ground, groundwater, water (permanent)
3. Traffic, direct and horizontal (variable)
4. Trees, roots and wind on trees (variable)
5. Storage (variable)

These categories of loads can be schematised in multiple ways, and in various combinations. For example, it is possible to have quay walls that are used mainly for the parking of cars, or quay walls containing trees over the full length. As a starting point in the model, only the self-weight and ground, groundwater and water forces are considered.

In chapter 4 the soil conditions are presented. With these values, the forces are calculated. An additional distributed force is added onto the soil side in steps of 10 kN/m to run the Diana model with different setups. In figure 6.1 the signs are displaced on a sketch of a quay wall.

The first step is to determine the soil pressures, with the dry and wet volumetric weights and the water level can be calculated with the following steps as described in Soil Mechanics by A. Verruijt. (Verruijt, 2007):

$$\begin{aligned} \sigma_{v1} &= \gamma_{dry} * z1 + q \\ \sigma_{v2} &= \gamma_{dry} * z1 + \gamma_{wet} * z2 \\ \sigma_{w} &= \gamma_{w} * z2 \\ \sigma_{ws} &= \gamma_{w} * z3 \end{aligned} \tag{6.1}$$

The effective soil stress is the soil stress minus the hydrostatic stress

$$\sigma_{v}^{'} = \sigma_{v2} - \sigma_{w} \tag{6.2}$$

The effective soil stress is the soil stress minus the hydraulic stress

$$\sigma_{v}^{'} = \sigma_{v2} - \sigma_{w} \tag{6.3}$$

The horizontal components can be calculated with the known cohesion and angle of internal friction of the sand layer, this goes by the following relation. Also, the resulting force can be calculated by integrating the area of the stress.

$$
\begin{aligned}
K_a &= \frac{1 - sin(\theta)}{1 + sin(\theta)} \\
\sigma_h &= K_a \sigma_v - 2 * c * \sqrt{K_a} \\
F_h &= 0.5 * h * K_a \sigma_v - 2 * h * c * \sqrt{K_a}
\end{aligned}
\tag{6.4}
$$

Symbol	Description	Value						Unit
q	distributed load	0	10	20	30	40	50	kN/m
σ_{v1}	vertical soil pressure 1	21,6	31,6	41,6	51,6	61,6	71,6	kN/m
σ_{v2}	vertical soil pressure 2	37,6	47,6	57,6	67,6	77,6	87,6	kN/m
$\sigma_v^{'}$	effective soil pressure	29,6	39,6	49,6	59,6	69,6	79,6	kN/m
σ_w	hydraulic pressure soil side	8,0	8,0	8,0	8,0	8,0	8,0	kN/m
σ_{ws}	hydraulic pressure water side	6,0	6,0	6,0	6,0	6,0	6,0	kN/m
σ_h	horizontal soil pressure	14,2	17,9	21,6	25,4	29,1	32,9	kN/m

Table 6.1: Forces on the quay wall

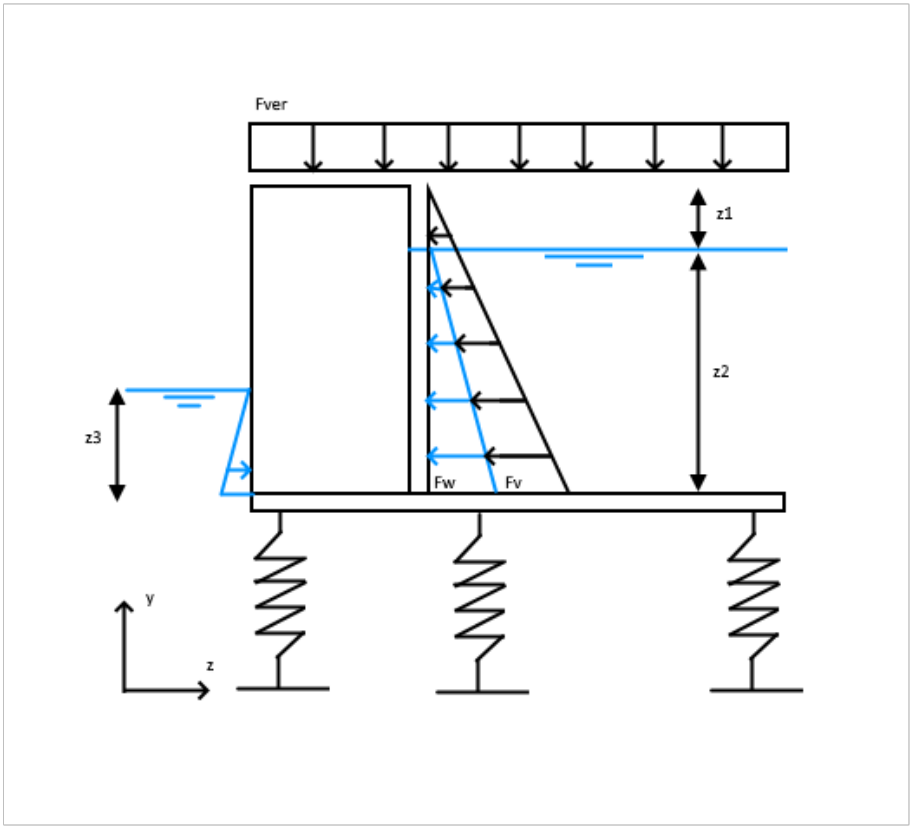

Figure 6.1: Acting loads on a quay wall

7

Numerical modelling of quay walls

The theory and strategies explained in this chapter are for references to the models used in chapters 8 and 9.

7.1. FEA Elements in 2D

The 2D models in Diana will work with a virtual thickness and so only in-plane loading is taken into account. An element that can be used for the modelling of masonry, as well as timber, is the CQ19M element. This is an eight noded quadrilateral plane stress element. In every node, it contains two degrees of freedom, displacement in x and y-direction.

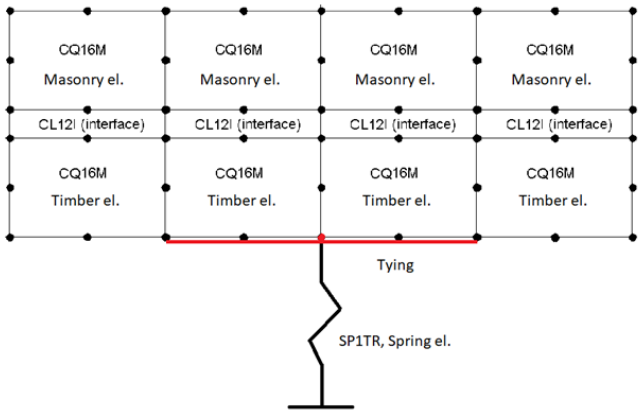

Figure 7.1: Connections of multiple elements and tyings of elements for pile behaviour

For the interface between the masonry and timber CQ16M elements, there is a CL12I element. This element fits the nodes of the CQ16M elements and contains in those nodes two degrees of freedom, displacements in x and y-direction. This interface element will work with the earlier specified Coulomb friction model.

The third element type used is the SP1TR. This is a one-node translation spring. The topology and variables as elongation and force can be found in figure 7.2.

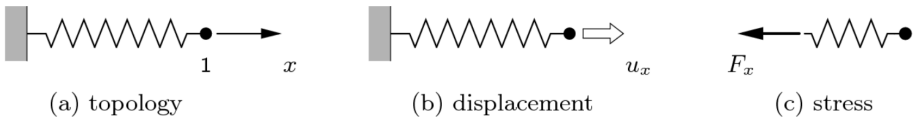

Figure 7.2: Definition of the SP1TR element (TNO DIANA BV, 2010)

The SP1TR element will be used to model the pile foundation. Under material properties in the input settings, the non-linear behaviour can be implemented via the force-displacement diagrams. The tying function will be used to simulate the one-noded element as a pile foundation with a larger diameter. The tying makes use of a master node and one or more slave nodes which will deform equally to the master node.

Figure 7.1 shows how the tying would be modelled in combination with the discussed other elements. The red node in the middle represents the SP1TR node, which is connected to two timber CQ16M elements. Along the red line, under the full edge of these two elements, the displacement in vertical direction would be exact to the vertical displacement of the red node. Depending on the element size, this could cover multiple elements to represent a pile with the desired diameter. Also visible is the CL12I interface layer between the timber and masonry elements which will be modelled with the discussed Coulomb friction interface. It is optional to remove this interface layer and then the masonry will be modelled directly to the timber, and the displacements of those connection nodes will be similar.

7.2. Types of modelling

As discussed in chapter two, masonry consists of brick and bed and head joints of mortar, see figure 7.3(a). To model masonry in finite element methods, there are multiple approaches. In literature (Lourenço, 2013) and (Paulo B. Lourenço, 1995), three main modelling types are discussed, differing in the detailing, from micro to macro level.

1. **Detailed micro-modelling**, see figure 7.3(b): separate continuum elements for the units of brick and mortar in bed and head joints. The interface between the elements of brick and mortar is a discrete element. Micro modelling is the most accurate approach but takes a lot of computational time and memory.

2. **Simplified micro-modelling**, see figure 7.3(c), (where the discontinuous line is the original brick size): The mortar joint properties and interface conditions are smeared out over a discontinuous element. The bricks dimensions are expanded to the middle of the joint layer, so that the geometry remains the same.

3. **Macro-modelling**, see figure 7.3(d): One continuous homogenised material without a distinction between brick, mortar and interfaces.

Both micro modelling approaches are of the best value when analysing small structural elements and aim to represent masonry using both material properties and the interface. Macro modelling is applicable for solid walls and large structures (Paulo B. Lourenço, 1995). The aim of this research is on a large quay wall its structural behaviour. For this reason, the masonry will be modelled in the finite element method with a macro model. The macro modelling makes use of additional material models.

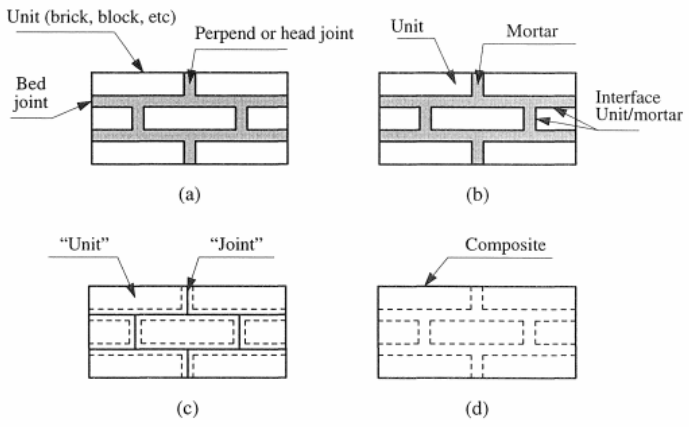

Figure 7.3: Modeling strategies for masonry structures: (a) masonry sample; (b) detailed micro-modeling; (c) simplified micro-modeling; (d) macro-modeling. (Paulo B. Lourenço, 1995)

7.3. Total Strain Crack Model

Multiple material models for masonry modelling in FEM software are found. In Diana, the newly developed Engineering Masonry Model is available and the Total Strain Crack Model. The Engineering Masonry model is a smeared failure model and can be applied in combination with regular plane stress (membrane) and curved shell elements for modelling failure of masonry walls into Diana (TNO DIANA BV, 2010). However, since the scope of the thesis is to determine the difference into a 2D and 3D analysis, the Engineering Masonry Model is not useable, since it would only be able to model membrane and shell elements. For this reason, the Total Strain Crack Model is used.

The Total Strain Crack Model is based on the modified compression field theory based on the research proposed by (Vecchio and Collins, 1986) as a model capable of reinforced concrete elements. The Strain Cracking model uses just like these theories a smeared cracking approach. In a smeared cracking approach, a certain crack is smeared over an area, as opposed to discrete cracking, where a crack forms at an exact location.

In the Total Strain Cracking Model, there are two options for modelling cracks, fixed and rotational. The fixed model fixes the direction of the crack after it starts cracking. When applying the rotational model, the direction has the possibility to change every time the stress-strain relationship differs. This relation is evaluated in the principal directions of the strain vector. In this study the rotational cracking model is chosen. For further reading on the background theory it is recommended to read the work of (van Noort, 2012) chapter 5 - Numerical modelling of masonry; (Grund, 2020) chapter 3.3 - Material models; (Verschuur, 2018) chapter 3 - Introduction to Diana with different models and possibilities.

The input for the Total Strain Crack Model consists of basic material properties as Young's Modulus and the Poisson's ratio, as defined in chapter 4 and predefined behaviour in tension, shear and compression.

In Diana, it is possible to choose a predefined function for the tensile behaviour of the TSCM. These relations can be found in figure 7.4. When masonry is modelled, the exponential relation for softening fits the curvature of brittle materials best when it is compared to the properties shown in chapter 4. However, for a more detailed study into the material properties of the masonry, a linear tensile behaviour is desirable. By doing so, the softening slope of all the compared materials can be modelled as slopes with parallel behaviour.

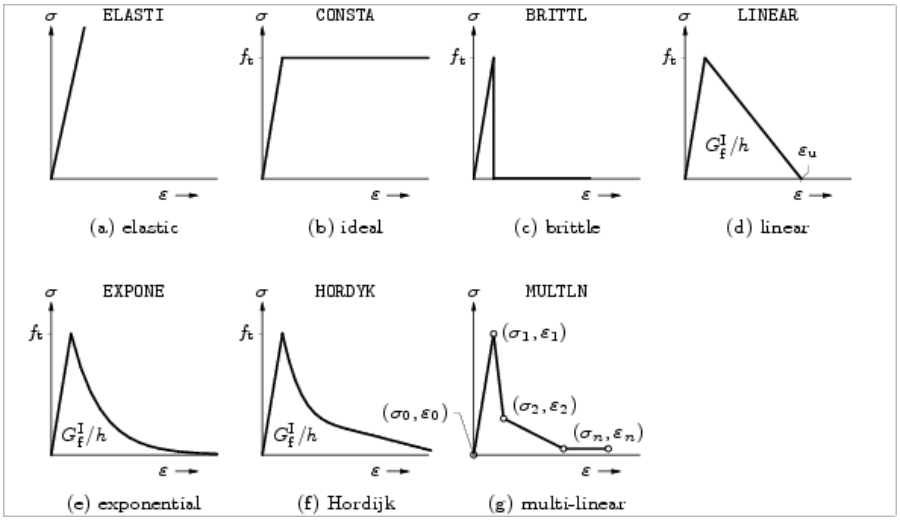

Figure 7.4: Tensile softening relations for the Total Strain Crack Model (TNO DIANA BV, 2010)

For the compressive stress-strain relationship, there are predefined options as well. These relations are shown in picture 7.5. Where the (c) Thorenfeldt and (g) parabolic are possible models for masonry. Since the Thorenfeldt curve fits the compression curve, as shown in chapter 5 slightly better, the Thorenfeldt curve is chosen in this thesis.

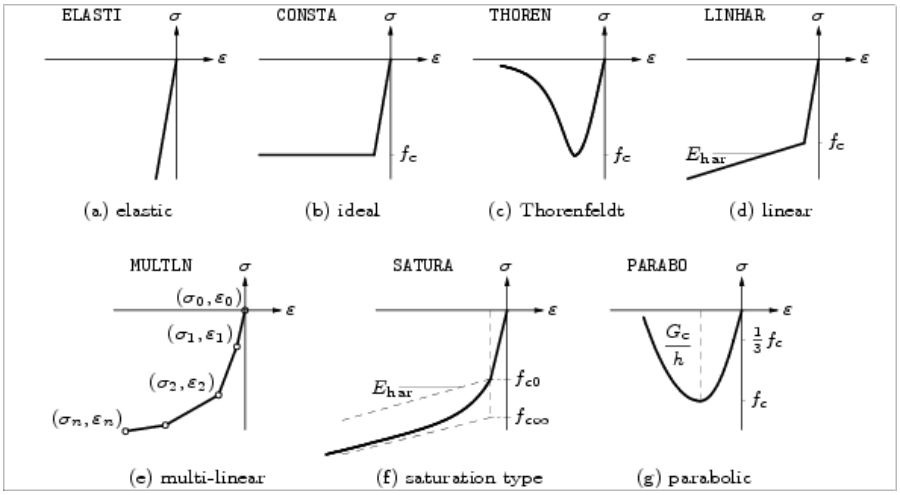

Figure 7.5: Compressive softening relations for the Total Strain Crack Model (TNO DIANA BV, 2010)

The Thorenfeldt curve is described by:

$$f = -f_p * \frac{\alpha}{\alpha_p} * \left(\frac{n}{n-(1-(\frac{\alpha}{\alpha_p})^{nk})}\right) \tag{7.1}$$

with:

$$n = 0.80 + \frac{f_{cc}}{17} \tag{7.2}$$

and:

$$k = \begin{cases} 1, & \text{if } \alpha_p < \alpha < 1 \\ 0.67 + \frac{f_{cc}}{62}, & \text{if } \alpha \leq \alpha_p \end{cases} \tag{7.3}$$

where f_p = peak stress and α_p = strain at which the peak stress is reached.

7.4. Coulomb friction model

For the modelling of the interface connection, which represents a mortar bind between the timber and masonry, a Coulomb friction interface is used, the specifics of the criterion can be found in figure 7.6. In this figure, c, is the cohesion between mortar and timber and ϕ is the angle of friction between the materials, both specified in chapter 5.

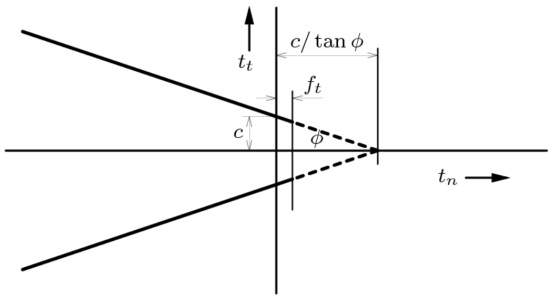

Figure 7.6: Coulomb Friction criterion (TNO DIANA BV, 2010)

In figure 7.6, f_t is a tensile limit which can be added to the interface. When this tensile cap is lower than the tensile strength of the masonry capacity, the interface would break before the masonry. With he tensile strength of mortar lower than the tensile strength of masonry it is recommended to look into the effects of this tensile limit of the interface.

8

Cross-sectional analysis

A 2D cross-section of a quay wall will be analysed in Diana FEA 10.2. In the analysis, the sensitivity of different parameters will be investigated. These parameters are the pile capacity, the properties of the masonry and the properties of the interface layer in between the masonry and the timber floor. As a starting load, there are the soil and water forces acting on the quay wall. An additional load, split up in a horizontal and vertical force, will be added with multiplication factors. The mentioned reference points of 20 and 25 mm will be added in the results to provide insight into the significance of the parameters.

For future research, the python code for all the material input, geometry and analysis method used in this chapter can be found in appendix I.

8.1. Model dimensions

In table 8.1 the dimensions used for the computational model are presented. The model's geometry is displayed in an exploded view in figure 8.1.

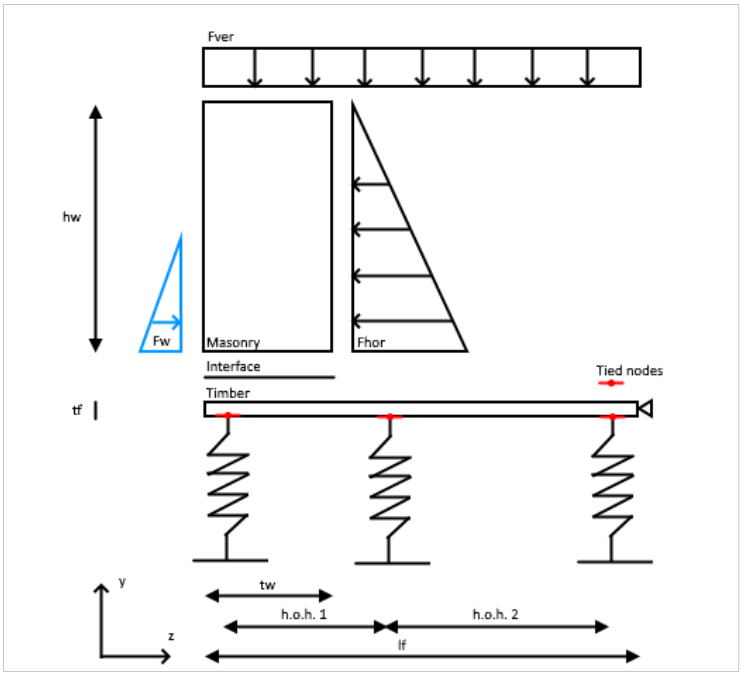

Figure 8.1: Components of the computational model in the cross sectional direction

Symbol	Description	Value	Unit
h_w	height of the wall	2.0 m	
t_w	thickness of the wall	0.8	m
h_f	height of the floor	0.1	m
l_f	length of the floor	2.8	m
$h.o.h._1$	pile distance 1-2	1.1	m
$h.o.h._2$	pile distance 2-3	1.3	m

Table 8.1: Dimensions of the cross sectional numerical model

The boundary conditions of the model are placed on the right side of the floor element and are fixed in the global x and z-axis. The tied nodes are fixed as discussed in chapter 7: Numerical modelling of quay walls.

8.2. Model structure

The finite element model in Diana FEA contains multiple element types. The masonry and timber elements are plane stress elements. For the interface layer, a 2D Coulomb friction line interface is used, and the spring translation springs. Further explanation about the element types and why these are chosen can be found in chapter 7, Numerical modelling of a quay wall.

	Masonry wall	Timber
Material model	TSRCM	Linear elastic isotropic
Element type	Plane stress (CQ16M)	Plane stress (CQ16M)
DOF's	ux, uy	ux, uy
Integration scheme	2x2	2x2
Mesh size [mm]	100	100
Thickness [mm]	1000	1000

Table 8.2: Discritesation masonry and timber in cross sectional model

	Interface	Piles
Material model	Coulomb friction	Boundary spring
Element type	2D Line interface (CL12I)	Translation spring (SP1TR)
DOF's	ux, uy	uy
Integration scheme	3 point Newton Cotes	1 point
Mesh size [mm]	100	
Thickness [mm]	1000	

Table 8.3: Discritesation interface and piles in cross sectional model

8.3. Input parameters

The timber elements are linear elastic and have the material properties as found in table 8.4.

Property	Parameter	Symbol	Value	Unit
Elasticity	Young's Modulus	E	7000	N/mm^2
	Poissoin's ratio	ν	0.3	-
	Density	ρ	350	kg/m^3

Table 8.4: Timber modelling properties cross sectional model

An overview of the masonry material properties used for the Total Strain Rotating Crack Model (TSRCM) can be found in table 8.5. As discussed in chapter 5, there are three types of structural failure: tilting, crack development and deformation. It is expected that the analyses of the cross sectional model would result in a stability problem and the structural failure occurring would be tilting. Hence it is chosen to only analyse one set of material properties for the masonry. These properties are based on the results found in literature (Jafari and Rots, 2016) of the Groningen masonry. The numbers presented in table 8.5 and used in the calculations are round of for thesis purpose.

Property	**Parameter**	**Symbol**	**Medium**	**Unit**
Elasticity	Young's Modulus	E	5000	N/mm^2
	Poissoin's ratio	ν	0.27	-
	Density	ρ	1775	kg/mm^3
	Shear Modulus	G_{xy}	3000	N/mm^2
Tension	Tensile strength	f_t	0.10	N/mm^2
	Fracture energy	G_f^I	0.015	N/mm
	Curve	-	Linear	-
Compression	Compressive strength	f_c	8	N/mm^2
	Curve	-	Thorenfeldt	-

Table 8.5: Masonry modelling properties cross sectional model

For the interface layer, the Coulomb friction model is used. An overview of the parameters used is presented in table 8.6. The stiffness parameters are found by equations 8.1 and 8.2. The tensile strength of the interface layer is chosen to be lower than the tensile strength of the masonry. This interface layer simulates a layer of mortar in between the masonry and timber, the tensile strength of mortar is lower than masonry. The final configuration that will be checked is when the materials are not modelled with an additional interface layer. This would result in a fully stiff connection.

Property	**Parameter**	**Symbol**	**None**	**Closed**	**Open**	**Unit**
Stiffness	Normal	k_n	-	50	5000	N/mm^3
	Shear	k_s	-	30	30	N/mm^3
Coulomb friction	Cohesion	c	-	0.575	0.575	N/mm
	Friction angle	ϕ	-	0.65	0.65	rad
	Opening model	Gapping model	-	-	Brittle	-
	Tensile strength	f_t	-	-	0.05	N/mm^2

Table 8.6: Interface layer properties cross sectional model

The stiffness in normal direction is determined by:

$$k_n = \frac{E}{l} = \frac{5000}{100} = 50N/mm^2 \tag{8.1}$$

The stiffness in shear direction is determined by:

$$k_s = \frac{G}{l} = \frac{3000}{100} = 30N/mm^2 \tag{8.2}$$

Where the letter l; in both parameters is the mesh size of the material.

The spring capacities' input parameters are presented in figure 8.2 and calculated using the formulas used in chapter 4. For different diameters of the foundation piles, different force-displacement diagrams are found and loaded into Diana. The specific values of the diagrams can be found in appendix D. In figure 8.2, the proposed numbers for Diana are presented versus the calculated ones. The solid lines are the calculated values and the dotted lines the proposed. The simplified force-displacement model is used because it was found

that for the longitudinal model, the more detailed the diagram, the longer the computational time. For research purposes, the preference was to keep the input for both models equal, and therefore the simplified force-displacement model is used in the cross-sectional analysis.

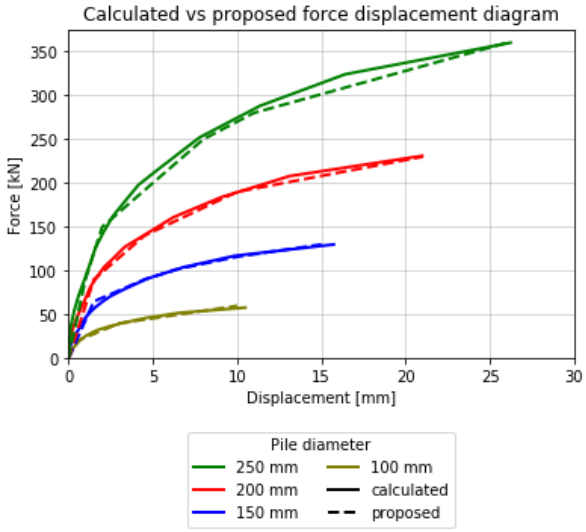

Figure 8.2: Force displacement diagram for non linear spring behaviour

8.4. Analysis method

The analyses in Diana are run in two load steps. First, the own weight of the structure combined with the forces of the soil and water are loaded onto the model. Secondly, an additional vertical distributed force and a triangular distributed horizontal force are loaded on the masonry work in a separate load step.

Load step 1	**Load**	load name	starting loads
		size	selfweight
		steps	1
		load name	hydraulic
		type	hor. trangular
		size	6 kN/m
		steps	1
		load name	soil
		type	hor. trangular
		size	18 kN/m
		steps	1
	Equilibrium iteration	max number iterations	50
		method	Newton Raphson
	Convergence norms	norm	force
		criterium	0.01
		norm	energy
		criterium	0.01
		satisfy both norms	yes
		no convergence	terminate

Table 8.7: Analysis method cross sectional model load step 1

Load step 2	**Load**	load name	Extra
		type	vert. distributed
		size	350 kN/m
		steps	50
		load name	soil
		type	hor. trangular
		size	18 kN/m
		steps	1
	Equilibrium iteration	max number iterations	100
		method	Newton Raphson
	Convergence norms	norm	force
		criterium	0.01
		norm	energy
		criterium	0.01
		satisfy both norms	yes
		no convergence	continue

Table 8.8: Analysis method cross sectional model load step 2

8.5. Results

Figure 8.4 presents the absolute deformations of the quay wall, measured at the tip of the masonry, in horizontal and vertical directions, see figure 8.3. This is done for three interface conditions, node-to-node, Coulomb friction criterion and a stiffer Coulomb friction criterion as presented in table 8.6. The following chapters will discuss the results of the different interface conditions in detail.

8.5.1. Node-to-node interface

In figure 8.4 on the left side, the results of the direct timber to masonry, node-to-node interface are displayed. The dark green lines, the 250 mm piles, show the results for a quay wall system with fully functioning piles; these results are considered as base results for the model. In the vertical direction, this means the system moves downwards until 26 mm for 360 kN, this is the maximum spring capacity in the model. In the horizontal direction, the displacements stay close to zero, and the system does not tilt over.
The remaining lines show the results for weaker piles, modelled with a lower ultimate displacement and force. Especially in the curves of the 150- and 100-millimetres piles, the results show a horizontal line. In vertical direction this is for the 150 millimetres pile around 15 mm, and the 100 millimetres around 10 mm, these are the ultimate displacements for both springs. After it reaches the ultimate displacement point, the pile fails, and the second pile, which is fully functioning, should take all the loads and therefore the displacement increases. After this jump, the model continues to displace until the two other piles reach their maximum capacity.

Lastly, the grey lines represent the behaviour of the quay wall system when the first pile has no structural capacity and is not modelled. By modelling it like this, the system starts to tilt over from the start.

In figure 8.5 the relative displacements in both directions are presented. These represent the displacements of the models minus the displacements of the model where all the piles are fully functioning. So, the displacements due to the pile foundation defects. For reference, the intervention points of the municipality of Amsterdam are added to the results. Now it follows that for a displacement of, 20 or 25 millimetres, the affected first pile should be degraded. When the pile is still relatively strong, 200 millimetres, the quay wall system will collapse due to the exceeding of the maximum pile capacity without reaching the intervention points of the municipality. Also, due to the modelling without an interface, the horizontal and vertical displacements follow the same curvature, where the path of the vertical displacement is governing.

Figure 8.3: Horizontal (l) and vertical (r) displacements of the quay wall in cross-sectional direction

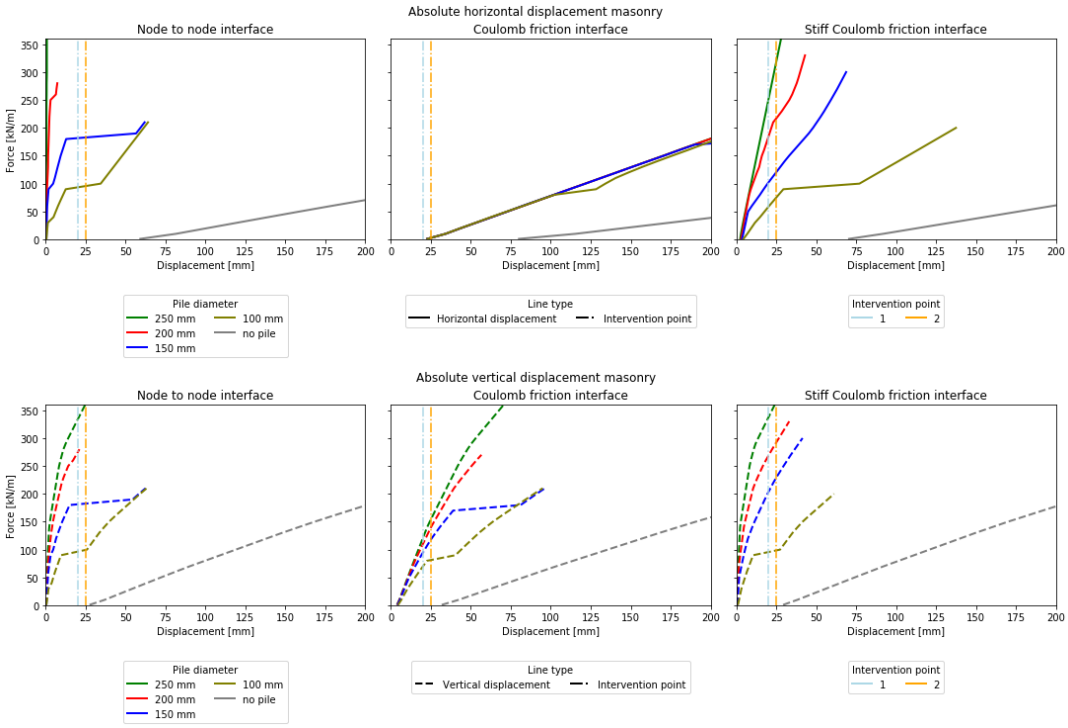

Figure 8.4: Absolute horizontal (top) and vertical (bottom) displacements using various interface conditions.

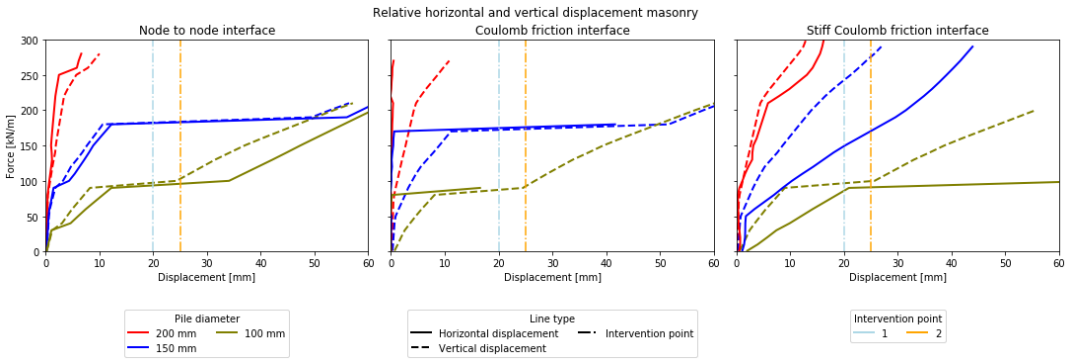

Figure 8.5: Relative horizontal and vertical displacements using various interface conditions.

Due to the modelling of the interface as a node to node connection from timber to masonry, tensile forces start to develop at this connection resulting in crack development. When the results are enlarged, see figure 8.6 for the enlarged results in the horizontal direction for the 100 millimetres pile, a second smaller jump is visible as well. At this point, see the red dot, the masonry starts to develop cracks, this occurs in an earlier stage than the failure of the pile, see the blue dot. For the location of the crack, see the right figure of 8.6. One could argue that this crack development would not occur in practice since the layer of mortar in between the masonry work and the timber floor would fail before the masonry would. For this reason, the second analysis would run with the discussed Coulomb friction model.

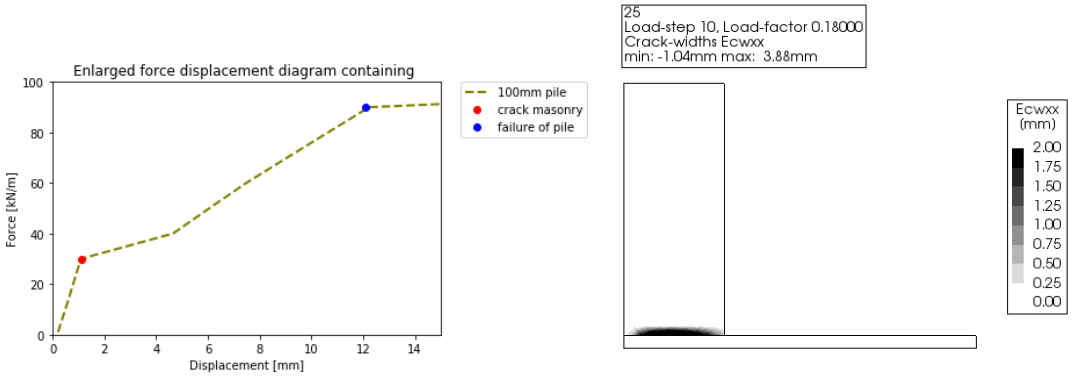

Figure 8.6: Location of crack and crack development over the force-displacement diagram

8.5.2. Coulomb friction interface

The absolute force-displacement diagram of the model using a Coulomb interface connection can be found in the middle of figure 8.4. In the middle figure of 8.5, the relative force-displacement diagrams are presented, the solid lines represent the horizontal displacement and the dashed lines the vertical displacement. Direct observation can be drawn with the Coulomb friction interface, there is no crack development in the model, the first jump in the displacement line is not visible in the results.

Besides the difference in crack development, the vertical displacement results show a similar displacement curve as the results for the node-to-node interface connection. However, the horizontal displacements differ significantly. This difference is the direct result of the interface layer, using a stiff node-to-node connection, the masonry layer can not slide from the timber floor. By using the Coulomb friction model, this sliding is possible.

What can be observed in the results is that for the 150- and 100-millimetres piles, the model again reaches its maximum pile capacity at the first pile row. After this, the already discussed jump occurs in the vertical direction. However, in the horizontal direction, the models tilts and is sliding over the timber floor. Although the relative displacements show results that can be expected, which concludes that the effect of the pile damage is taken into account in the model, the analyses absolute force-displacements diagrams show displacements in the horizontal direction of over 200 millimetres while modelled with a perfect set of piles. These extreme values and the tilting of the quay wall would not occur in practice, so an increased stiffness is proposed.

8.5.3. Coulomb friction interface - increased stiffness

The stiffness of the interface layer is adapted to modify the behaviour of the force-displacement diagrams. Observed is that after a jump in the vertical direction, the interface layer stretches and the displacement between the timber and masonry layer are exceeding. To counteract this, the third interface setup is used with a stiffer connection in the normal direction.

The absolute force-displacement diagram of the model using the stiffer Coulomb interface criterion can be found on the right side of figure 8.4. On the right side in figure 8.5, the relative force-displacement di-

agrams are presented. Again, in the vertical direction, the curvatures follow a similar path as observed in the results containing no interface and a weaker interface condition. The horizontal displacement for the 100 millimetres pile results eventually in a displacement of 121 millimetres before the model diverges due to the exceeding of the maximum pile capacity. To conclude, a lower force-displacement diagram results in large horizontal displacements due to tilting of the masonry.

For vertical displacements and loading in vertical direction, it is observed that the quay wall system can be loaded over the maximum load of the first pile row when modelled weaker. In table 8.9 the designed and enforced maximum loads and displacements in the vertical direction are displayed for the interface using a increasing stiffness.

Pile [mm]	**Design load [kN]**	**Design disp. [mm]**	**Max load [kN]**	**Max disp. [mm]**
250	360	26	360	28
200	230	21	330	43
150	130	15	300	69
100	60	10	200	137
0	0	0	200	515

Table 8.9: Interface layer properties cross sectional model

It is notable that the quay wall system can function while its vertical supports are degraded. The second and third pile rows absorb the forces when the first pile row structurally failed.

8.6. Conclusion

In the results presented above, all analyses run until divergence. Eventually, the analyses diverge and stop running due to the overloading of the maximum pile capacity. So, even though the system is modelled with perfect piles, displacements, and divergence occur.

In general it can be concluded that the modelling of a (partly) failing pile foundation in the cross-sectional direction provides little insight in hidden structural capacity within the masonry of the quay wall. While modelling with a reduced pile capacity the results present a decrease in the force-displacement diagrams, but eventually the quay walls tilt over.

The vertical displacement curvatures follow the given force-displacement diagrams in the springs, after the failure of the first pile row, the second and third pile row absorb and distribute these forces until failure of these piles and the model diverges. The vertical displacement curvatures found for the different researched interface conditions differ slightly in magnitude but follow the same displacement path. The observed vertical jumps in displacement are the result of the abrupt failure of the foundation piles in the model. Since the researched failure mechanism is the structural failure of the foundation piles, this is a logical response in the model, but field experiments should be performed to test the post-peak behaviour of pile foundations.

The displacement in the vertical direction is governing for the initial displacement in the horizontal direction, but the interface setup is governing for the magnitude of the displacements.

When modelled using a direct connection of masonry to timber, the horizontal displacement of the quay walls displaces along the same curvature as the vertical displacement. For an interface layer modelled using the Coulomb friction criterion, the stiffness of the interface determines the horizontal displacement of the quay wall. By making this connection stiffer, the displacement curvature moves to the displacement curvature found by using a direct interface. Using an interface to flexible, the quay wall slides over the masonry, and horizontal displacement occurs without horizontal constraints to hold the quay wall back.

This constraint to hold the masonry back, is the masonry wall itself. Figure 8.7 presents, on the left side, the deformed state of the cross-sectional model, where tilting and sliding of the masonry wall can occur without those constraints. On the right side, the top view is presented, where the masonry is constrained in horizontal

movement by the wall itself. In the middle figure, this constraint is predicted in the vertical direction.

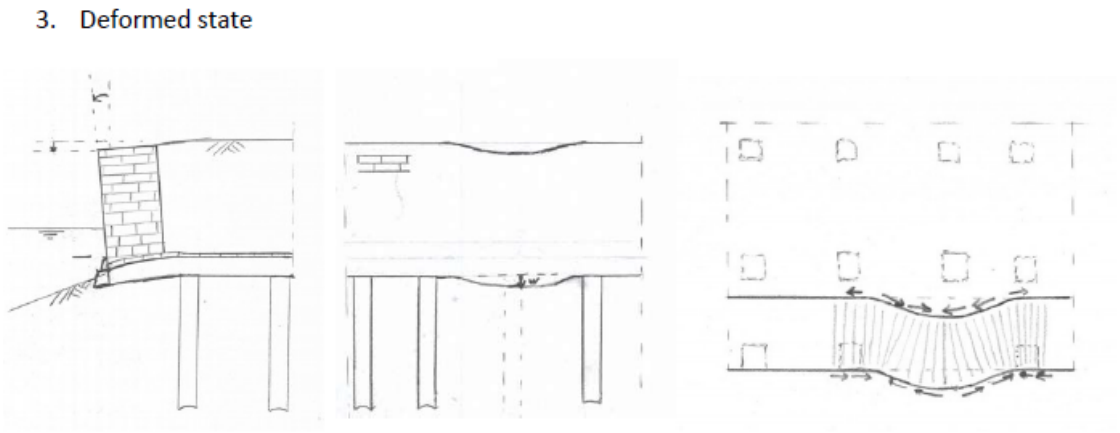

Figure 8.7: Deformed stage of quay walls under the condition of a partly failing pile foundation. (l) Cross section, (m) longitudinal section and (r) top view.

In this chapter the springs functioned as a vertical displacement constraint and without a function in horizontal direction. When figure 8.7 is observed, the vertical springs can be applied in the longitudinal direction of the quay wall and not in the top view. So, chapter 9 focuses on the analysis in the longitudinal direction as presented in the middle of figure 8.7. Here, the goal is to observe a constraint in vertical displacement by the masonry wall itself. It is notable that there should be a constraint in horizontal direction in the top view of the quay, this analysis is outside the scope of the study.

9

Longitudinal analysis

The longitudinal section of a quay wall are analysed in Diana FEA 10.2, in a later stage, some results are verified in Diana FEA 10.4 to check if divergence would occur later. In the analysis the sensitivity of different parameters are investigated. These parameters are the pile capacity, the properties of the masonry and the relevancy of the supporting timber floor. As a starting load the self weight of the structure is enforced and secondly an additional load will be added in smaller load steps. The mentioned reference points of 20 and 25 mm will be added in the results to provide insight in the significance of the parameters.

For future research the python code for all the material input, geometry and analysis method used in this chapter can be found in appendix I.

9.1. Model geometry

In table 9.1 the dimensions used for the computational model are presented. The geometry of the model is displayed in an exploded view in figure 9.1.

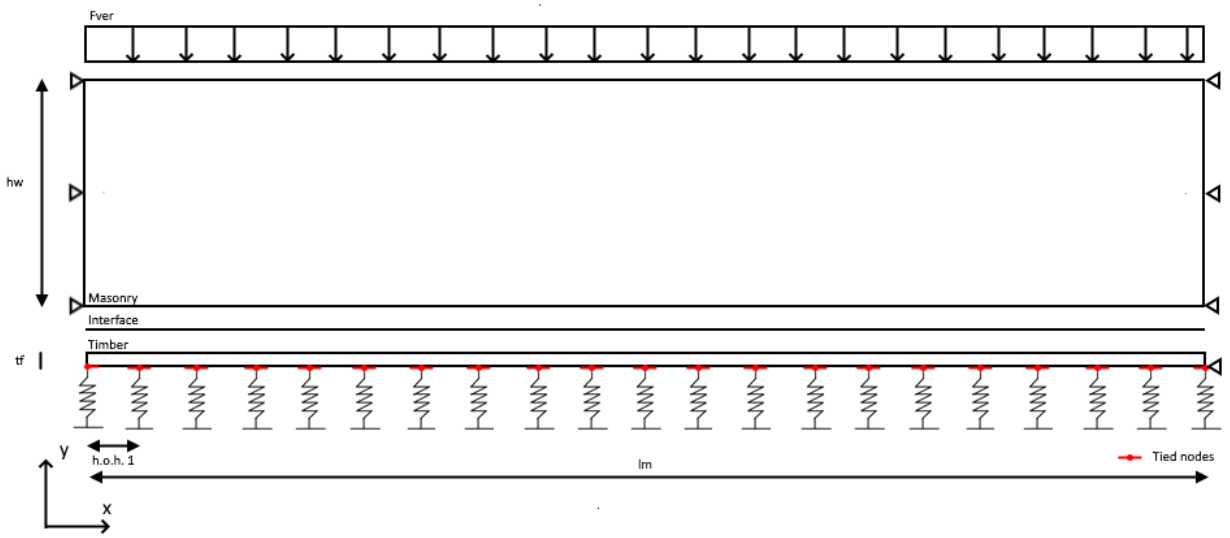

Figure 9.1: Components of the computational model in the longitudinal direction

The boundary conditions of the model are placed on both sides of the floor and masonry element and are fixed in the global x and z-axis. The tied nodes are fixed as discussed in chapter 7.

Symbol	Description	Value	Unit
h_w	height of the wall	2.0	m
t_w	thickness of the wall	0.8	m
t_f	height of the floor	0.1	m
l_m	length of the wall	22	m
$h.o.h._1$	pile distance	1.1	m
F_{ver}	Distributed vertical force	variable	kN/m

Table 9.1: Dimensions of the longitudinal numerical model

9.2. Model structure

The finite element model in Diana FEA contains multiple elements. In the longitudinal analysis, out of plane loads are not taken into account, so the masonry and timber elements are plane stress. For the interface layer, a 2D Coulomb friction line interface is used and the for the foundation piles, translation springs. Further explanation about the element types and why these are chosen can be found in chapter 7, Numerical modelling of a quay wall.

	Masonry wall	**Timber**
Material model	TSRCM	Linear elastic isotropic
Element type	Plane stress (CQ16M)	Plane stress (CQ16M)
DOF's	ux, uy	ux, uy
Integration scheme	2x2	2x2
Mesh size [mm]	100	100
Thickness [mm]	100	100
	Interface	**Piles**
Material model	Coulomb friction	Boundary spring
Element type	2D Line interface (CL12I)	Translation spring (SP1TR)
DOF's	ux, uy	uy
Integration scheme	3 point Newton Cotes	1 point
Mesh size [mm]	100	
Thickness [mm]	100	

Table 9.2: Discritesation masonry, timber, interface and piles

9.3. Input parameters

The timber elements are linear elastic and have the material properties as found in table 9.3.

Property	Parameter	Symbol	Value	Unit
Elasticity	Young's Modulus	E	7000-14000	N/mm^2
	Poisson's ratio	ν	0.3	-
	Density	ρ	1775	kg/m^3

Table 9.3: Timber modelling properties

An overview of the masonry material properties used for the Total Strain Rotating Crack Model can be found in table 9.4. There are three different classifications modelled to work with in Diana, strong, medium and weak masonry.

These properties are based on the results found in literature of the Groningen masonry. For thesis purpose

these numbers are round of. The fracture energy is chosen so that the softening slope of the masonry in tension is parallel. See fig 9.2, for the three different stress strain curvatures in tension.

Property	**Parameter**	**Symbol**	**Strong**	**Medium**	**Weak**	**Unit**
Elasticity	Young's Modulus	E	7500	5000	2500	N/mm^2
	Poisson's ratio	ν	0.27	0.27	0.27	-
	Density	ρ	1775	1775	1775	kg/mm^3
Tension	Tensile strength	f_t	0.15	0.10	0.05	N/mm^2
	Fracture energy	G_f^I	0.035	0.015	0.004	N/mm
	Curve	-	Linear	Linear	Linear	-
Compression	Compressive strength	f_c	12	8	4	N/mm^2
	Curve	-	Thorenfeldt	Thorenfeldt	Thorenfeldt	-

Table 9.4: Masonry modelling properties

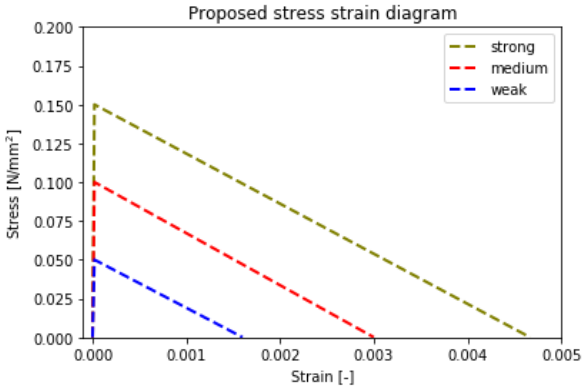

Figure 9.2: Tensile softening for different material properties

For the interface layer the Coulomb friction model is used. An overview of the parameters used is presented in table 9.5, these are determined by the following equations:
The stiffness in normal direction is determined by:

$$k_n = \frac{E}{l} = \frac{5000}{100} = 50N/mm^2 \tag{9.1}$$

The stiffness in shear direction is determined by:

$$k_s = \frac{G}{l} = \frac{3000}{100} = 30N/mm^2 \tag{9.2}$$

Where the letter l; in both parameters is the mesh size of the material. Just like in chapter 8 the stiffness of the interface layer in normal direction k_n is made 100 times stronger to normalize the displacements of the interface layer, due to the forces in compression. To counter this, the model is also tested using an interface layer with a tensile maximum capacity.

Property	Parameter	Symbol	Closed	Open	Unit
Stiffness	Normal	k_n	5000	5000	N/mm^3
	Shear	k_s	30	30	N/mm^3
Coulomb friction	Cohesion	c	0.2	0.2	N/mm
	Friction angle	ϕ	0.65	0.65	degrees
	Tensile strength	f_t	-	0.05	N/mm^2

Table 9.5: Interface layer properties

The final material properties that are put into Diana are the spring capacities. With the formulas used in chapter 4, for different diameters of the foundation piles, different force-displacement diagrams are found and loaded into Diana. The specific values of the diagrams can be found in appendix D. In figure 9.3 the proposed numbers for Diana are presented versus the calculated ones. Where the solid lines are the calculated values and the dotted lines the proposed. The simplified force-displacement model is used because it was found that; the more detailed the diagram, the longer the computational time of the model and divergence occurs earlier.

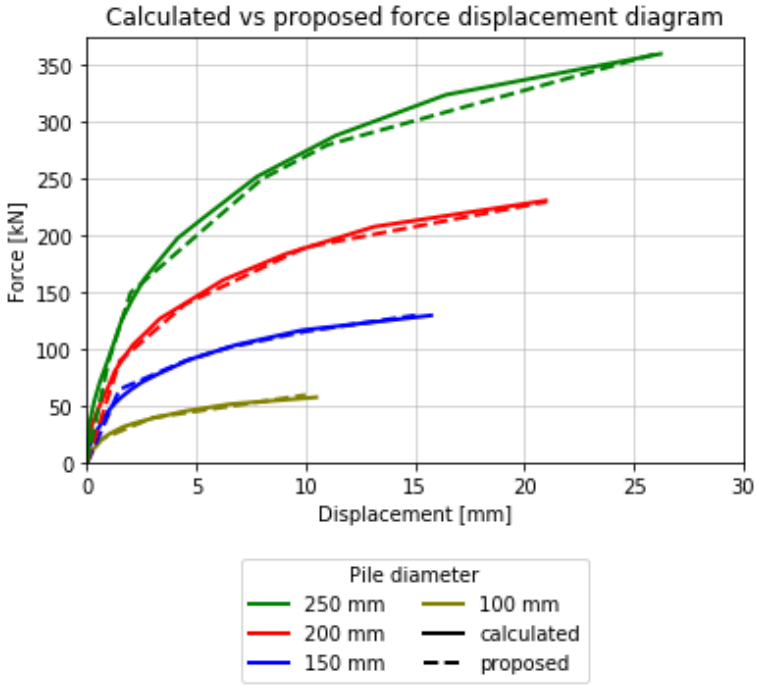

Figure 9.3: Force displacement diagram for non linear spring behaviour

9.4. Analysis method

The analyses in Diana is run in two load steps. First the own weight of the structure is loaded onto the model, secondly an additional distributed force is loaded on top of the masonry work in a separate load step.

Load step 1	**Load**	load name	own weight
		size	selfweight
		steps	1
	Equilibrium iteration	max number interations	100
		method	Newton Raphson
	Convergence norms	norm	force
		criterium	0.01
		norm	energy
		criterium	0.01
		satisfy both norms	yes
		no convergence	terminate
Load step 2	**Load**	load name	additional
		type	distributed
		size	200-500 kN/m
		steps	50
	Equilibrium iteration	max number iterations	100
		method	Newton Raphson
	Convergence norms	norm	force
		criterium	0.01
		norm	energy
		criterium	0.01
		satisfy both norms	yes
		no convergence	continue

Table 9.6: Analysis method

9.5. Results

The following sub-chapters will go into detail about the results found performing analysis in the longitudinal direction of the quay wall. Chapter 9.5.1 will present the results for the analyses to different pile capacities and the number of total affected amount of piles. Thereafter in chapter 9.5.2, the effects of the different material properties are studied. In chapter 9.5.3, the effect of the timber floor will be analysed by removing the floor, creating a stiff floor and a floor that has been split up in parts. Finally, in chapter 9.5.4, the effect of the post-peak behaviour of the foundation pile is presented. In appendix F a crack pattern is presented for reference and understanding, only the masonry is analysed without any constraints. These results show similar behaviour as found by (Grund, 2020).

The results in chapter 9.5.1 will be presented using both the absolute displacement of the quay wall and the relative displacements to the model using only foundation piles of 250 millimetres, the strongest setup. The results after this chapter will only contain the relative displacements since these represent the displacements due to a failing pile foundation.

For all chapters containing results, the first analysis will be on the vertical displacement of the quay wall. The displacements in the figures are measured at the centre, the top point of the wall. The different displacements can answer which parameters have the most influence on the behaviour of quay walls.

Besides the displacement, there are figures containing the stress development in the masonry wall; these figures help to answer the question: how do forces distribute in masonry work in failing conditions of a quay wall?

9.5.1. Influence of pile capacity and affected amount of piles

This section shows the results obtained from the analyses performed for a masonry wall setup with medium strength masonry, various pile diameters and a various amount of affected piles.

In figure 9.5 on the next page, the force-displacement curvatures are presented for a total of 20 different setups. The figure on the rights side presents the amount of pile that are failing under the quay wall, starting from a single pile to eventually seven failing piles. The graphs on the left side, present the absolute vertical deformation of the quay wall, the graphs in the middle show the displacement relative to the displacement of the model using only 250 millimetres foundation piles. This is done exactly as in chapter 8, where the cross-sectional results are discussed. Due to the modelling of the pile foundation as springs, the quay wall will deform even when all piles modelled, use the strongest force-displacement diagram. By presenting the relative displacements, only the displacements due to the failing pile foundation are presented.

What can be observed from figure 9.5 and especially for the results of the top three graphs representing the failure of a single pile, three piles and 5 piles in a row, is that the piles modelled with a weaker force-displacement diagram have a horizontal jump, to the line where no timber piles are modelled (grey), in their curvature. After the jump, the displacements follow the line which is representing the displacement when no piles are modelled. This horizontal jump in the displacement curve represents the point where the foundation pile fails, and the functioning surrounding piles have to take over.

This effect is less visible for the curvature representing a 200 mm pile and for all lines in the model where seven piles have a weaker pile capacity. If the reaction forces in the piles are analysed, see figure 9.4, it is concluded why for the 200 millimetres pile curvature the jump is not possible. In the example of figure 9.4, three piles are modelled weaker than the strong 250 millimetres pile. On the left side, the reaction forces at pile A are presented, for models using no pile to a 200 millimetres pile. On the right side, the reaction forces for pile B are presented; this is the first 250 millimetres pile.

It is noticeable that when the maximum pile capacities are reached for the 100 and 150 millimetres pile lines at location A, the pile at location B is not at the piles maximum loading capacity and the line jumps to the line without a pile foundation. Pile B reaches its maximum loading of 360 kN at a distributed force of 220 kN. When the 200 millimetres pile hits the maximum load of 225 kN at a distributed force of 250 kN/m, this is already over the maximum loading that pile B can absorb, so pile B fails, which leads to failure of all piles and divergence of the analysis. When the number of piles with a defect is at seven, the jump is not possible for all pile configurations. It is recommended to model the quay walls without piles instead of piles with a lesser force-displacement diagram.

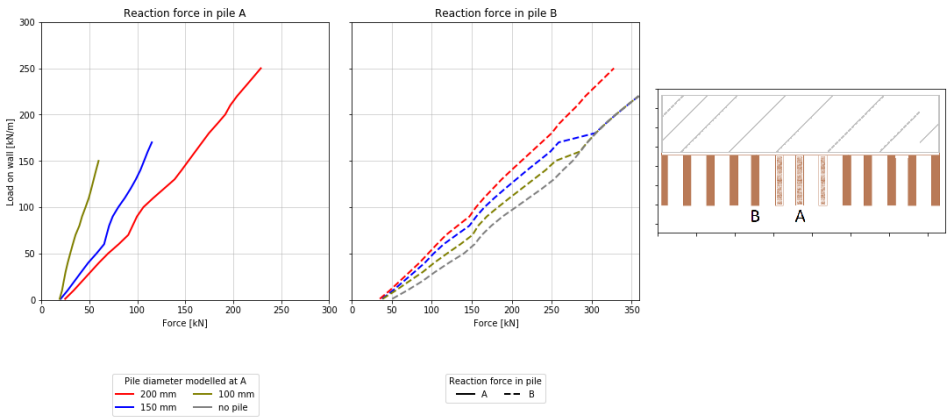

Figure 9.4: Reaction forces under the quay wall for different piles

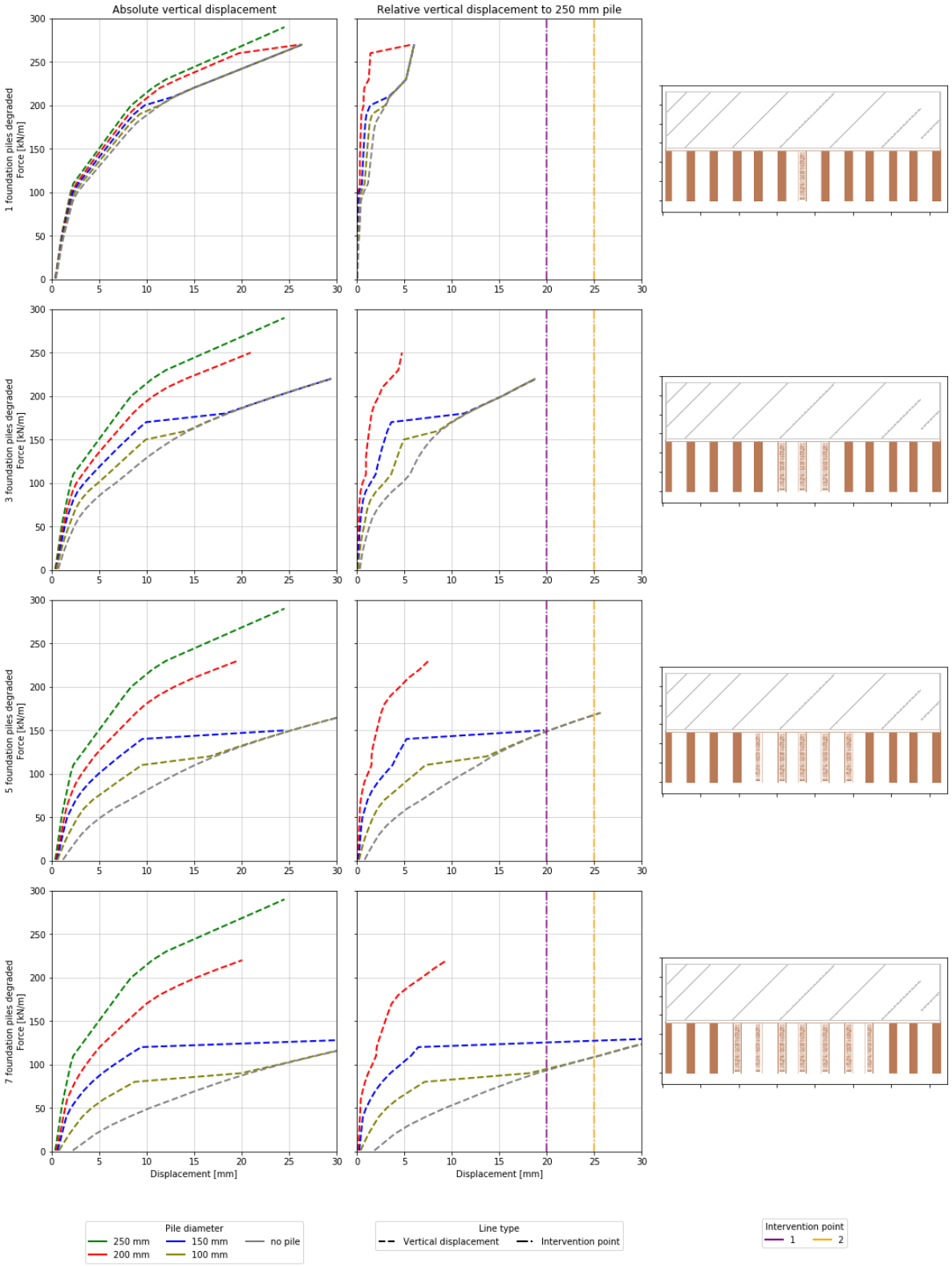

Figure 9.5: Vertical displacements for various pile capacities and affected amount of piles

To answer how forces distribute under a failing pile condition figure 9.7 displays the stress distribution for two different models, in appendix G the same figure can be found in colour. Since the results are symmetric, for both models, half the results are presented side by side to compare easily. The left side results represent a model where the three piles are modelled with a 200 millimetres pile, and the results on the right side represent a model where three piles are not modelled at all.The models' results using piles with 150 or 100 millimetres piles end up with the same stress distribution as the model were the piles are gone, just like were the displacements go to the same values as the models without piles.

In figure 9.7 tensile stress is presented in red and compression in blue. At every row the load on top of the quay wall is increased, the steps presented are for 1: own weight of the quay wall, 2: 50 kN/m, 3: 100 kN/m, 3: 150 kN/m, 4: 250 kN/m left and 220 kN/m right.

Observed are two different patterns. For the model without piles, there is tensile stress present from the first load step stretching over the full length of the quay wall, which is not supported. This tensile strength is present in the masonry as well as in the timber beam, the effect of this is studied in chapter 9.5.3. When the loads increase the zone under compression is increasing until the point where a full compression arch is formed.

The stress distributions for the models on the left side of figure 9.7 are primarily for the tensile stresses different. There is also an arch present in compression, but due to the supporting piles, the arch in compression is less. However, the tensile stresses form not over the full length but only in between the supporting piles. This has consequences for crack formation. See figure 9.6 for the final strain at the moment before the failure of the quay wall.

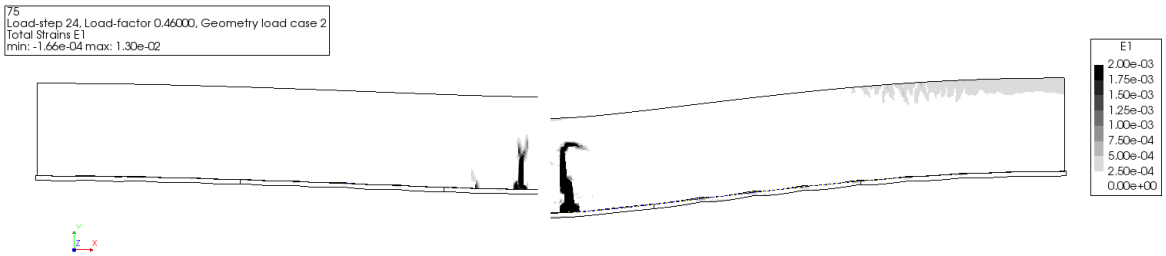

Figure 9.6: Final strain for three piles modelled as 200 mm pile (l) and no piles (r) at maximum load.

Figure 9.6 might give the impression that for crack development, both models behave similarly. But the occurring strains on the rights side start at a distributed force of 90 kN/m, and for the left side, this starts to develop around 200 kN/m just before the models start to diverge due to the overloading of the maximum pile capacity.

To conclude, the results show a different force-displacement curvature, but for weaker piles, the final displacement is similar to the analysis modelling no piles. For crack propagation, it is observed that modelling weaker piles results in smaller cracks than running an analysis using no piles.

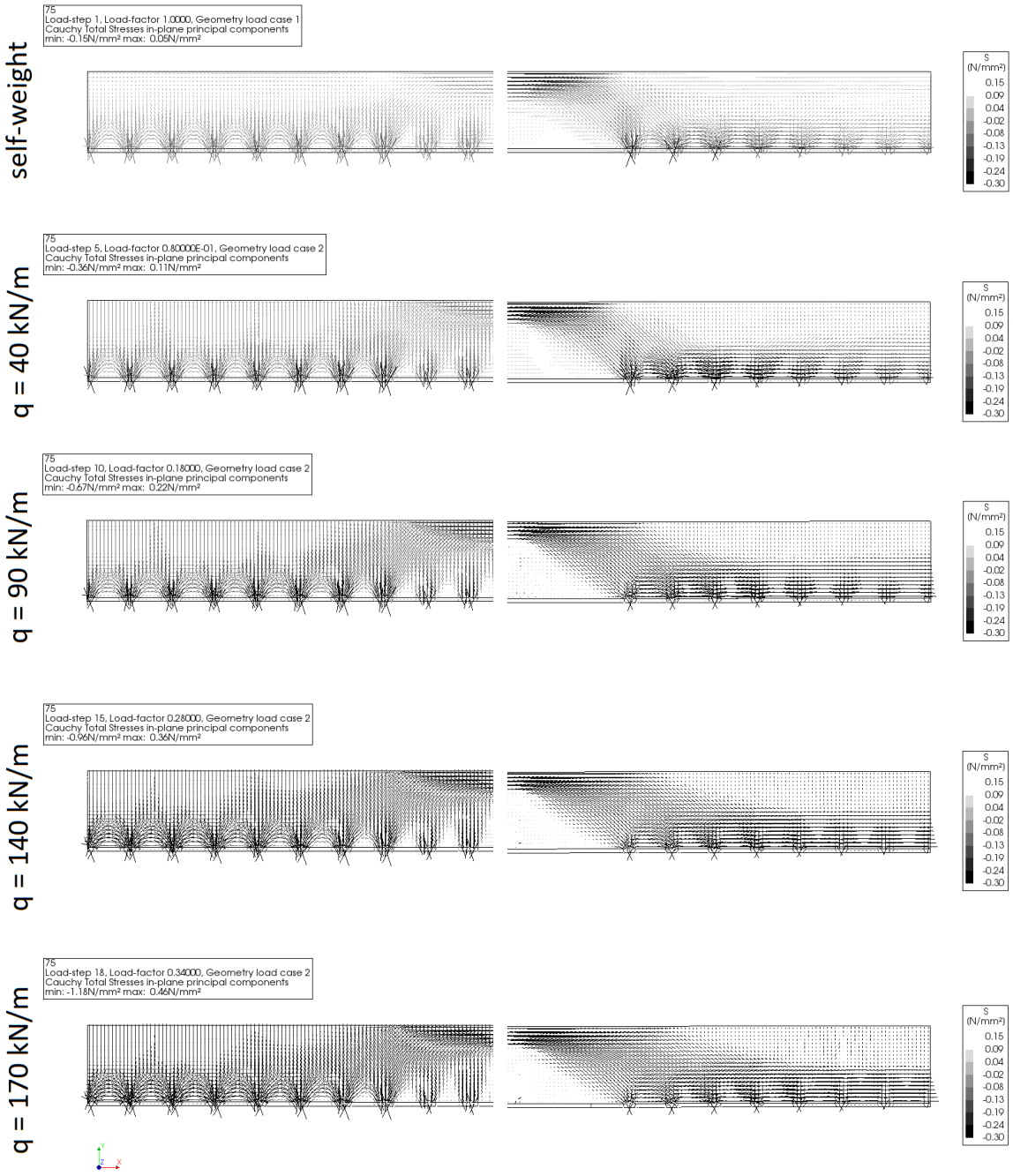

Figure 9.7: Stress distribution for three piles modelled as 200 mm pile (l) and no piles (r) under a increasing load.

9.5.2. Influence of material properties

This sections shows the results obtained from the analysis performed for three different masonry configurations as specified in table 9.4. Similar as in previous chapters, the results presented in figure 9.9 display the behaviour of the quay wall for various pile diameters, with one, three, five and seven pile defects. The absolute displacements are not presented since the relative displacements due to pile defects are most relevant.

The results in figure 9.9 show that for the strong and medium masonry configurations the displacements curvatures follow similar paths. Especially prior to the pile failure, the displacements are equal. After the pile failure and for the models containing no pile support, the deformations are governed by the material quality. From a growing foundation defect over the length of the quay wall this displacement difference starts to grow.

Secondly, what can clearly be observed from figure 9.9, is the difference in displacement for the weaker masonry configuration compared to the two other configurations. If in figure 9.9 the results of 3 failing foundation piles for weak masonry are observed, the jump in displacement from the 100 millimetres pile diameter curve to the curvature without a pile foundation occurs at a lower load, 70 against 150 kN/m. The explanation for this is the tensile strength of the materials and the crack propagation. In figure 9.8 the strains in the masonry for the weak and medium masonry configuration are plotted. This displays a strain development for the weak masonry configuration and none for the medium masonry configuration.

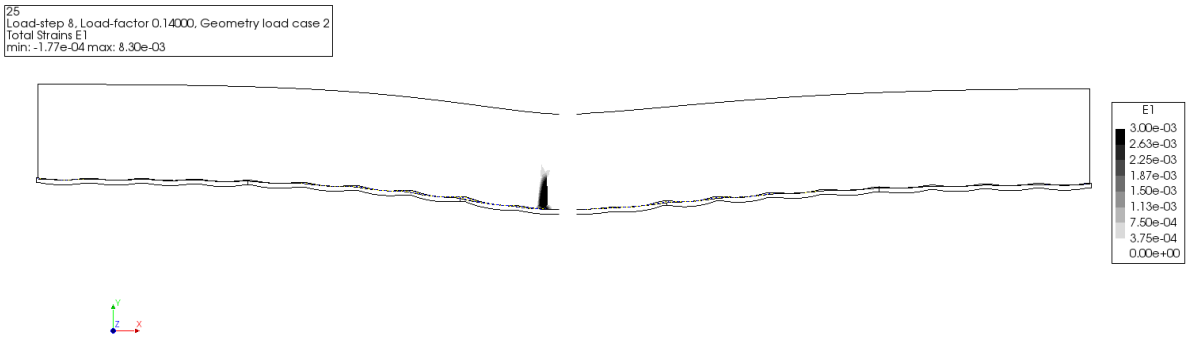

Figure 9.8: Strain at 70 kN/m for weak (l) and medium (r) masonry configurations

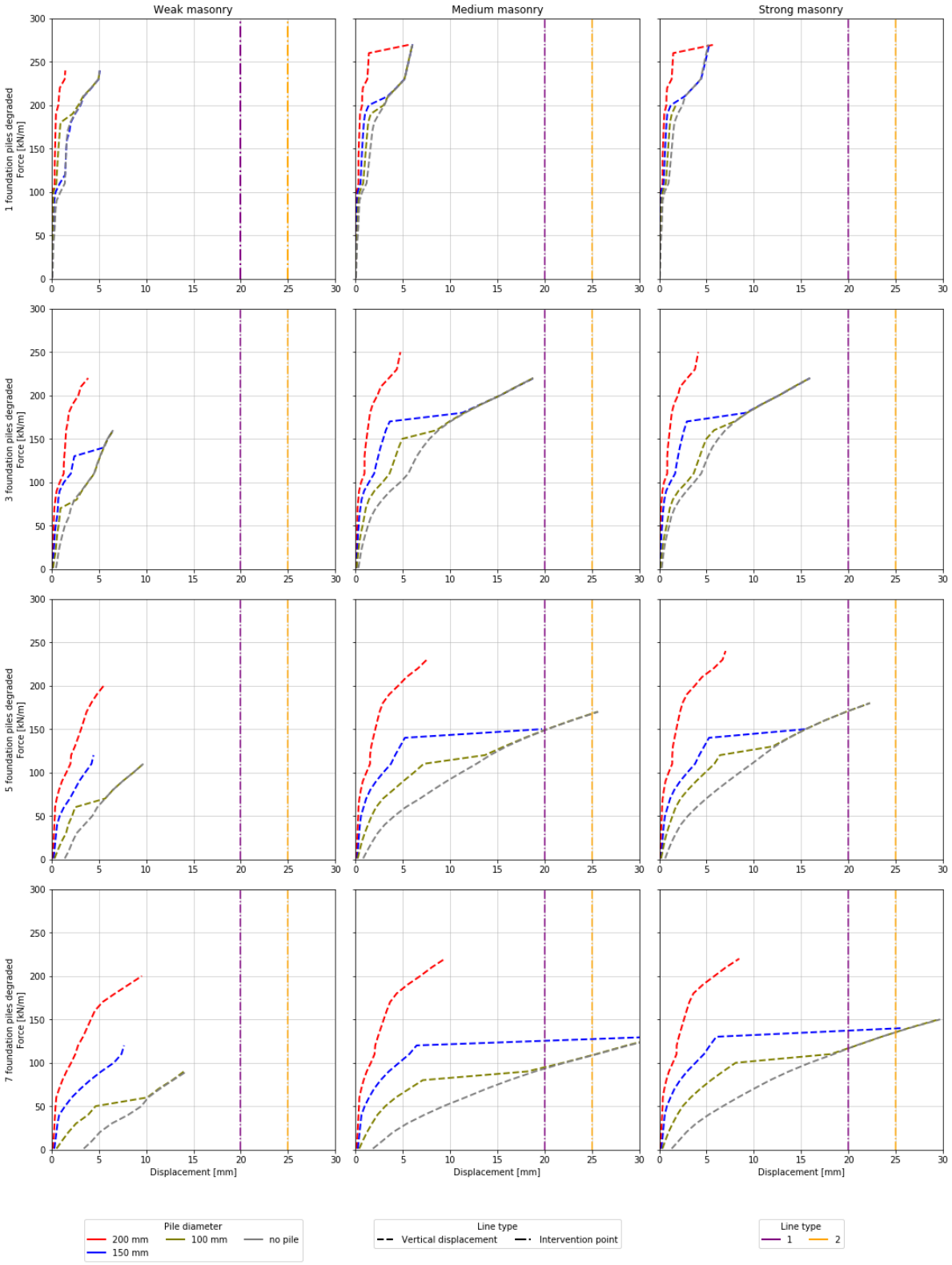

Figure 9.9: Vertical displacements for various masonry properties

9.5.3. Influence of timber floor design

As observed in chapter 9.5.2, tensile stress develops at the bottom of the masonry and in the timber floor. The observed cracks are the direct result of the tensile stress at the bottom of the masonry. This chapter focuses on the effects this timber floor has on the quay wall system.

Figure 9.10 presents three different floor modifications. In the longitudinal analysis, the options of no floor and the continuous floor are used. Second to that, the continuous floor is analysed using a higher stiffness for the timber. In figure 9.10, the top sketches represent the top view of the floor and the bottom sketches the front view. Presented on the far right, the continuous floor used in the analyses before. Here the floor elements are overlapping over the length of the floor. For this setup two different stiffnesses of the timber floor are compared. Secondly, on the left, the floor is removed from the model, and the piles are connected directly to the masonry.

Finally, in the middle, a split up in the floor elements of 5.5 metres long is used. Here the floor element is continuous over the depth of the floor. The results can be found in appendix H, the results differ significantly compared to the two other models. After discussions, it is concluded that this setup of the model is, from an engineering point of view, inefficient and not logical to be found in Amsterdam.

no floor, split floor, continuous floor

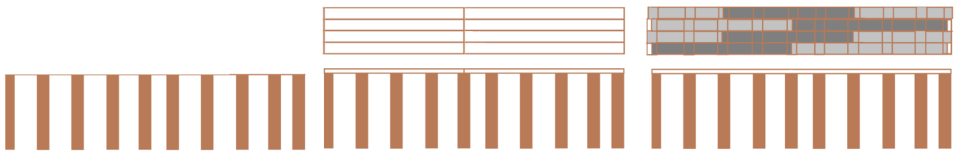

;

Figure 9.10: Sketches for timber floor setups

Figure 9.12 presents the results for the different floor setups. Directly notable is that the displacements for a quay wall system containing a stiff floor connection (both setups) or no floor are similar. When the strains are observed, the removal of the timber floor results into a different strain formation. Figure 9.11 displays the strains of the models were 5, 150 millimetres piles were modelled. It can be concluded that the cracks start similar to a vertical crack in both models. When the floor is removed, the crack development results in a horizontal crack at the tip of the vertical crack. The model using the timber floor does not form this horizontal crack but a second vertical crack propagates.

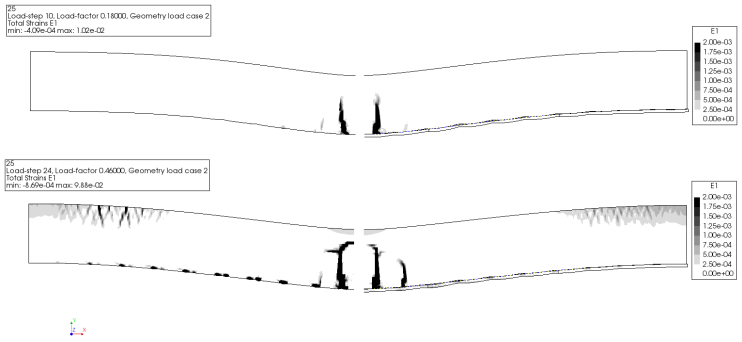

Figure 9.11: Strain for model without the floor elements (l) and with floor elements (r)

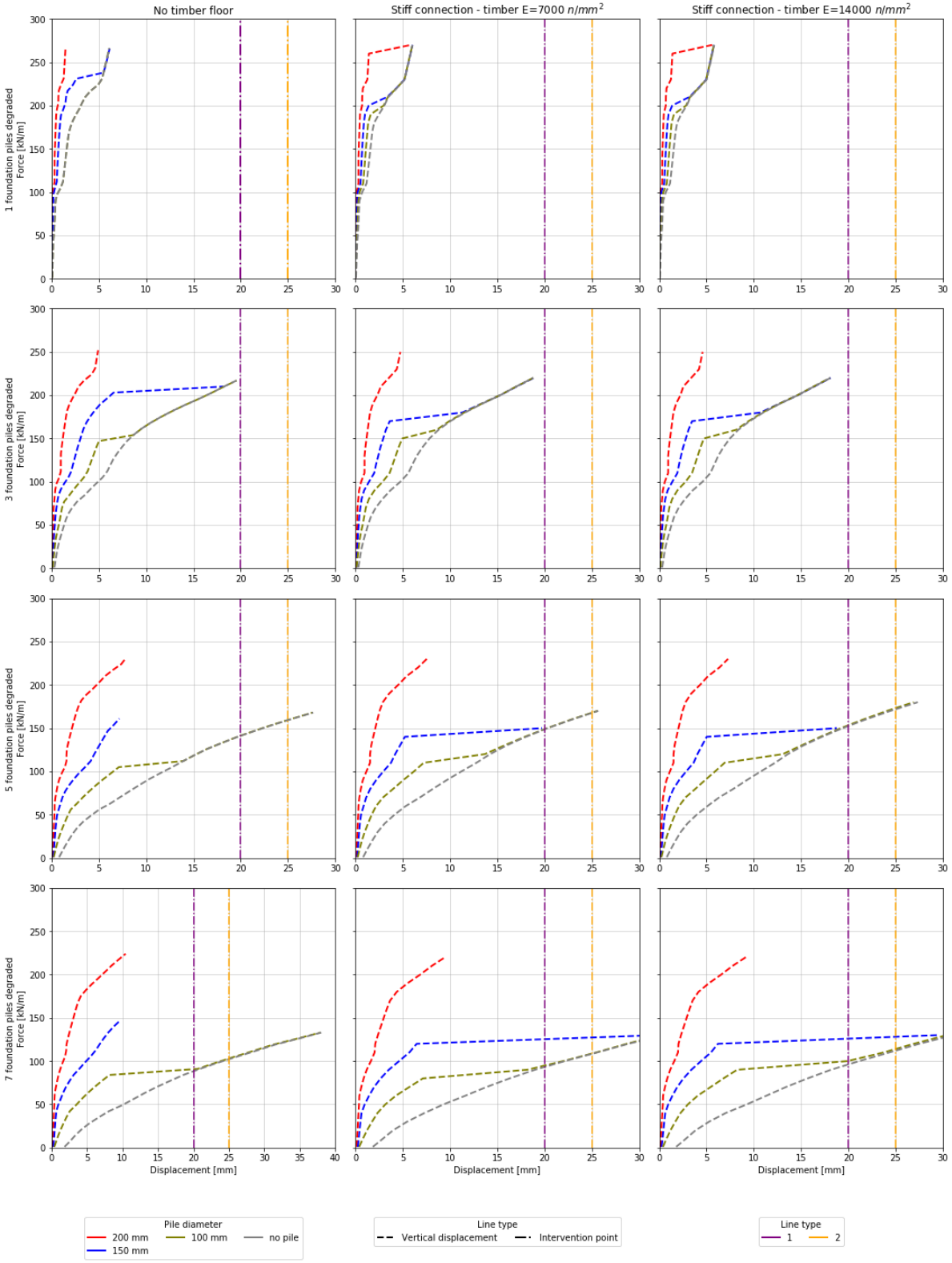

Figure 9.12: Vertical force-displacement diagrams for various floor setups

9.5.4. Influence of post-peak behaviour foundation pile

This section covers the results obtained from the analysis performed for two different types of pile failure. In results presented before, it is found that the model has difficulty with the abrupt failure of the pile foundation. A second post-peak pile behaviour has opted to study the significance of this abrupt failure.

Figures 9.13 and 9.14 are added to discuss the relevance of the post-peak pile behaviour in the setup of the model. Schematised on the left side is the basic situation of a solid pile connected to the timber floor. One step to the right, due to rotting, the top part of the timber is degraded and contains a smaller pile diameter. The third sketch presents the modelling strategy, over the full length of the pile, the reduced pile diameter is assumed to calculate the force-displacement diagrams for different pile diameters, see figure 9.14 on the left side.

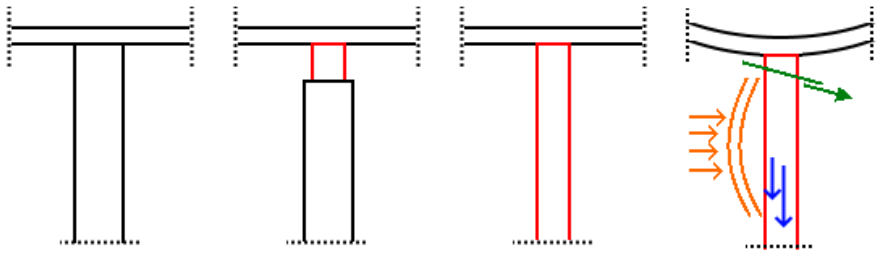

Figure 9.13: Sketches of the defected timber foundation pile to floor connection

Then, for the final sketch on figure 9.13, due to loading, the timber floor is deformed to the maximum deformation, and the foundation pile fails. Three possible failure mechanism can occur, brittle failure (green line), the connection fails, and the bearing capacity reduced abruptly to zero, see figure 9.14 right side. Secondly, plastic failure, (blue line) figure 9.13, the connection remains intact; the pile is loaded to its maximum capacity, continuous deformation without absorbing extra loads, see figure 9.14 plastic failure line. Finally, quasi-brittle behaviour, the orange mechanism in figure 9.13 and force-displacement curve in figure 9.14, where the pile continuous to deform under a reduced maximum bearing capacity.

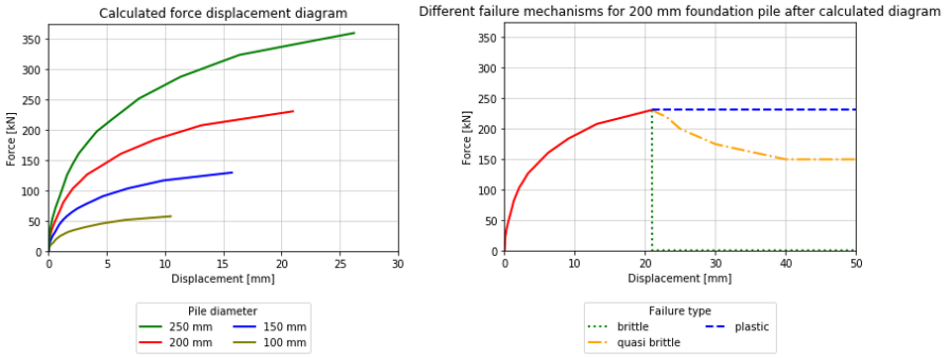

Figure 9.14: Force-displacement curvatures for the post-peak behaviour of the pile configurations

The quasi-brittle behaviour is hard to predict, so the remainder of this chapter focuses on the difference between the brittle and plastic failure of the pile foundation. The brittle failure mechanism was used in the previous chapter, resulting in jumps for the displacement in the quay wall. Figure 9.15 presents the results for both post-peak behaviours of the foundation piles.

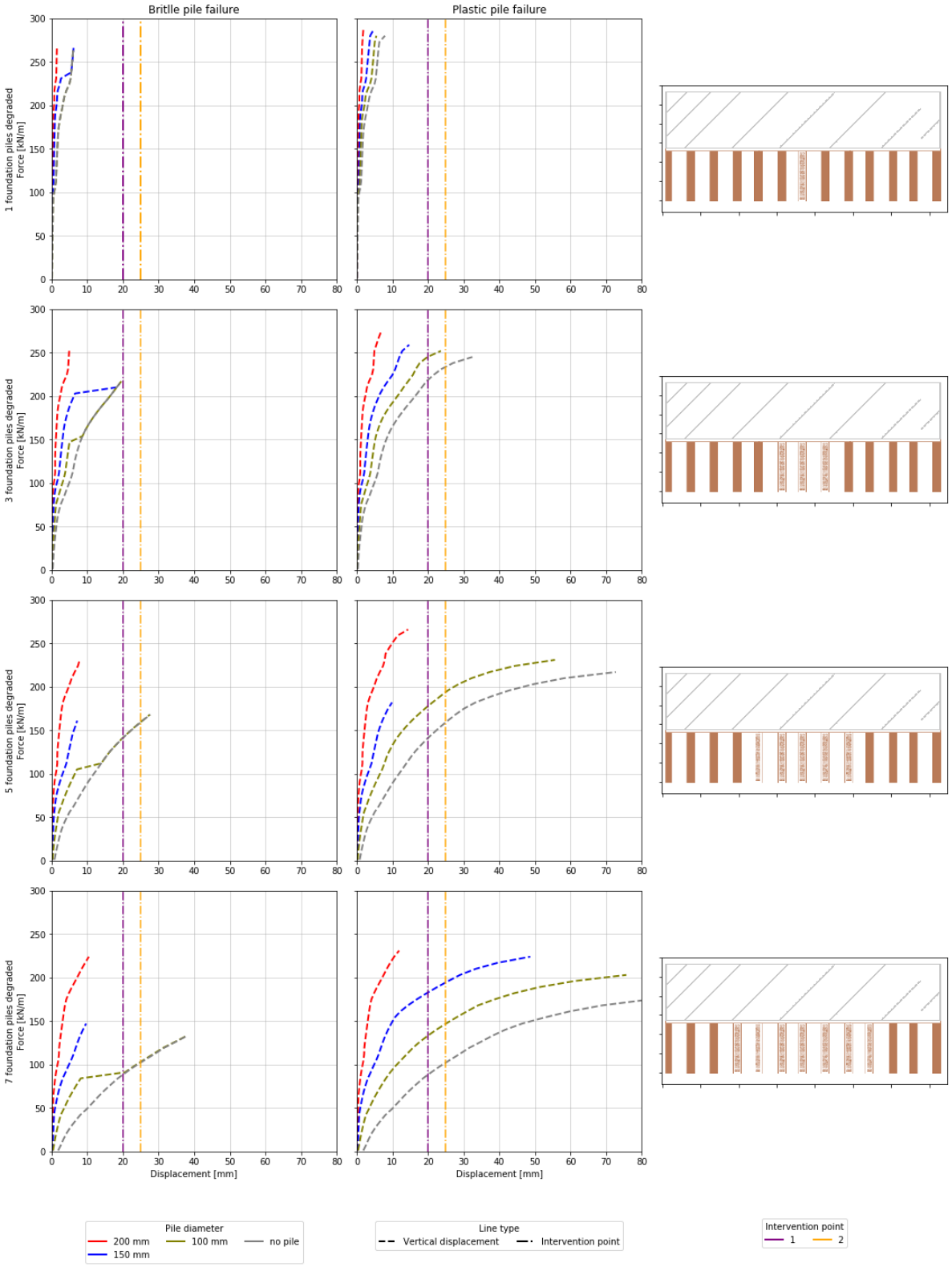

Figure 9.15: Vertical force-displacement diagrams for brittle and plastic failure mechanisms for foundation piles

Figure 9.15 displays significant differences in the force-displacement curvatures. The observed vertical jumps in displacement only occur for brittle pile failure. The plastic post-peak pile behaviour results in a continuous deformation of the quay wall. Since for the failure of three piles, the displacement jump is visible, the reaction forces in the piles are examined for both failure mechanisms in figure 9.16.

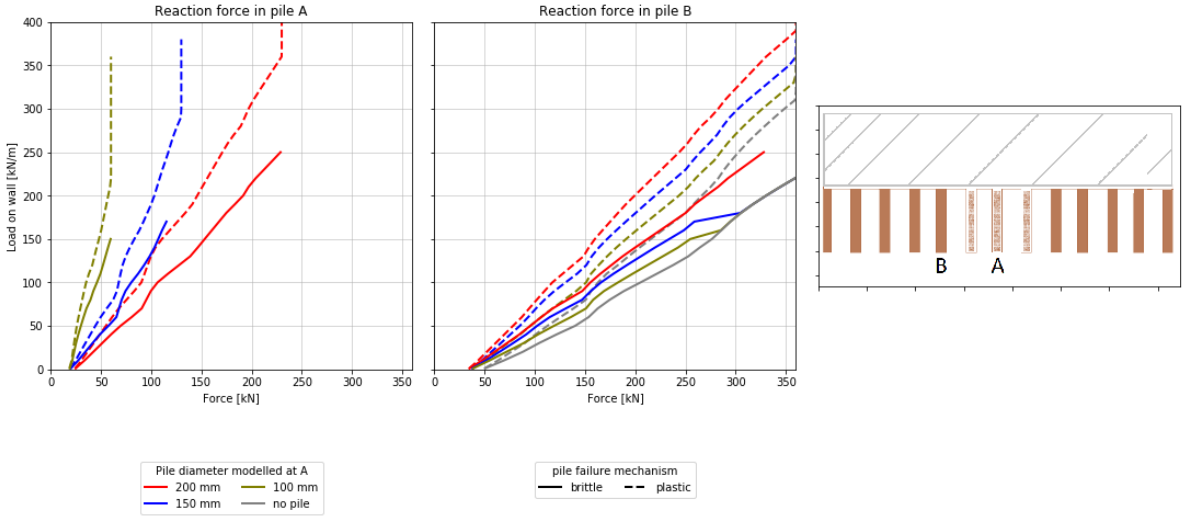

Figure 9.16: Reaction forces in pile foundation for brittle and plastic failure mechanisms

The presented figure concludes that for brittle failure, the pile forces for the functioning surrounding piles (B) reach their maximum bearing capacity in an earlier stage and this will lead to a domino effect of failure. When a plastic failure mechanism is modelled, loads are spread more evenly. This jump in vertical displacement results in a horizontal crack at the tip of the already formed vertical crack, see figure 9.17. Here, the masonry strains are plotted, for both models, the displacement is exact at 7.1 millimetres before the foundation failure, directly after the brittle failure, the difference in displacements between both models is 6.7 millimetre and a horizontal cracks start to develop.

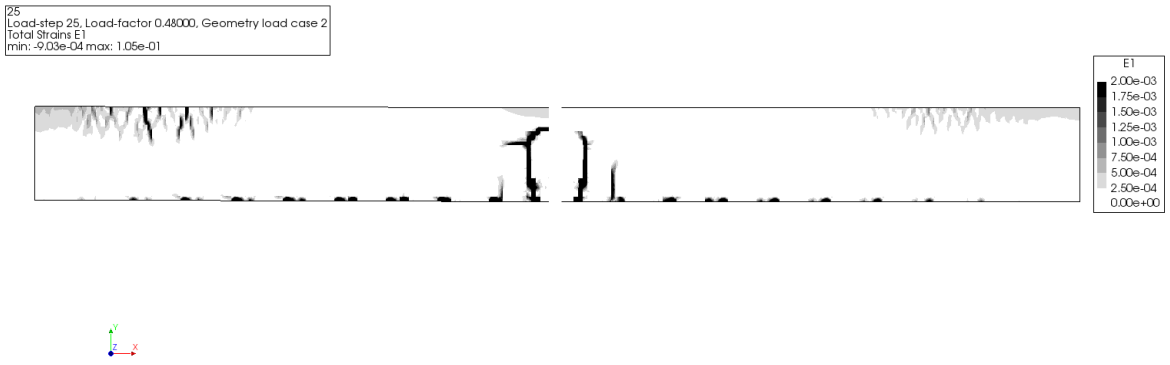

Figure 9.17: Crack development for brittle (l) and plastic (r) pile failure

9.6. Conclusion

This chapter concludes that in the longitudinal direction of the quay wall there is a hidden structural capacity compared to the cross-sectional direction. By removing a single foundation pile, the masonry combined with the floor distributes the forces to the functioning foundation piles.

It is found that the scale of the foundation defect over the length of the wall contains the most significant

influence in the behaviour of the quay wall in terms of displacement and crack formation.

The connection between the timber floor and foundation pile is an important indicator for the crack development and the redistribution of forces. When this connection remains intact, the area of the masonry wall in tension is divided, resulting in multiple smaller cracks between piles. When piles fail brittle, or when there are no piles modelled, the models result in a single or two large cracks.

The analyses on material properties show that the influence of the Young's Modulus in combination with the tensile strength and crack energy, is significant for the weakest configuration. Displacements evolve faster, and cracks develop at lower displacements. The maximum observed displacement before the model its divergence, is significantly lower than the displacements found for the medium and strong masonry configurations. Finally, for the weak masonry configuration, the model diverges due to the crack development at displacement levels lower than the intervention points set by the municipality.

The research to the effects of the timber floor concludes that modelling of the floor results into a different stress distribution. The floor combined with residual strength in the timber piles results in multiple smaller cracks in contrast to the concluded larger and horizontal cracks when the timber floor is removed. The researched Young's Moduli of the timber floor have no significant influence on the vertical displacements of the quay wall.

Finally, the results to the post-peak behaviour of a failing pile foundation conclude a beneficial effect when a plastic pile failure mechanism is used. However, if figure 9.13 is interpreted correctly, brittle failure of foundation piles would be expected when the connection to the timber floor is in poor condition due to rotting. It is unclear how the connection fails precisely, but for foundation piles in good condition (250 and 200 millimetres), it is beneficial for the analysis to model a plastic failure mechanism. For the weaker pile, 150 millimetres, it is proven that the model can function using a brittle failure mechanism; the brittle failure results in a vertical displacement jump, and this consequently results in a horizontal crack in the quay wall.

10

Discussion

In the performed research, assumptions are made and simplifications applied due to various reasons. The choices made influence the results of this research. In this chapter, the most critical assumptions and simplifications are discussed, and the effects of these decisions are elaborated.

- In this research, it is assumed that the only occurring failure mechanism is the structural failure of the timber foundation pile. The structural failure of the foundation pile is observed in Amsterdam. However, it is also found that multiple failure mechanisms are observed simultaneously. The order in which this is evolving is assumed to be, first the failure of the foundation pile after which other failure mechanisms develop like, masonry cracking or tilting of the masonry wall.

  If different failure mechanisms had been analysed, like the structural failure of the kesp or timber floor, the displacement and structural behaviour of the masonry wall would differ.

- The thickness of the piles is considered to be even over the full length of the pile. In reality, the thickness measured at the top of the pile would differ from the bottom of the foundation pile, due to tapering, the top would be thicker than the bottom. In this research, the piles are considered an input parameter. The analyses are focused on the behaviour of the masonry wall, an additional study to the state and reaction forces in the timber piles is needed to study the effect of a varying pile diameter of the length of a pile.

  A second assumption is made about the piles and the connection to the timber floor. It is assumed that this connection is still intact, and only the connecting pile diameter is affected. In practice, however, this connection can be entirely gone for various reasons; for that reason, the option without a foundation pile is studied.

  A final simplification about the piles is that they only support the quay wall system in the vertical direction. For the analysis in both directions, but especially in the cross-sectional analysis, using a lateral constraint for the timber pile would be more correct.

- The masonry is modelled using a macro model. This means that the brick and mortar are not modelled separately but by using a smeared material based on the material properties of both brick and mortar. Additionally, by making use of symmetry in the affected number of piles, unrealistic scenarios are created. In practice, the cracking in brick and mortar would not develop as symmetric as the obtained results. More logical is that one crack would develop and another would stop.

  The solution to this would be to run a micro model of the masonry wall. With this method, the brick and mortar are modelled as two different materials and connected by interface layers. The downside is, there are more parameters to analyse, and the computational time and data storage would rise. It is

debatable, considering the magnitude of the problems in Amsterdam, whether a micro model would be beneficial.

- The chosen masonry model, the Total Strain Rotating Crack Model (TSRCM), is considered to diverge sooner than other models like the Engineering Masonry Model (EMM). This is studied by (Grund, 2020). By choosing the EMM, the anisotropic behaviour of the material could have been implemented. In this research, with the chosen TSRCM, masonry is considered as an isotropic material.

  However, the TSRCM can be used in 3D models, since this was the goal of the research at the start, the TSRCM was chosen. To conclude, the results could have represented masonry better when the Engineering Masonry Model would have been used. The results in this thesis can, however, be used as a reference for a 3D model using the Total Strain Rotating Crack Model.

- The performed analyses are done in a 2D regular plane stress model. The thickness and the already discussed anisotropic behaviour are not taken into account. By doing so, a second simplification, that a masonry wall is a single wythe (a vertical layer of the wall, with one brick thickness), is implemented. In practice, the masonry wall is about 800 millimetres thick, containing multiple wythes of bricks. While the stacking of the masonry alongside the wall is visible, it is not visible over the depth of the wall. The material strength, cohesion and interaction of bricks and mortar can vary in the depth of the wall.

  For these 2D analyses, these assumptions are necessary, but in a 3D study, this effect can be modelled. There are experiments required to obtain knowledge on the behaviour and structure of masonry over the depth of the wall to model the quay wall in 3D.

- At the beginning of the thesis, simplifications have been made on the timber elements. The kesp and sloof are not modelled as elements. The timber floor was modelled as a continuous element and considered as linear elastic. In a later stage, this timber floor is split up in part to analyse the benefit in the distribution of tensile forces in the quay wall system. When analysing this it is assumed that either the floor works as a tensile beam, or the floor has no function at all.

  The decision to not implement the kesp and watersloof into the model affects the results. For the 2D cross-sectional analysis, not modelling the watersloof resulted in the removal of the horizontal constraint and the sliding of the masonry wall as a whole. To counter the effect of the sliding, the quay wall was modelled with a direct node-to-node connection. Modelling the kesp would have been beneficial for the vertical stability in the cross-sectional analysis since this is a thicker beam than the timber floor and would deform less. However, it was chosen to model the same elements in both models. The kesp would not have been present in the longitudinal analysis.

- To ensure that displacements occur in the model, a distributed load is enforced on the top of the quay wall. This type of loading results in a displacement that is also evenly distributed over the full length of the wall. While this is a possibility to model the effects of a failing pile foundation, it does not take into account the actual loading in practice, where lower dynamic loading by traffic and due to that cycles of loading and unloading occurs.

  In the model point loads are not taken into account; these point loads would represent trees or parked cars along the quay wall. In practice, these point loads at the location of a foundation defect result in higher displacements; that is why one of the controlling measurements is the removal of parking spots and trees. This study has not focused on this type of loading.

- It is found that the municipality of Amsterdam measures the quay walls monthly. To ensure the stability observations are done to the horizontal and vertical displacements. There are two intervention points; after the quay walls displace 20 or 25 millimetres in either direction, control measures have to

be placed. In this research, these values are used as reference points in the result sections to put a perspective on the severity of the displacements found.

The reference points are used as indicators on the severity of the displacements in both directions. Due to the modelling strategy of a 2D analysis in respect to the actual 3D quay wall, the observed displacements might pass the reference points under an earlier load or state of foundation defect than it would in practice. This is observed best for the horizontal displacements in the cross-sectional analysis where the resulting displacements out-scale the intervention points. To counter this, the longitudinal model represents displacements values in the norm of the intervention points but does not take out of plane loading into account.

- Finally, the research focused on two 2D directions of a quay wall, the cross-sectional and longitudinal, see figure 10.1 (l) and (m). The cross-sectional results presented instability issues and tilting of the masonry wall as the failure mechanism. The longitudinal model presents multiple indicators for hidden structural capacity which are not visible in the cross-sectional direction. However, the longitudinal analysis does not take out of plane loading into account. This results into a model which can not tilt and examines the cracking behaviour of the masonry. Ultimately it would have been beneficial to study the top view (10.1 (r)) as well, the boundaries for tilting could have been analysed and implemented into the study. By doing so, it would have provided knowledge on a turning point, where the longitudinal analysis would have transferred into a stability issue presented in the cross-sectional analysis.

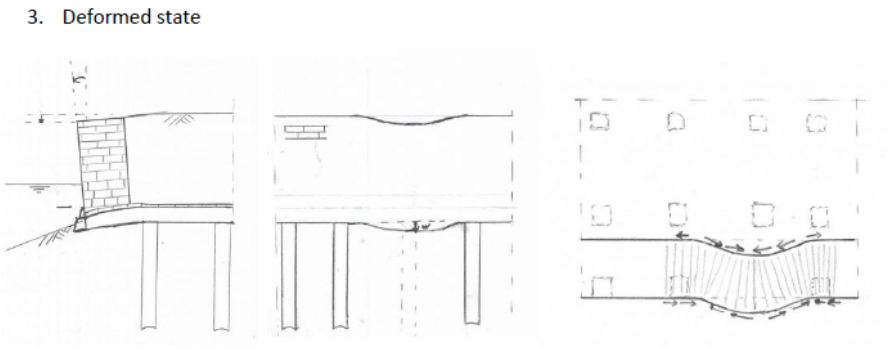

Figure 10.1: Deformed stage of quay walls under the condition of a partly failing pile foundation. (l) cross-section, (m) longitudinal section and (r) top view.

11

Conclusions and recommendations

The city of Amsterdam contains about 1600 bridges and 600 kilometres of quay walls. Of these walls, about 200 kilometres are of masonry walls placed on a timber floor and founded on timber piles. These quay walls are sometimes over 100 years old. Due to the increasing loads in the past century and the degrading of material properties in the masonry wall and timber elements, the quay walls are in bad shape. In recent years the number of quay walls failing in Amsterdam has risen. When designing a quay wall, most of the times, a cross-sectional analysis is used to calculate the desired dimensions to withstand the loads. When this calculation is performed on a quay wall which is already over 100 years old containing a failing pile foundation, the quay wall should fail. However, many of the quay walls under the condition of a partly failing foundation, are deforming, but still standing.

The main objective of the research, as formulated in chapter 1.3, was:

Obtaining more insight into the structural behaviour of quay walls by looking at the redistribution of forces in multiple directions of the quay wall system when it is partly failing.

It can be concluded that the finite element models created in this research fulfil the objective. However, it is found that the quay walls in Amsterdam behave as a complex system, the conclusions made in this chapter are for a specific set of parameters and limitations discussed in chapter 10. Before concluding on the main research questions, the sub-questions will be answered.

11.1. Conclusions

11.1.1. Sub-research questions

How to model the failure mechanism of a (partly) failing pile foundation of a quay wall?

Chapters 2 to 7 give an overview of the literature study to answer this questions. To model the effects of the failure mechanism, a model is created using the following elements: the masonry work gravity weight wall, the timber floor and timber foundation piles. A model containing as few components as possible is created, and only the components present in both the longitudinal and cross-sectional section of the quay wall are implemented. In literature, it is found that the timber beam between the foundation piles and the floor does not have to be modelled when it is assumed that the beam is not displaced horizontally (so for this failure mechanism neglected). The effects of the horizontal displacement constraint in the quay wall, the waterloof, can be modelled in the cross-sectional analysis as an increased cohesion between the masonry and

timber floor, which results in higher shear stresses before the masonry would slide off the timber floor.

For the elements modelled, the timber foundation piles and floor, and masonry wall, literature provided material properties. Since there is no data available for the masonry properties in Amsterdam, data found from tests on masonry in Groningen is used. These masonry studies provided material properties for clay bricks from before 1940 and came closest to the masonry in the Amsterdam quay walls. It is chosen to model the masonry of the wall using a macro model with smeared material properties instead of modelling the brick and mortar as separate elements. To model masonry, the Total Strain Rotating Crack Model is used. The advantage of this model is that it can be used in a 3D analysis to continue research on quay wall systems. During the research, a report came out that the Engineering Masonry Model provided more accurate but similar results for 2D analysis on masonry (Grund, 2020).

Literature provided that the pine and spruce are used in Amsterdam as timber elements in quay walls. In the reference case at the Groenburgwal, it is found that the floor is made of pine, which is modelled using the lowest strength classification found in Amsterdam C14. There is no data known about the interface between the timber floor and masonry wall, which would be a layer of mortar. Results from an experimental study, where the angle of friction and cohesion of brick and timber were studied, are used. This cohesion and angle of friction are modelled as a Coulomb friction interface between the masonry and timber elements.

The last element to model the failure mechanism is the foundation pile. It is found that the timber piles are made of spruce and for quay walls are founded in the first sand layer of Amsterdam at about -8 meters N.A.P. With the method of Koppejan, the shaft and base resistance of a timber pile are calculated for various pile diameters from 250 till 100 millimetres. The base resistance is about 90 to 95 per cent of the total bearing capacity The decision is made to only model the base resistance using a non-linear force-displacement diagram. By using various pile diameters as input data, the importance of a reduced foundation pile is analysed in the models.

How do forces distribute in the masonry work of a quay wall in failing condition?

The answer to the sub-question is split into two parts, this since the effects of the failing pile foundation are studied in the cross-sectional and longitudinal direction.

Cross-sectional analysis
For the cross-sectional direction, tilting of the quay wall system and sliding of the masonry wall in the horizontal direction are the occurring patterns. Three different interface conditions between the masonry and timber floor are analysed and concluded is that a direct node-to-node interface would represent the most realistic results. Using the node-to-node interface condition, the model could endure the horizontal soil pressure. Due to the stiffness of the connection, tensile stresses develop into horizontal cracks at the location of this interface between the masonry wall and the timber floor.

The decision to not model the horizontal displacement constraint as an element but as an additional cohesion did not prove to be a realistic modelling option since values for the horizontal displacement rose significantly. Because the sliding of the wall occurs separately from the floor, there is no build-up in tension, and there will be no crack development at the interface condition.

For all researched interfaces, the relation between a decrease in pile diameter (bearing capacity) and in an increase in displacements is found. It can be concluded that from the point where the first pile row reaches its maximum bearing capacity and the vertical restraint dissolves, the quay wall starts to tilt. When the problem is analysed without the presence of a first pile row from the start of the analysis, tilting occurs directly.

Finally, it can be concluded that modelling the quay wall in the cross-sectional direction provides little insight into the redistribution of forces in the masonry of the quay wall. It is observed that the problem develops into a stability issue and without the constraints in the masonry wall the model tilts over.

Longitudinal analysis
In the analysis of the longitudinal direction, only the vertical displacements are analysed. In the analysis in this direction, only the first pile row is modelled. It can be concluded that after pile failure, the piles on the sides absorb the additional loads. By increasing the number of piles that show a defect, it is observed that the first fully functioning piles on the sides, absorb most of the loads.

In terms of displacement, it can be concluded that for a single pile failure the maximum vertical displacement found is less than 10 millimetres, noted that this only occurs at loads close to maximum bearing capacity of the foundation piles (275 kN/m) and therefore unlikely to occur in practice. Furthermore, it can be concluded that by increasing the deflected amount of piles, the deformations increase as well and consequently the crack development.

It is found that an arch in compression is formed in the wall, between the first modelled piles without any defects. In the timber floor as well as on the bottom of the masonry wall, tensile stresses develop, which will result in crack development in the masonry.

It can be concluded that the first cracks to develop are vertical cracks at the bottom of the masonry. For larger distances of pile defects, it is observed that vertical crack propagation arises at the top of the masonry wall where the foundation piles function. There can be multiple cracks formed next to each other.

Horizontal cracks appear at the tip of the first vertical crack in the middle of the masonry at the centre of the pile defects.

Observed is a notable difference in the location of crack propagation for weaker masonry when there are no piles modelled, weaker masonry will develop into one vertical crack in the centre of the foundation defect. When for the same weaker masonry, the foundation piles are still connected to the quay walls but modelled with a smaller pile diameter, multiple smaller cracks occur between the defected foundation piles.

Which input parameters have the most influence on the behaviour of the masonry work of the quay wall?

The scale of the foundation defect over the length of the wall contains the most significant influence in the behaviour of the quay wall in terms of displacement.

The reduced strength in the timber pile provides temporary stability in both the cross-sectional and longitudinal direction of the model. It is also concluded that the connections spread the tensile stresses, resulting in multiple smaller cracks.

A brittle failure mechanism for the foundation piles results in a jump in displacement and horizontal crack formation. This brittle failure mechanism works best for the smallest modelled pile of 150 millimetres. Plastic failure of the foundation pile results in larger deformations and a better running model since the model does not diverge due to the over exceeding of the maximum bearing capacity.

The researched material properties conclude that for weaker masonry displacements arise at lower loads and cracks develop at lower displacements. Also, the maximum observed displacement before the divergence of the model is significantly lower than the displacements found for the medium and strong masonry configurations.

The research to the effects of the timber floor concludes that modelling of the floor effects the stress distribution. The floor in combination with residual strength in the timber piles results in multiple smaller cracks in contrast to the presented larger and horizontal cracks when the timber floor is removed.

How do the combined results of the cross-sectional and longitudinal directions provide insight in hidden structural capacity?

The cross-sectional analyses result into a stability issue without residual strength presented in the masonry and timber elements. The problems transfers into a question of strength when the analyses are performed in the longitudinal direction. Here the already discussed parameters, masonry strength and scale and severity of the foundation defect are constants which provide hidden structural capacity to the quay wall system.

It has to be noted that this sub-question is only partially answered. The results are kept separate and so the conclusions are formed.

11.1.2. Main research questions

The main research question of the thesis, as stated in chapter 1.3, was:

How can 2D analyses of quay walls, in multiple directions, under the condition of a partly failing foundation, provide insight into the hidden structural capacity within the masonry?

This research concludes that the modelling of foundation defects of quay walls in the longitudinal direction provides hidden structural capacity, which is not visible in the cross-sectional analysis. The length of the foundation defect, the quality of the pile and floor connection, the failure mechanism of the structurally failing foundation pile, and the masonry quality are the studied parameters. It is concluded that the severeness and length of the foundation defect is the most significant impact parameter.

The cross-sectional analysis of structural failure in the first pile row evolves into a stability issue. Residual strength in the failing pile provides some temporary stability, but ultimately the masonry wall tilts over.

By analysing the quay wall in the longitudinal direction, it is proven that after the structural failure of a foundation pile, the masonry in the quay wall system distributes the forces to functioning foundation piles. By increasing the amount of structurally failing foundation piles, the deformations increase and cracks develop before the failure of the quay wall.

It is concluded that the quality of the masonry contains a direct link to the maximum occurring displacement and crack propagation.

The modelling of the pile degradation as a decrease in pile diameter yet connected to the wall, concludes as an improvement in the stress distribution and consequently a decrease in crack propagation.

For a brittle structural failure of the foundation pile, it is found that in the vertical force-displacement diagram a jump is observed, resulting in a horizontal crack at the tip of the already formed vertical crack.

The examined effect of the function of the timber floor presents no significant difference in the force-displacement diagrams. The timber floor ensures the spreading of the tensile forces resulting in multiple smaller cracks, without the timber floor, after the vertical crack a horizontal crack forms at the tip.

11.2. Recommendations

Since the quay wall system is a complex system, containing multiple failure mechanisms, load combinations and material and soil parameters, not all could be covered in the scope of this study. Therefore future research could investigate the following topics:

- The material properties used to model masonry are based on research about Groningen masonry. It is recommended to perform experiments to the material properties of the brick and mortar used in the

Amsterdam quay walls. Besides the material properties, the stacking of the bricks in the depth of the wall should be analysed to perform computational analysis of the masonry with different strengths in the depth of the wall.

- The intervention points used in this research are formed by the municipality of Amsterdam. Indications of a defect in the pile foundation are observed at lower values than the stated 20 and 25 millimetres. For that reason, it is recommended to research the reliability of these intervention points.

  Secondly, to perform this study and to ensure that the measures at the reach of the interventions points are active before critical failure might occur, there are more measurements and data required to the displacements and state of the quay walls in Amsterdam.

- The created models are 2D, recommended is to research the failure mechanism of a failing pile foundation using a 3D model. The model should contain loading combinations using out-of-plane and in-plane loading. Secondly, dynamic loading for traffic over and point loads to resemble trees on the quay wall should be implemented in future research.
- The results show a great difference for the modelling options of the post-peak behaviour of the load-displacement diagrams of the foundation piles. Recommended is to study the failure mechanisms of the tip of a degraded foundation pile.
- This research focused on the structural failure of the pile foundation. The remaining failure mechanisms were put out of the scope; future research should focus on the remaining failure mechanisms and implement combinations into the study.

Bibliography

Abbot. Understanding-wythe-masonry-restoration. https://www.abbotbuilding.com/understanding-wythe-masonry-restoration/.

Andrés, J. and Barraza, C. (2012). Numerical model for nonlinear analysis of masonry walls. Technical report.

AT5 (2019). *Verschillende kades tijdens Canal Parade afgesloten wegens instortingsgevaar*. https://www.at5.nl/artikelen/195729/verschillende-kades-tijdens-canal-parade-afgesloten-wegens-instortingsgevaar

Cobouw (2017). *Amsterdamse kademuur ingestort*. https://www.cobouw.nl/bouwbreed/nieuws/2017/12/amsterdamse-kademuur-ingestort-101256053.

Couzy, M. and Koops, R. (2019). Financieel onheil dreigt 'de nieuwe lente' te verpesten. https://www.parool.nl/nieuws/financieel-onheil-dreigt-de-nieuwe-lente-te-verpesten~ba1c800c/.

CUR commissie 186 (2013). *Binnenstedelijke kademuren*. SBRCURnet, Rotterdam.

de Gans, W. (2011). *De bodem onder Amsterdam: een geologische stadswandeling*. TNO.

de Gijt, J. (2010). *A History of Quay Walls - Techniques, types, costs and future*. PhD thesis, Delft University of Technology.

de Groot, A. (2019). Structural window design for in-plane seismic strengthening. Master's thesis, Delft University of Technology.

de Vent, I. (2011). *Structural damage in masonry*. PhD thesis, Technische Universiteit Delft.

DINO loket (1999). S25g00127. Online.

DINO loket (2011). B25g2892. Online.

Gemeente Amsterdam (2018). Marktbijeenkomst 9 oktober 2018 innovatiepartnerschap kademuren. PowerPoint presentation.

Gemeente Amsterdam (2019a). Actieplan bruggen en kademuren. PowerPoint presentation.

Gemeente Amsterdam (2019b). Het grootste probleem van de kades zit onder water. https://www.amsterdam.nl/nieuws/nieuws/probleem-kades/.

Gemeente Amsterdam (2019c). Voorzorgsmaatregelen bij 10 kademuren in de binnenstad. https://www.amsterdam.nl/projecten/kademuren/nieuws-kademuren/maatregelen-10-slechte-kademuren/.

Grund, M. (2020). Urban quay walls - a numerical study to recognize foundation defects via masonry damage patterns. Master's thesis, Technische Universiteit Delft.

Jafari, S. and Rots, J. (2016). Summary report for the characterization of original groningen masonry.

Klaassen, D. R., ing. P. Nelemans, and ir. P. den Nijs (2013). Richtlijn voor onderzoek naar houten paalfundering. *Land+Water*, (3).

Klaassen, R. (2013). Heipalen in water en grond. PowerPoint presentation.

Knuppe, J. (2019). Restlevensduurbepaling van de amsterdamse kademuur.

Kruyswijk, M. (2019). Staat van kademuren is nog slechter dan gedacht. https://www.parool.nl/nieuws/staat-van-kademuren-is-nog-slechter-dan-gedacht~b299b057/?referer=https%3A%2F%2Fwww.google.com%2F.

Library of congress. The heerengracht (main canal), amsterdam, holland, between ca. 1890 and ca. 1900. https://www.loc.gov/pictures/collection/pgz/item/2001698757/.

Lourenço, P. B. (1996). *Computational strategies for masonry structures*. PhD thesis, Technische Universiteit Delft.

Lourenço, P. B. (2013). Computational strategies for masonry structures:multi-scale modelling, dynamics, engineering applications and other challenges. Technical report, University of Minho.

Movares (2019). *Kades Amsterdam, Beheersmaatregelen bij calamiteiten (D90-AST-KA-1806570)*, 2.0 edition.

Naval Facilities Engineering Command (1986). *Foundations and Earth Structures*, 7.02 edition.

NEN-EN-1912 (2012). Hout voor constructieve toepassingen - sterkteklassen - toewijzing van visuele sorteringsklassen en houtsoorten. Technical report.

NEN-EN-1997 (2012). Nationale bijlage bij nen-en 1997-1 eurocode 7: Geotechnisch ontwerp - deel 1: Algemene regels. Technical report.

Pande, G., Kralj, B., and Middleton, J. (1994). Analysis of the compressive strength of masonry given by the equation $f_k = k(f_b')^{\alpha}(f_m)^{\beta}$. $TheStructuralEngineer, Volume71(1)$.

Paulo B. Lourenço, Jan G. Rots, J. B. (1995). Two approaches for the analysis of masonry structures: micro and macro-modeling. Technical report, Delft University of Technology.

Roubos, A. (2019). *Enhancing reliability-based assessments of quay walls*. PhD thesis, Delft University of Technology.

Sas, F. (2007). *De houten paalfundering doorgezaagd*, 2006/2007 edition.

Schmidt, T. (1990). Native wood fence posts. Technical report, University of Nebraska - Lincoln.

Strikvoort, I. (2014). Old quay walls - proposal for a method for analysing the remaining lifespan. Master's thesis, Delft University of Technology.

Swedish Wood. Wood grades. https://www.swedishwood.com/about_wood/choosing-wood/wood-grades/.

TNO DIANA BV (2010). *DIANA Finite Element Analysis User's Manual*, 9.4 edition.

Urban Capture. Huidenstraat-herengracht, amsterdam, the netherlands. http://www.urbancapture.com/20130208-huidenstraat-herengracht-amsterdam-the-netherlands/.

van Daatselaar, F. (2019). The geotechnical bearing capacity of old timber piles. Master's thesis, Technische Universiteit Delft.

van Noort, J. (2012). Computational modelling of masonry structures. Master's thesis, Delft University of Technology.

Vecchio, F. J. and Collins, M. P. (1986). The modified compression-field theory for reinforced concrete elements subjected to shear. Technical Report 83-22, ACI Journal.

Vermeer, G. (2003). Metselwerk in de oude binnenstad van amsterdam. *Binnenstad*, 203.

Verruijt, A. (2007). *Soil Mechanics*. VSSD. revised by S. van Baars.

Verschuur, R. (2018). Effective concrete tension zone - a thesis on the comparison of the effective concrete tension zone between finite element analyses using diana and eurocode 2 and jones method. Master's thesis, Technische Universiteit Delft.

A

Overview control measures

Gr.	Nr.	Maatregel	Inzet [d]	Bezwijkmechanismen									
				1	2	3	4	5	6	7	8	9	10
A	1	Reductie van de verkeersbelasting	1	x		x		x	x	x		x	x
A	2	Lichter aanvulmateriaal achter de kade	7+	x		x		x	x	x		x	x
B	1	Verticale damwand voor de kadeconstructie aangevuld met zand. (optioneel geschoord)	7+			x		x	x	x	x	x	x
B	2	Verticale damwand met stempel niet aangevuld met zand. (optioneel geschoord)	7+			x		x	x	x		x	x
B	3	Kleine stalen palen in het water ondersteunen de kade (vloer) verticaal	7+	x									
B	4	Grote stalen palen in het water ondersteunen de kade (vloer) verticaal en horizontaal	7+	x		x			x	x		x	
B	5	Stempelconstructie tussen kade en overzijde	1-7			x		x		x		x	
B	6	Buispaal/juk en raamwerk met stempel	7+			x		x		x		x	
B	7	Ponton ondersteunt de kade (vloer) verticaal	1-7	x					x				
B	8	Constructie (afgezonken) aangevuld met zand	1			x		x	x	x		x	x
C	1	Stalen palen door metselwerk	7+	x		x			x			x	
C	2	Erosie scherm waterzijde	7+			x					x		
C	3	Horizontale ankers landzijde	7+			x		x		x		x	
C	4	Buispaal landzijde met horizontaal anker	7+			x						x	
D	1	Geotextiel boven de vloer	7+								x		
D	2	Injecteren boven de vloer	7+								x		
E	1	Injecteren onder de vloer	7+	x					x		x		x
E	2	Grondkerend scherm landzijde onder de vloer	7+			x				x	x	x	

Figure A.1: Overview control measures (Movares, 2019)

B

Soil measurements

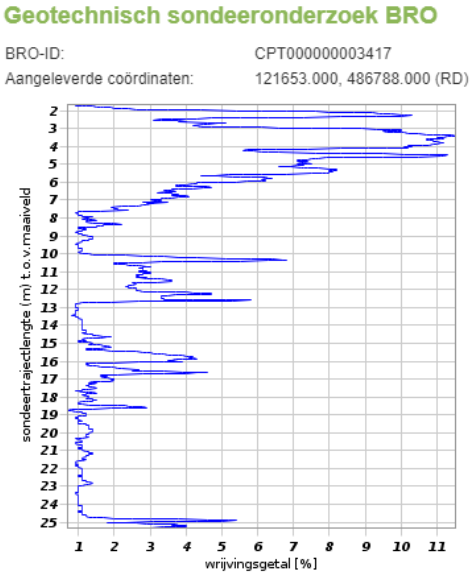

(a) Geotechnical measurements S25G00127 (DINO loket, 1999)

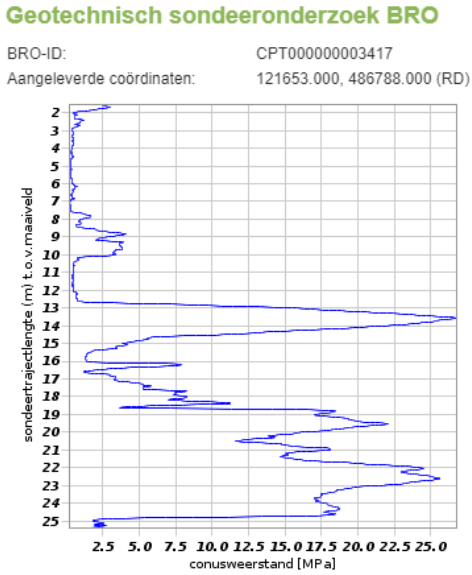

(b) Geotechnical measurements S25G00127 (DINO loket, 1999)

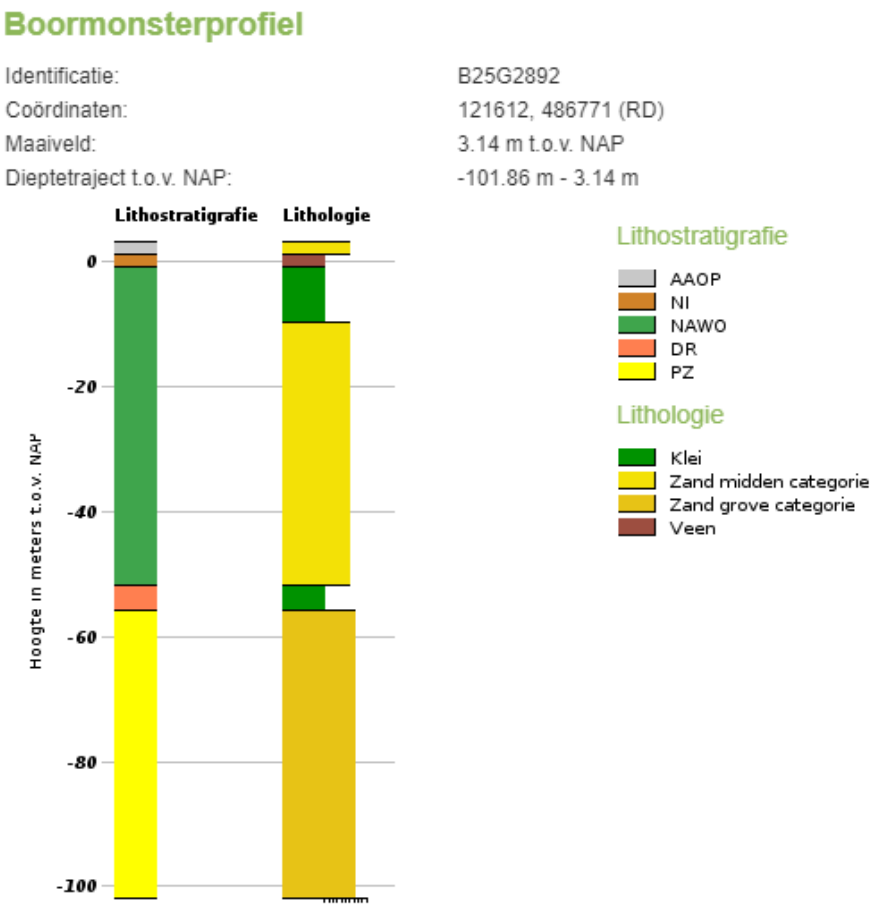

Figure B.2: Geotechnical measurements B25G2892 (DINO loket, 2011)

C

Material properties

Karakteristieke eigenschappen en sterkteklassen van gezaagd naaldhout													
Eigenschap	**C14**	**C16**	**C18**	**C20**	**C22**	**C24**	**C27**	**C30**	**C35**	**C40**	**C45**	**C50**	**Eenheid**
$f_{m,k}$	14	16	18	20	22	24	27	30	35	40	45	50	N/mm^2
$E_{0,mean}$	7	8	9	9,5	10	11	11,5	12	13	14	15	16	kN/mm^2
ρ_{mean}	350	370	380	400	410	420	430	460	470	480	520	520	kg/m^3
ρ_k	290	310	320	330	340	350	360	380	390	400	440	430	kg/m^3
$f_{t;0;k}$	7,2	8,5	10	11,5	13	14,5	16,5	19	22,5	26	30	33,5	N/mm^2
$f_{t;90;k}$	0,4	0,4	0,4	0,4	0,4	0,4	0,4	0,4	0,4	0,4	0,4	0,4	N/mm^2
$f_{c;0;k}$	16	17	18	19	20	21	22	24	25	27	29	30	N/mm^2
$f_{c;90;k}$	2,0	2,2	2,2	2,3	2,4	2,5	2,5	2,7	2,7	2,8	2,9	3,0	N/mm^2
$f_{v;k}$	3,0	3,2	3,4	3,6	3,8	4,0	4,0	4,0	4,0	4,0	4,0	4,0	N/mm^2
$E_{0,05}$	4,7	5,4	6,0	6,4	6,7	7,4	7,7	8,0	8,7	9,4	10,1	10,7	kN/mm^2
$E_{90,mean}$	0,23	0,27	0,30	0,32	0,33	0,37	0,38	0,40	0,43	0,47	0,50	0,53	kN/mm^2
G_{mean}	0,44	0,50	0,56	0,59	0,63	0,69	0,72	0,75	0,81	0,88	0,94	1,00	kN/mm^2
$G_{0,05}$	0,29	0,34	0,38	0,40	0,42	0,46	0,48	0,50	0,54	0,59	0,63	0,67	kN/mm^2
Tabel 1. Karakteristieke eigenschappen en sterkteklassen van gezaagd naaldhout													

Figure C.1: Timber material properties (NEN-EN-1912, 2012)

Material property	Symbol	Unit	Clay							
			(pre 1945)				(post 1945)			
			Average	Lower bound	Upper bound	C.o.V.	Average	Lower bound	Upper bound	C.o.V.
Flexural strength of masonry unit	$f_{mu,t}$	MPa	6.43	0.71	17.35	0.53	4.29	1.30	8.79	0.41
Compressive strength of masonry in the direction perpendicular to bed joints	$f_{m,v}$	MPa	10.76	1.30	32.40	0.42	14.31	4.50	28.60	0.42
Elastic chord modulus of masonry in the direction perpendicular to bed joints	$E_{m,v}$	GPa	7.44	1.27	19.92	0.66	7.35	1.20	15.60	0.50
Fracture energy in compression for loading perpendicular to bed joints	$G_{fc,v}$	N/mm	27.06	5.53	70.64	0.77	20.58	5.29	37.37	0.46
Compressive strength of masonry in the direction parallel to bed joints	$f_{m,h}$	MPa	9.51	7.60	11.73	0.20	11.00	7.41	14.23	0.23
Elastic chord modulus of masonry in the direction parallel to bed joints	$E_{m,h}$	GPa	6.56	3.78	10.60	0.51	5.47	4.76	6.33	0.10
Fracture energy in compression for loading parallel to bed joints	$G_{fc,h}$	N/mm	30.94	30.84	31.04	0.005	31.55	22.80	40.30	0.39
Average of compressive strength in vertical and horizontal direction	f_m	MPa	10.13				12.65			
Average of elastic chord modulus in vertical and horizontal direction	E_m	GPa	7.00				6.41			
Average of fracture energy in vertical and horizontal direction	G_{fc}	N/mm	29.00				26.07			
Masonry shear modulus	G_m	GPa	2.92				2.67			
Masonry bending strength with the moment vector parallel to the bed joints and in the plane of the wall	f_{x1}	MPa	-	-	-	-	0.33	0.26	0.42	0.24
Masonry bending strength with the moment vector orthogonal to the bed joint and in the plane of the wall	f_{x2}	MPa	0.83	0.55	1.28	0.47	1.12	0.59	1.68	0.27
Masonry bending strength with the moment vector orthogonal to the plane of the wall	f_{x3}	MPa	0.61	0.29	1.12	0.20	0.63	0.11	1.40	0.57
Masonry flexural bond strength between brick and mortar	$f_{b,bj}$	MPa	0.38	0.03	1.00	0.57	0.32	0.00	0.95	0.72
*Masonry uniaxial bond strength between brick and mortar	f_b	MPa	0.25	0.02	0.67	0.38	0.21	0.00	0.64	0.42
Masonry (bed joint) initial shear strength	f_{v0}	MPa	0.30	0.17	0.43	0.29	0.47	0.15	0.84	0.46
Masonry (bed joint) shear friction coefficient	μ	-	0.80	0.50	1.23	0.37	0.76	0.45	1.12	0.30
**Fracture energy in shear	G_{fs}	N/mm	0.33				0.93			
***Fracture energy in tension	G_{ft}	N/mm	0.035				0.035			

Figure C.2: Groningen masonry material properties (Jafari and Rots, 2016)

D

Pile input

Force-displacement values for a 250 mm diameter pile			
shaft displacement [mm]	**shaft force [kN]**	**base displacement [mm]**	**base force [kN]**
0.000	0	0.000	0
0.050	1	0.068	18
0.104	2	0.133	36
0.169	3	0.333	54
0.261	4	0.605	72
0.399	5	0.950	90
0.540	6	1.278	108
0.716	7	1.595	126
0.959	8	2.075	144
1.189	9	2.625	162
1.459	10	3.378	180
1.784	11	4.155	198
2.135	12	5.338	216
3.000	14	7.770	252
4.486	16	11.353	288
6.587	18	16.403	324
10.372	20	26.215	360

Force-displacement values for a 200 mm diameter pile			
shaft displacement [mm]	**shaft force [kN]**	**base displacement [mm]**	**base force [kN]**
0.000	0	0	0
0.050	1	0.054	12
0.104	2	0.106	23
0.169	2	0.266	35
0.261	3	0.484	46
0.399	4	0.76	58
0.540	5	1.022	69
0.716	5	1.276	81
0.959	6	1.66	92
1.189	7	2.1	104
1.459	8	2.702	115
1.784	9	3.324	127
2.135	9	4.27	138
3.000	11	6.216	161
4.486	13	9.082	184
6.587	14	13.122	208
10.372	16	20.972	231

Force-displacement values for a 150 mm diameter pile			
shaft displacement [mm]	**shaft force [kN]**	**base displacement [mm]**	**base force [kN]**
0.000	0	0	0
0.050	1	0.041	6
0.104	1	0.08	13
0.169	2	0.2	19
0.261	2	0.363	26
0.399	3	0.57	32
0.540	4	0.767	39
0.716	4	0.957	45
0.959	5	1.245	52
1.189	5	1.575	58
1.459	6	2.027	65
1.784	6	2.493	71
2.135	7	3.203	78
3.000	8	4.662	91
4.486	9	6.812	104
6.587	11	9.842	117
10.372	12	15.729	130

Force-displacement values for a 100 mm diameter pile			
shaft displacement [mm]	**shaft force [kN]**	**base displacement [mm]**	**base force [kN]**
0.000	0	0	0
0.050	0	0.027	3
0.104	1	0.053	6
0.169	1	0.133	9
0.261	2	0.242	12
0.399	2	0.38	14
0.540	2	0.511	17
0.716	3	0.638	20
0.959	3	0.83	23
1.189	4	1.05	26
1.459	4	1.351	29
1.784	4	1.662	32
2.135	5	2.135	35
3.000	5	3.108	40
4.486	6	4.541	46
6.587	7	6.561	52
10.372	8	10.486	58

E

Formulas of Pande et al

In order to determine Young's moduli, Poisson's ratios and shear moduli a script is created containing the formulas provided by Pande. In the equations it is assumed that there is a perfect bond between the elements, no slippage between masonry and joints. Also assumed, the dimensions of any of the constituents are small compared to the dimensions of the masonry panel. (Pande et al., 1994)

One layer of masonry units with perpend joints

For the elastic constants of the masonry holds:

$$\begin{aligned} \frac{\bar{\nu}_{yx}}{\bar{\nu}_{xy}} &= \frac{\bar{E}_y}{\bar{E}_x} \\ \frac{\bar{\nu}_{zy}}{\bar{\nu}_{yz}} &= \frac{\bar{E}_z}{\bar{E}_y} \\ \frac{\bar{\nu}_{zx}}{\bar{\nu}_{xz}} &= \frac{\bar{E}_z}{\bar{E}_x} \end{aligned} \tag{E.1}$$

Relative dimensions of masonry units and perpend joints are defined as: (for input reference see picture on the next page)

$$\begin{aligned} t_b &= \frac{l_b}{l_b + t_{hj}} \\ t_m &= \frac{t_{hj}}{l_b + t_{hj}} \end{aligned} \tag{E.2}$$

Which satisfy:

$$t_b + t_m = 1.0 \tag{E.3}$$

Defining:

$$\begin{aligned} \alpha &= \frac{t_m E_m (1-\nu_b^2) + t_b E_b (1-\nu_m^2)}{(1-\nu_m^2)(1-\nu_b^2)} \\ \zeta &= \frac{t_m \nu_m E_m (1-\nu_b^2) + t_b \nu_b E_b (1-\nu_m^2)}{(1-\nu_m^2)(1-\nu_b^2)} \\ \chi_b &= \frac{t_b \nu_b}{1-\nu_b} \\ \chi_m &= \frac{t_m \nu_m}{1-\nu_m} \\ \chi &= \chi_b + \chi_m \end{aligned} \tag{E.4}$$

Poisson's ratios can be calculated as:

$$\begin{aligned} \nu'_{yz} &= \frac{\zeta}{\alpha} \\ \nu'_{zx} = \nu'_{yx} &= \chi(1-\nu'_{yz}) \end{aligned} \tag{E.5}$$

And Young's moduli:

$$\begin{aligned} E'_y = E'_z &= \alpha - \zeta\nu'_{zy} \\ \frac{1}{E'_x} &= \frac{t_m}{E_m} + \frac{t_b}{E_b} + 2\chi_m\left(\frac{\nu'_{zx}}{E'_z} - \frac{\nu_m}{E_m}\right) + 2\chi_b\left(\frac{\nu'_{zx}}{E'_z} - \frac{\nu_b}{E_b}\right) \end{aligned} \tag{E.6}$$

Other Poisson's ratios can be calculated using formulas in E.1:

$$\begin{aligned} \nu'_{xz} &= \nu'_{zx}\frac{E'_x}{E'_z} \\ \nu'_{zy} &= \nu'_{yz}\frac{E'_z}{E'_y} \\ \nu'_{xy} &= \nu'_{yx}\frac{E'_x}{E'_y} \end{aligned} \tag{E.7}$$

Shear moduli of this layer are:

$$\begin{aligned} \frac{1}{G'_{xy}} = \frac{1}{G'_{xz}} &= \frac{t_m}{G_m} + \frac{t_b}{G_b} \\ G'_{yz} &= t_m G_m + t_b G_b \end{aligned} \tag{E.8}$$

Stack of layers of masonry units, perpendicular joints and bed joints will be considered

The new relative dimensions are defined as:

$$\begin{aligned} t_m &= \frac{t_{bj}}{h_b + t_{bj}} \\ t' &= \frac{h_b}{h_b + t_{bj}} \end{aligned} \tag{E.9}$$

And a set of parameters as:

$$\begin{aligned} \alpha &= \frac{t_m E_m}{1-\nu_m^2} + \frac{t' E'_x}{1-\nu'_{xz}\nu'_{zx}} \\ \zeta &= \frac{t_m \nu_m E_m}{1-\nu_m^2} + \frac{t' E'_z \nu'_{xz}}{1-\nu_m^2} \\ \chi_m &= \frac{t_m \nu_m}{1-\nu_m} \\ \chi' &= \frac{t'(\nu'_{zy} + \nu'_{zx}\nu'_{xy})}{1-\nu'_{xz}\nu'_{zx}} \\ \chi &= \chi_m + \chi' \\ \lambda_m &= \chi_m \\ \lambda' &= \frac{t'(\nu'_{xy} + \nu'_{zy}\nu'_{xz})}{1-\nu'_{xz}\nu'_{zx}} \\ \lambda &= \lambda_m + \lambda' \end{aligned} \tag{E.10}$$

Equivalent mechanical properties of the panel can now be obtained:

$$
\begin{aligned}
\bar{\nu}_{zx} &= \frac{\zeta}{\alpha} \\
\bar{\nu}_{zy} &= \chi - \frac{\lambda\zeta}{\alpha} \\
\bar{\nu}_{xy} &= \lambda - \frac{\chi\zeta}{\beta} \\
\bar{E}_z &= \frac{\alpha\beta - \zeta^2}{\alpha} \\
\bar{E}_x &= \frac{\alpha\beta - \zeta^2}{\beta} \\
\frac{1}{\bar{E}_y} &= \frac{t_m}{E_m} + \frac{t'}{E'_y} + \chi_m\left(\frac{\bar{\nu}_{xy}}{\bar{E}_z} - \frac{\nu_m}{E_m}\right) + \chi'\left(\frac{\bar{\nu}_{zy}}{\bar{E}_z} - \frac{\nu'_{zy}}{E'_z}\right) + \lambda_m\left(\frac{\bar{\nu}_{xy}}{\bar{E}_x} - \frac{\nu_m}{E_m}\right) + \lambda'\left(\frac{\bar{\nu}_{xy}}{\bar{E}_x} - \frac{\nu'_{xy}}{E'_x}\right)
\end{aligned}
\tag{E.11}
$$

Using identities defined by using equation E.1 other Poisson's ratios can be obtained:

$$
\begin{aligned}
\bar{\nu}_{yx} &= \bar{\nu}_{xy}\frac{\bar{E}_y}{\bar{E}_x} \\
\bar{\nu}_{xz} &= \bar{\nu}_{zx}\frac{\bar{E}_x}{\bar{E}_z} \\
\bar{\nu}_{yz} &= \bar{\nu}_{zy}\frac{\bar{E}_y}{\bar{E}_z}
\end{aligned}
\tag{E.12}
$$

Finally, the shear moduli are given as:

$$
\begin{aligned}
\frac{1}{\bar{G}_{xy}} &= \frac{t_m}{G_m} + \frac{t'}{G'_{xy}} \\
\bar{G}_{xz} &= t_m G_m + t' G'_{xz} \\
\frac{1}{\bar{G}_{yz}} &= \frac{t_m}{G_m} + \frac{t'}{G'_{yz}}
\end{aligned}
\tag{E.13}
$$

Using the material properties with the bar a masonry panel or wall can be treated as a homogeneous material with orthotropic properties instead of a composite material.

For formulas E.2 and E.9, figure E.1 shows the relevant dimensions of brick and mortar. Where $t_{hj} = t_{mh}$ and $t_{bj} = t_{mb}$.

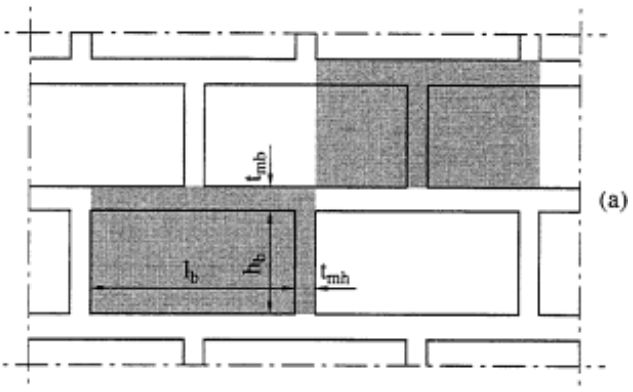

Figure E.1: Masonry terminology (Paulo B. Lourenço, 1995)

F

Basic crack pattern for masonry

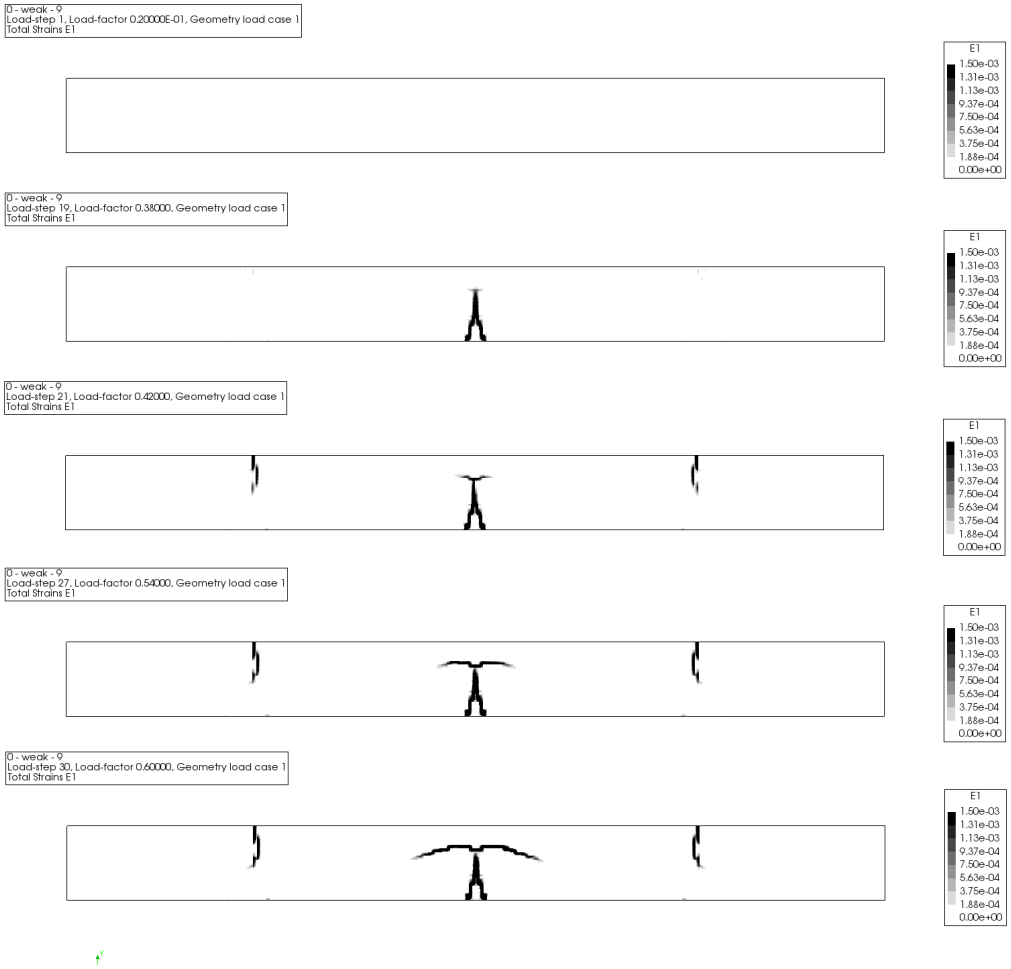

Figure F.1: Basic crack pattern for masonry without timber floor support

G

Stress distribution in colour

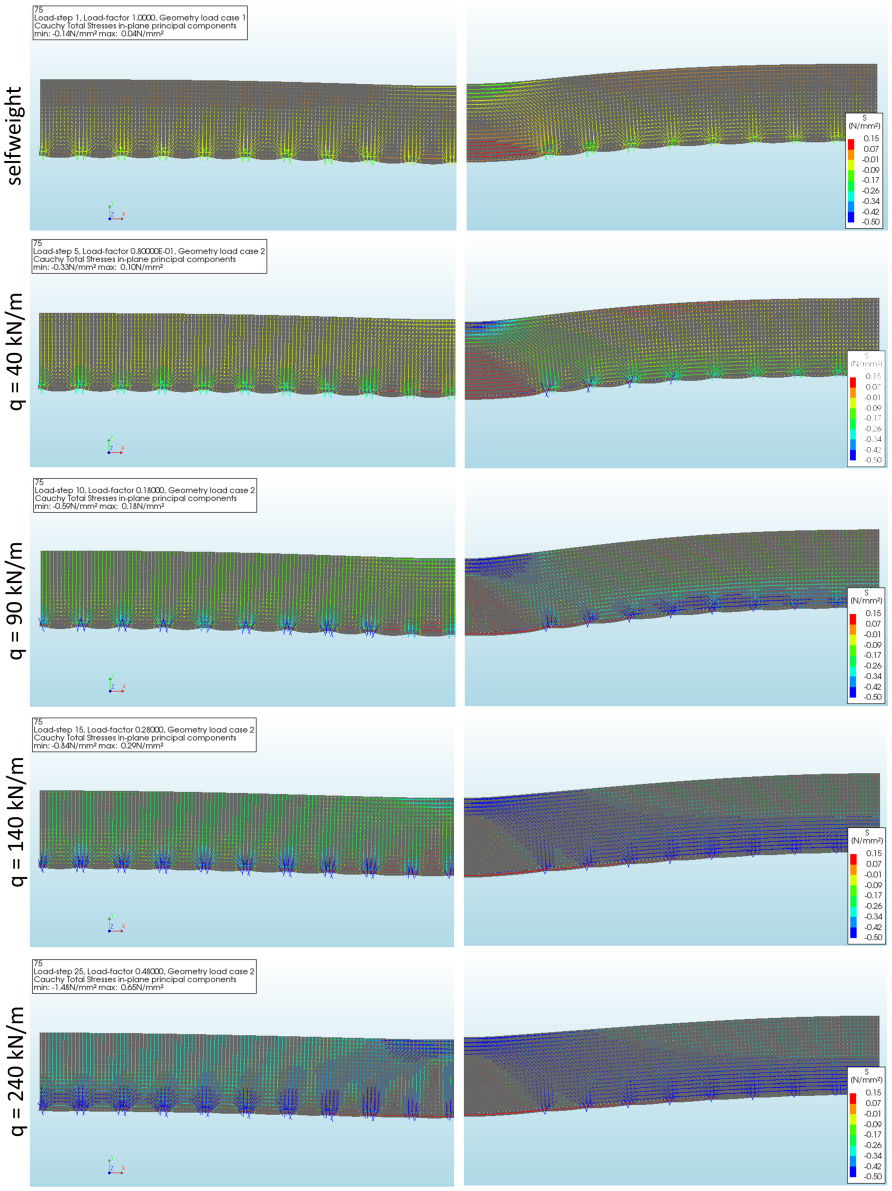

Figure G.1: Stress distribution for three piles modelled as 200 mm pile (l) and no piles (r) under a increasing load

H

Results split timber floor

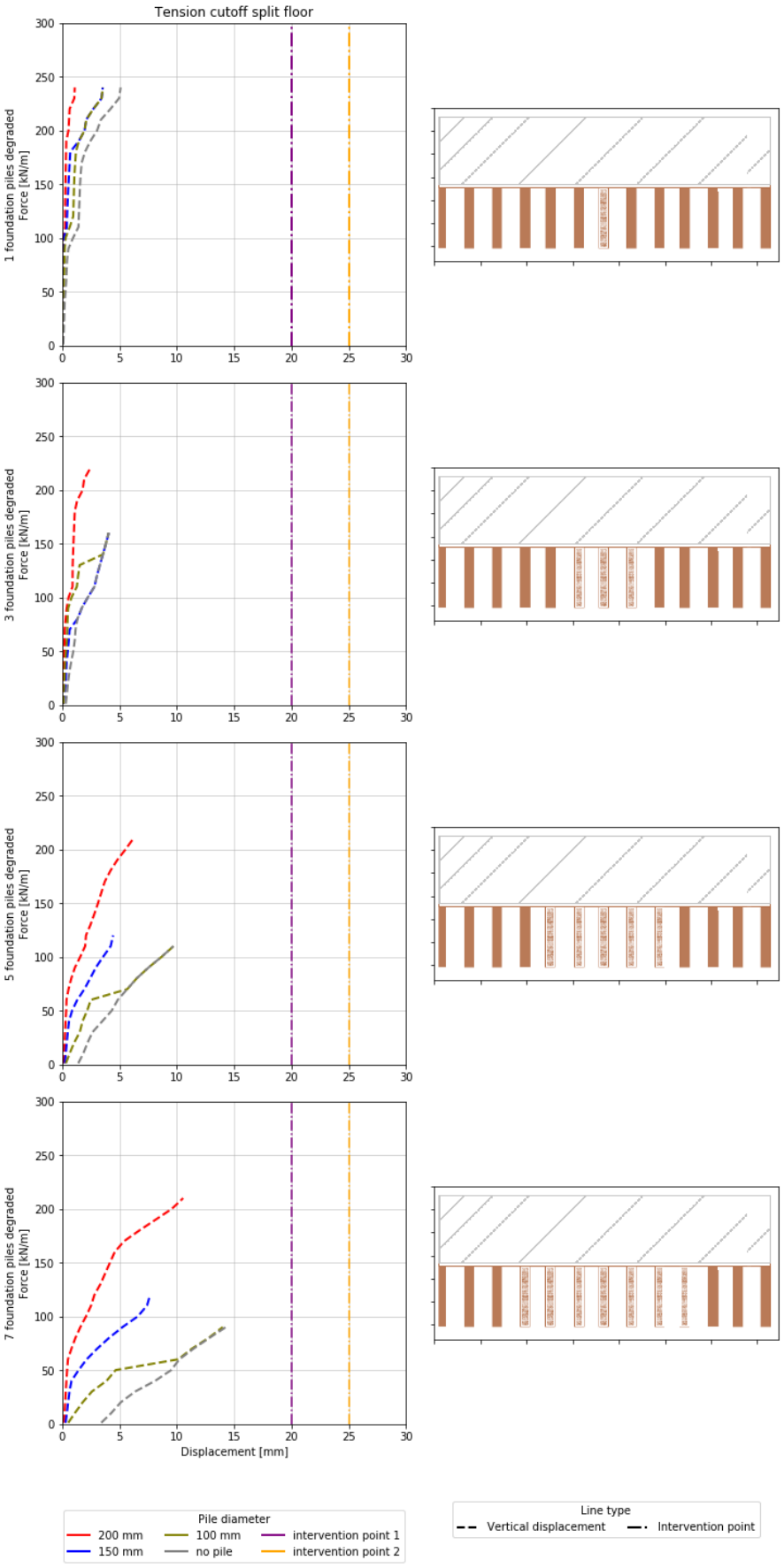

Figure H.1: Vertical displacements for tension cutoff - split floor setup

Python code for Diana FEA

UNITS

```
setUnit( "LENGTH", "MM" )
setUnit( "MASS", "T" )
setUnit( "ANGLE", "RAD" )
```

MATERIAL INPUT

```
addMaterial( "Masonry good", "CONCR", "TSCR", [] )
setParameter( MATERIAL, "Masonry good", "LINEAR/ELASTI/YOUNG", 7500 )
setParameter( MATERIAL, "Masonry good", "LINEAR/ELASTI/POISON", 0.27 )
setParameter( MATERIAL, "Masonry good", "LINEAR/MASS/DENSIT", 1.775e-09 )
setParameter( MATERIAL, "Masonry good", "MODTYP/TOTCRK", "ROTATE" )
setParameter( MATERIAL, "Masonry good", "TENSIL/TENCRV", "LINEAR" )
setParameter( MATERIAL, "Masonry good", "TENSIL/TENSTR", 0.15 )
setParameter( MATERIAL, "Masonry good", "TENSIL/GF1", 0.035 )
setParameter( MATERIAL, "Masonry good", "COMPRS/COMCRV", "THOREN" )
setParameter( MATERIAL, "Masonry good", "COMPRS/COMSTR", 12 )

addMaterial( "Masonry medium", "CONCR", "TSCR", [] )
setParameter( MATERIAL, "Masonry medium", "LINEAR/ELASTI/YOUNG", 5000 )
setParameter( MATERIAL, "Masonry medium", "LINEAR/ELASTI/POISON", 0.27 )
setParameter( MATERIAL, "Masonry medium", "LINEAR/MASS/DENSIT", 1.775e-09 )
setParameter( MATERIAL, "Masonry medium", "MODTYP/TOTCRK", "ROTATE" )
setParameter( MATERIAL, "Masonry medium", "TENSIL/TENCRV", "LINEAR" )
setParameter( MATERIAL, "Masonry medium", "TENSIL/TENSTR", 0.5 )
setParameter( MATERIAL, "Masonry medium", "TENSIL/GF1", 0.015 )
setParameter( MATERIAL, "Masonry medium", "COMPRS/COMCRV", "THOREN" )
setParameter( MATERIAL, "Masonry medium", "COMPRS/COMSTR", 8 )

addMaterial( "Masonry bad", "CONCR", "TSCR", [] )
setParameter( MATERIAL, "Masonry bad", "LINEAR/ELASTI/YOUNG", 2500 )
setParameter( MATERIAL, "Masonry bad", "LINEAR/ELASTI/POISON", 0.27
) setParameter( MATERIAL, "Masonry bad", "LINEAR/MASS/DENSIT", 1.775e-09 )
setParameter( MATERIAL, "Masonry bad", "MODTYP/TOTCRK", "ROTATE" )
setParameter( MATERIAL, "Masonry bad", "TENSIL/TENCRV", "LINEAR" )
setParameter( MATERIAL, "Masonry bad", "TENSIL/TENSTR", 0.5 )
setParameter( MATERIAL, "Masonry bad", "TENSIL/GF1", 0.004 )
setParameter( MATERIAL, "Masonry bad", "COMPRS/COMCRV", "THOREN" )
setParameter( MATERIAL, "Masonry bad", "COMPRS/COMSTR", 4 )
```

```
addMaterial( "Paal 100", "SPRING", "LINETR", [] )
setParameter( MATERIAL, "Paal 100", "LINETR/SPRING", 100000 )
setParameter( MATERIAL, "Paal 100", "LINETR/SPTYPE", "DIAGRA" )
setParameter( MATERIAL, "Paal 100", "LINETR/DIAGRA/DUFX", [] )
setParameter( MATERIAL, "Paal 100", "LINETR/DIAGRA/DUFX", [ 0, 0, 1, 90000, 2, 150000, 8,
250000, 11, 280000, 26, 360000, 26.1, 0, 100, 0] )

addMaterial( "Paal half", "SPRING", "LINETR", [] )
setParameter( MATERIAL, "Paal half", "LINETR/SPRING", 50000 )
setParameter( MATERIAL, "Paal half", "LINETR/SPTYPE", "DIAGRA" )
setParameter( MATERIAL, "Paal half", "LINETR/DIAGRA/DUFX", [] )
setParameter( MATERIAL, "Paal half", "LINETR/DIAGRA/DUFX", [ 0, 0, 1, 90000, 2, 150000, 8,
250000, 11, 280000, 26, 360000, 26.1, 0, 100, 0 ] )

addMaterial( "Paal 75", "SPRING", "LINETR", [] )
setParameter( MATERIAL, "Paal 75", "LINETR/SPRING", 60000 )
setParameter( MATERIAL, "Paal 75", "LINETR/SPTYPE", "DIAGRA" )
setParameter( MATERIAL, "Paal 75", "LINETR/DIAGRA/DUFX", [] )
setParameter( MATERIAL, "Paal 75", "LINETR/DIAGRA/DUFX", [
0,0,1.5,90000,4.5,140000,10,190000,21,230000, 21.1, 0, 100, 0 ] )

addMaterial( "Paal 50", "SPRING", "LINETR", [] )
setParameter( MATERIAL, "Paal 50", "LINETR/SPRING", 20000 )
setParameter( MATERIAL, "Paal 50", "LINETR/SPTYPE", "DIAGRA" )
setParameter( MATERIAL, "Paal 50", "LINETR/DIAGRA/DUFX", [] )
setParameter( MATERIAL, "Paal 50", "LINETR/DIAGRA/DUFX", [
0,0,1.5,65000,4.5,90000,6.5,102000,10,116000,15,130000, 15.1, 0, 100, 0 ] )

addMaterial( "Paal 25", "SPRING", "LINETR", [] )
setParameter( MATERIAL, "Paal 25", "LINETR/SPRING", 7000 )
setParameter( MATERIAL, "Paal 25", "LINETR/SPTYPE", "DIAGRA" )
setParameter( MATERIAL, "Paal 25", "LINETR/DIAGRA/DUFX", [] )
setParameter( MATERIAL, "Paal 25", "LINETR/DIAGRA/DUFX", [
0,0,0.5,20000,3,40000,6,50000,10,60000, 10.1, 0, 100, 0 ] )

addMaterial( "Paal 100 plastic", "SPRING", "LINETR", [] )
setParameter( MATERIAL, "Paal 100 plastic", "LINETR/SPRING", 100000 )
setParameter( MATERIAL, "Paal 100 plastic", "LINETR/SPTYPE", "DIAGRA" )
setParameter( MATERIAL, "Paal 100 plastic", "LINETR/DIAGRA/DUFX", [] )
setParameter( MATERIAL, "Paal 100 plastic", "LINETR/DIAGRA/DUFX", [ 0, 0, 1, 90000, 2,
150000, 8, 250000, 11, 280000, 26, 360000, 100, 360000] )

addMaterial( "Paal half plastic", "SPRING", "LINETR", [] )
setParameter( MATERIAL, "Paal half plastic", "LINETR/SPRING", 50000 )
setParameter( MATERIAL, "Paal half plastic", "LINETR/SPTYPE", "DIAGRA" )
setParameter( MATERIAL, "Paal half plastic", "LINETR/DIAGRA/DUFX", [] )
setParameter( MATERIAL, "Paal half plastic", "LINETR/DIAGRA/DUFX", [ 0, 0, 1, 90000, 2,
150000, 8, 250000, 11, 280000, 26, 360000, 100, 360000 ] )

addMaterial( "Paal 75", "SPRING", "LINETR", [] )
setParameter( MATERIAL, "Paal 75 plastic", "LINETR/SPRING", 60000 )
setParameter( MATERIAL, "Paal 75 plastic", "LINETR/SPTYPE", "DIAGRA" )
setParameter( MATERIAL, "Paal 75 plastic", "LINETR/DIAGRA/DUFX", [] )
setParameter( MATERIAL, "Paal 75 plastic", "LINETR/DIAGRA/DUFX", [
0,0,1.5,90000,4.5,140000,10,190000,21,230000, 100, 230000 ] )
```

addMaterial("Paal 50", "SPRING", "LINETR", [])
setParameter(MATERIAL, "Paal 50 plastic", "LINETR/SPRING", 20000)
setParameter(MATERIAL, "Paal 50 plastic", "LINETR/SPTYPE", "DIAGRA")
setParameter(MATERIAL, "Paal 50 plastic", "LINETR/DIAGRA/DUFX", [])
setParameter(MATERIAL, "Paal 50 plastic", "LINETR/DIAGRA/DUFX", [
0,0,1.5,65000,4.5,90000,6.5,102000,10,116000,15,130000, 100, 130000])

addMaterial("Paal 25", "SPRING", "LINETR", [])
setParameter(MATERIAL, "Paal 25 plastic", "LINETR/SPRING", 7000)
setParameter(MATERIAL, "Paal 25 plastic", "LINETR/SPTYPE", "DIAGRA")
setParameter(MATERIAL, "Paal 25 plastic", "LINETR/DIAGRA/DUFX", [])
setParameter(MATERIAL, "Paal 25 plastic", "LINETR/DIAGRA/DUFX", [
0,0,0.5,20000,3,40000,6,50000,10,60000, 100, 60000])

addMaterial("Interface low", "INTERF", "FRICTI", [])
setParameter(MATERIAL, "Interface low", "LINEAR/IFTYP", "LIN2D")
setParameter(MATERIAL, "Interface low", "LINEAR/ELAS2/DSNY", 5000)
setParameter(MATERIAL, "Interface low", "LINEAR/ELAS2/DSSX", 30)
setParameter(MATERIAL, "Interface low", "COULOM/COHESI", 0.2)
setParameter(MATERIAL, "Interface low", "COULOM/PHI", 0.65)
setParameter(MATERIAL, "Interface low", "COULOM/PSI", 0)

addMaterial("Interface cross", "INTERF", "FRICTI", [])
setParameter(MATERIAL, "Interface cross", "LINEAR/IFTYP", "LIN2D")
setParameter(MATERIAL, "Interface cross", "LINEAR/ELAS2/DSNY", 30)
setParameter(MATERIAL, "Interface cross", "LINEAR/ELAS2/DSSX", 5000)
setParameter(MATERIAL, "Interface cross", "COULOM/COHESI", 0.55)
setParameter(MATERIAL, "Interface cross", "COULOM/PHI", 0.65)
setParameter(MATERIAL, "Interface cross", "COULOM/PSI", 0)

addMaterial("Timber", "MCSTEL", "ISOTRO", [])
setParameter(MATERIAL, "Timber", "LINEAR/MASS/DENSIT", 0.35e-09)
setParameter(MATERIAL, "Timber", "LINEAR/ELASTI/POISON", 0.3)
setParameter(MATERIAL, "Timber", "LINEAR/ELASTI/YOUNG", 7000)

ELEMENT GEOMETRIES

addGeometry("Element geometry 1", "SHEET", "MEMBRA", [])
setParameter(GEOMET, "Element geometry 1", "THICK", 800)
addGeometry("Line", "LINE", "STLIIF", [])
setParameter(GEOMET, "Line", "LIFMEM/THICK", 800)
addGeometry("paalelement", "POINT", "SPRING", [])
setParameter(GEOMET, "paalelement", "AXIS", [0, -1, 0])

GEOMETRY LONGITUDINAL
createSheet("Masonry sheet", [[-11000, 0, 0],[-11000, 2000, 0],[11000, 2000, 0],[11000, 0, 0]])

createSheet("Timber sheet", [[-11000, 0, 0],[-11000, -100, 0],[-10900, -100, 0],[-10000, -100, 0],[-9900, -100, 0],[-9800, -100, 0],[-8900, -100, 0],[-8800, -100, 0],[-8700, -100, 0],[-7800, -100, 0],[-7700, -100, 0],[-7600, -100, 0],[-6700, -100, 0],[-6600, -100, 0],[-6500, -100, 0],[-5600, -100, 0],[-5500, -100, 0],[-5400, -100, 0],[-4500, -100, 0],[-4400, -100, 0],[-4300, -100, 0],[-3400, -100, 0],[-3300, -100, 0],[-3200, -100, 0],[-2300, -100, 0],[-2200, -100, 0],[-2100, -100, 0],[-1200, -100, 0],[-1100, -100, 0],[-1000, -100, 0],[-100, -100, 0],[0, -100, 0],[100, -100, 0],[1000, -100, 0],[1100, -100, 0],[1200, -100, 0],[2100, -100, 0],[2200, -100, 0],[2300, -100, 0],[3200, -100, 0],[3300, -100, 0],[3400, -100, 0],[4300, -100, 0],[4400, -100, 0],[4500, -100, 0],[5400, -100, 0],[5500, -100, 0],[5600, -100, 0],[6500, -100, 0],[6600, -100, 0],[6700, -100, 0],[7600, -100, 0],[7700, -100, 0],[7800, -100, 0],[8700, -100, 0],[8800, -100, 0],[8900, -100, 0],[9800, -100, 0],[9900, -100, 0],[

```
10000, -100, 0 ],[ 10900, -100, 0 ],[ 11000, -100, 0 ],[ 11000, 0, 0 ]] )
```

BOUNDARY LONGITUDINAL

```
addSet( GEOMETRYSUPPORTSET, "Geometry support set 1" )
createLineSupport( "sidel", "Geometry support set 1" )
setParameter( GEOMETRYSUPPORT, "sidel", "AXES", [ 1, 2 ] )
setParameter( GEOMETRYSUPPORT, "sidel", "TRANSL", [ 1, 0, 0 ] )
setParameter( GEOMETRYSUPPORT, "sidel", "ROTATI", [ 0, 0, 0 ] )
attach( GEOMETRYSUPPORT, "sidel", "Masonry sheet", [[ -11000, 1000, 0 ]] )
attach( GEOMETRYSUPPORT, "sidel", "Timber sheet", [[ -11000, -50, 0 ]] )
addSet( GEOMETRYSUPPORTSET, "Geometry support set 1" )
createLineSupport( "sider", "Geometry support set 1" )
setParameter( GEOMETRYSUPPORT, "sider", "AXES", [ 1, 2 ] )
setParameter( GEOMETRYSUPPORT, "sider", "TRANSL", [ 1, 0, 0 ] )
setParameter( GEOMETRYSUPPORT, "sider", "ROTATI", [ 0, 0, 0 ] )
attach( GEOMETRYSUPPORT, "sider", "Masonry sheet", [[ 11000, 1000, 0 ]] )
attach( GEOMETRYSUPPORT, "sider", "Timber sheet", [[ 11000, -50, 0 ]] )
```

LOADS LONGITUDINAL

```
addSet( GEOMETRYLOADSET, "Geometry load case 2" )
addSet( GEOMETRYLOADSET, "Geometry load case 1" )

createModelLoad( "own", "Geometry load case 1" )

createLineLoad( "top", "Geometry load case 2" )
setParameter( GEOMETRYLOAD, "top", "FORCE/VALUE", -500 )
setParameter( GEOMETRYLOAD, "top", "FORCE/DIRECT", 2 )
attach( GEOMETRYLOAD, "top", "Masonry sheet", [[ 0, 2800, 0 ]] )

addGeometryLoadCombination( "" )
setGeometryLoadCombinationFactor( "Geometry load combination 1", "Geometry load case 1", 1 )
addGeometryLoadCombination( "" )
setGeometryLoadCombinationFactor( "Geometry load combination 2", "Geometry load case 2", 1 )
```

CONNECTIONS LONGITUDINAL

```
createConnection( "timber-masonry", "INTER", SHAPEEDGE )
setParameter( GEOMETRYCONNECTION, "timber-masonry", "MODE", "AUTO" )
attachTo( GEOMETRYCONNECTION, "timber-masonry", "SOURCE", "Masonry sheet", [[ 0, 0, 0 ]] )
setElementClassType( GEOMETRYCONNECTION, "timber-masonry", "STLIIF" )
assignMaterial( "Interface low", GEOMETRYCONNECTION, "timber-masonry" )
assignGeometry( "Line", GEOMETRYCONNECTION, "timber-masonry" )
setParameter( GEOMETRYCONNECTION, "timber-masonry", "FLIP", False )
resetElementData( GEOMETRYCONNECTION, "timber-masonry" )

createConnection( "goed1l", "BNDSPR", SHAPEVERTEX )
attachTo( GEOMETRYCONNECTION, "goed1l", "SOURCE", "Timber sheet", [[ -11000, -100, 0 ]] )
setElementClassType( GEOMETRYCONNECTION, "goed1l", "SPRING" )
assignMaterial( "Paal 100", GEOMETRYCONNECTION, "goed1l" )
assignGeometry( "paalelement", GEOMETRYCONNECTION, "goed1l" )
setParameter( GEOMETRYCONNECTION, "goed1l", "FLIP", False )

createConnection( "goed2l", "BNDSPR", SHAPEVERTEX )
attachTo( GEOMETRYCONNECTION, "goed2l", "SOURCE", "Timber sheet", [[ -9900, -100, 0 ]] )
```

```
setElementClassType( GEOMETRYCONNECTION, "goed2l", "SPRING" )
assignMaterial( "Paal 100", GEOMETRYCONNECTION, "goed2l" )
assignGeometry( "paalelement", GEOMETRYCONNECTION, "goed2l" )
setParameter( GEOMETRYCONNECTION, "goed2l", "FLIP", False )

createConnection( "goed3l", "BNDSPR", SHAPEVERTEX )
attachTo( GEOMETRYCONNECTION, "goed3l", "SOURCE", "Timber sheet", [[ -8800, -100, 0 ]] )
setElementClassType( GEOMETRYCONNECTION, "goed3l", "SPRING" )
assignMaterial( "Paal 100", GEOMETRYCONNECTION, "goed3l" )
assignGeometry( "paalelement", GEOMETRYCONNECTION, "goed3l" )
setParameter( GEOMETRYCONNECTION, "goed3l", "FLIP", False )

createConnection( "goed4l", "BNDSPR", SHAPEVERTEX )
attachTo( GEOMETRYCONNECTION, "goed4l", "SOURCE", "Timber sheet", [[ -7700, -100, 0 ]] )
setElementClassType( GEOMETRYCONNECTION, "goed4l", "SPRING" )
assignMaterial( "Paal 100", GEOMETRYCONNECTION, "goed4l" )
assignGeometry( "paalelement", GEOMETRYCONNECTION, "goed4l" )
setParameter( GEOMETRYCONNECTION, "goed4l", "FLIP", False )

createConnection( "goed5l", "BNDSPR", SHAPEVERTEX )
attachTo( GEOMETRYCONNECTION, "goed5l", "SOURCE", "Timber sheet", [[ -6600, -100, 0 ]] )
setElementClassType( GEOMETRYCONNECTION, "goed5l", "SPRING" )
assignMaterial( "Paal 100", GEOMETRYCONNECTION, "goed5l" )
assignGeometry( "paalelement", GEOMETRYCONNECTION, "goed5l" )
setParameter( GEOMETRYCONNECTION, "goed5l", "FLIP", False )

createConnection( "goed6l", "BNDSPR", SHAPEVERTEX )
attachTo( GEOMETRYCONNECTION, "goed6l", "SOURCE", "Timber sheet", [[ -5500, -100, 0 ]] )
setElementClassType( GEOMETRYCONNECTION, "goed6l", "SPRING" )
assignMaterial( "Paal 100", GEOMETRYCONNECTION, "goed6l" )
assignGeometry( "paalelement", GEOMETRYCONNECTION, "goed6l" )
setParameter( GEOMETRYCONNECTION, "goed6l", "FLIP", False )

createConnection( "goed7l", "BNDSPR", SHAPEVERTEX )
attachTo( GEOMETRYCONNECTION, "goed7l", "SOURCE", "Timber sheet", [[ -4400, -100, 0 ]] )
setElementClassType( GEOMETRYCONNECTION, "goed7l", "SPRING" )
assignMaterial( "Paal 100", GEOMETRYCONNECTION, "goed7l" )
assignGeometry( "paalelement", GEOMETRYCONNECTION, "goed7l" )
setParameter( GEOMETRYCONNECTION, "goed7l", "FLIP", False )

createConnection( "goed8l", "BNDSPR", SHAPEVERTEX )
attachTo( GEOMETRYCONNECTION, "goed8l", "SOURCE", "Timber sheet", [[ -3300, -100, 0 ]] )
setElementClassType( GEOMETRYCONNECTION, "goed8l", "SPRING" )
assignMaterial( "Paal 100", GEOMETRYCONNECTION, "goed8l" )
assignGeometry( "paalelement", GEOMETRYCONNECTION, "goed8l" )
setParameter( GEOMETRYCONNECTION, "goed8l", "FLIP", False )

createConnection( "goed1r", "BNDSPR", SHAPEVERTEX )
attachTo( GEOMETRYCONNECTION, "goed1r", "SOURCE", "Timber sheet", [[ 11000, -100, 0 ]] )
setElementClassType( GEOMETRYCONNECTION, "goed1r", "SPRING" )
assignMaterial( "Paal 100", GEOMETRYCONNECTION, "goed1r" )
assignGeometry( "paalelement", GEOMETRYCONNECTION, "goed1r" )
setParameter( GEOMETRYCONNECTION, "goed1r", "FLIP", False )

createConnection( "goed2r", "BNDSPR", SHAPEVERTEX )
attachTo( GEOMETRYCONNECTION, "goed2r", "SOURCE", "Timber sheet", [[ 9900, -100, 0 ]] )
```

```
setElementClassType( GEOMETRYCONNECTION, "goed2r", "SPRING" )
assignMaterial( "Paal 100", GEOMETRYCONNECTION, "goed2r" )
assignGeometry( "paalelement", GEOMETRYCONNECTION, "goed2r" )
setParameter( GEOMETRYCONNECTION, "goed2r", "FLIP", False )

createConnection( "goed3r", "BNDSPR", SHAPEVERTEX )
attachTo( GEOMETRYCONNECTION, "goed3r", "SOURCE", "Timber sheet", [[ 8800, -100, 0 ]] )
setElementClassType( GEOMETRYCONNECTION, "goed3r", "SPRING" )
assignMaterial( "Paal 100", GEOMETRYCONNECTION, "goed3r" )
assignGeometry( "paalelement", GEOMETRYCONNECTION, "goed3r" )
setParameter( GEOMETRYCONNECTION, "goed3r", "FLIP", False )

createConnection( "goed4r", "BNDSPR", SHAPEVERTEX )
attachTo( GEOMETRYCONNECTION, "goed4r", "SOURCE", "Timber sheet", [[ 7700, -100, 0 ]] )
setElementClassType( GEOMETRYCONNECTION, "goed4r", "SPRING" )
assignMaterial( "Paal 100", GEOMETRYCONNECTION, "goed4r" )
assignGeometry( "paalelement", GEOMETRYCONNECTION, "goed4r" )
setParameter( GEOMETRYCONNECTION, "goed4r", "FLIP", False )

createConnection( "goed5r", "BNDSPR", SHAPEVERTEX )
attachTo( GEOMETRYCONNECTION, "goed5r", "SOURCE", "Timber sheet", [[ 6600, -100, 0 ]] )
setElementClassType( GEOMETRYCONNECTION, "goed5r", "SPRING" )
assignMaterial( "Paal 100", GEOMETRYCONNECTION, "goed5r" )
assignGeometry( "paalelement", GEOMETRYCONNECTION, "goed5r" )
setParameter( GEOMETRYCONNECTION, "goed5r", "FLIP", False )

createConnection( "goed6r", "BNDSPR", SHAPEVERTEX )
attachTo( GEOMETRYCONNECTION, "goed6r", "SOURCE", "Timber sheet", [[ 5500, -100, 0 ]] )
setElementClassType( GEOMETRYCONNECTION, "goed6r", "SPRING" )
assignMaterial( "Paal 100", GEOMETRYCONNECTION, "goed6r" )
assignGeometry( "paalelement", GEOMETRYCONNECTION, "goed6r" )
setParameter( GEOMETRYCONNECTION, "goed6r", "FLIP", False )

createConnection( "goed7r", "BNDSPR", SHAPEVERTEX )
attachTo( GEOMETRYCONNECTION, "goed7r", "SOURCE", "Timber sheet", [[ 4400, -100, 0 ]] )
setElementClassType( GEOMETRYCONNECTION, "goed7r", "SPRING" )
assignMaterial( "Paal 100", GEOMETRYCONNECTION, "goed7r" )
assignGeometry( "paalelement", GEOMETRYCONNECTION, "goed7r" )
setParameter( GEOMETRYCONNECTION, "goed7r", "FLIP", False )

createConnection( "goed8r", "BNDSPR", SHAPEVERTEX )
attachTo( GEOMETRYCONNECTION, "goed8r", "SOURCE", "Timber sheet", [[ 3300, -100, 0 ]] )
setElementClassType( GEOMETRYCONNECTION, "goed8r", "SPRING" )
assignMaterial( "Paal 100", GEOMETRYCONNECTION, "goed8r" )
assignGeometry( "paalelement", GEOMETRYCONNECTION, "goed8r" )
setParameter( GEOMETRYCONNECTION, "goed8r", "FLIP", False )

createConnection( "slecht1r", "BNDSPR", SHAPEVERTEX )
attachTo( GEOMETRYCONNECTION, "slecht1r", "SOURCE", "Timber sheet", [[ 1100, -100, 0 ]] )
setElementClassType( GEOMETRYCONNECTION, "slecht1r", "SPRING" )
assignMaterial( "Paal 25", GEOMETRYCONNECTION, "slecht1r" )
assignGeometry( "paalelement", GEOMETRYCONNECTION, "slecht1r" )
setParameter( GEOMETRYCONNECTION, "slecht1r", "FLIP", False )

createConnection( "slecht2r", "BNDSPR", SHAPEVERTEX )
attachTo( GEOMETRYCONNECTION, "slecht2r", "SOURCE", "Timber sheet", [[ 2200, -100, 0 ]] )
```

```
setElementClassType( GEOMETRYCONNECTION, "slecht2r", "SPRING" )
assignMaterial( "Paal 25", GEOMETRYCONNECTION, "slecht2r" )
assignGeometry( "paalelement", GEOMETRYCONNECTION, "slecht2r" )
setParameter( GEOMETRYCONNECTION, "slecht2r", "FLIP", False )

createConnection( "slecht1l", "BNDSPR", SHAPEVERTEX )
attachTo( GEOMETRYCONNECTION, "slecht1l", "SOURCE", "Timber sheet", [[ -1100, -100, 0 ]] )
setElementClassType( GEOMETRYCONNECTION, "slecht1l", "SPRING" )
assignMaterial( "Paal 25", GEOMETRYCONNECTION, "slecht1l" )
assignGeometry( "paalelement", GEOMETRYCONNECTION, "slecht1l" )
setParameter( GEOMETRYCONNECTION, "slecht1l", "FLIP", False )

createConnection( "slecht2l", "BNDSPR", SHAPEVERTEX )
attachTo( GEOMETRYCONNECTION, "slecht2l", "SOURCE", "Timber sheet", [[ -2200, -100, 0 ]] )
setElementClassType( GEOMETRYCONNECTION, "slecht2l", "SPRING" )
assignMaterial( "Paal 25", GEOMETRYCONNECTION, "slecht2l" )
assignGeometry( "paalelement", GEOMETRYCONNECTION, "slecht2l" )
setParameter( GEOMETRYCONNECTION, "slecht2l", "FLIP", False )

createConnection( "slecht1m", "BNDSPR", SHAPEVERTEX )
attachTo( GEOMETRYCONNECTION, "slecht1m", "SOURCE", "Timber sheet", [[ 0, -100, 0 ]] )
setElementClassType( GEOMETRYCONNECTION, "slecht1m", "SPRING" )
assignMaterial( "Paal 25", GEOMETRYCONNECTION, "slecht1m" )
assignGeometry( "paalelement", GEOMETRYCONNECTION, "slecht1m" )
setParameter( GEOMETRYCONNECTION, "slecht1m", "FLIP", False )

createConnection( "goedzijl", "BNDSPR", SHAPEVERTEX )
attachTo( GEOMETRYCONNECTION, "goedzijl", "SOURCE", "Timber sheet", [[ -11000, -100, 0 ]] )
setElementClassType( GEOMETRYCONNECTION, "goedzijl", "SPRING" )
assignMaterial( "Paal half", GEOMETRYCONNECTION, "goedzijl" )
assignGeometry( "paalelement", GEOMETRYCONNECTION, "goedzijl" )
setParameter( GEOMETRYCONNECTION, "goedzijl", "FLIP", False )

createConnection( "goedzijr", "BNDSPR", SHAPEVERTEX )
attachTo( GEOMETRYCONNECTION, "goedzijr", "SOURCE", "Timber sheet", [[ 11000, -100, 0 ]] )
setElementClassType( GEOMETRYCONNECTION, "goedzijr", "SPRING" )
assignMaterial( "Paal half", GEOMETRYCONNECTION, "goedzijr" )
assignGeometry( "paalelement", GEOMETRYCONNECTION, "goedzijr" )
setParameter( GEOMETRYCONNECTION, "goedzijr", "FLIP", False )
```

TYINGS LONGITUDINAL

```
addSet( GEOMETRYTYINGSET, "Geometry tying set 1" )
addSet( GEOMETRYTYINGSET, "Geometry tying set 2" )

createPointTying( "p1", "Geometry tying set 2" )
setParameter( GEOMETRYTYING, "p1", "AXES", [ 1, 2 ] )
setParameter( GEOMETRYTYING, "p1", "TRANSL", [ 0, 1, 0 ] )
setParameter( GEOMETRYTYING, "p1", "ROTATI", [ 0, 0, 0 ] )
attachTo( GEOMETRYTYING, "p1", "SLAVE", "Timber sheet", [[ -9750, -100, 0 ],[ -9850, -100, 0 ]] )
attachTo( GEOMETRYTYING, "p1", "MASTER", "Timber sheet", [[ -9900, -100, 0 ]] )

createPointTying( "p2", "Geometry tying set 2" )
setParameter( GEOMETRYTYING, "p2", "AXES", [ 1, 2 ] )
setParameter( GEOMETRYTYING, "p2", "TRANSL", [ 0, 1, 0 ] )
setParameter( GEOMETRYTYING, "p2", "ROTATI", [ 0, 0, 0 ] )
```

```
attachTo( GEOMETRYTYING, "p2", "SLAVE", "Timber sheet", [[ -8950, -100, 0 ],[ -8750, -100, 0 ]] )
attachTo( GEOMETRYTYING, "p2", "MASTER", "Timber sheet", [[ -8800, -100, 0 ]] )

createPointTying( "p3", "Geometry tying set 2" )
setParameter( GEOMETRYTYING, "p3", "AXES", [ 1, 2 ] )
setParameter( GEOMETRYTYING, "p3", "TRANSL", [ 0, 1, 0 ] )
setParameter( GEOMETRYTYING, "p3", "ROTATI", [ 0, 0, 0 ] )
attachTo( GEOMETRYTYING, "p3", "SLAVE", "Timber sheet", [[ -7850, -100, 0 ],[ -7650, -100, 0 ]] )
attachTo( GEOMETRYTYING, "p3", "MASTER", "Timber sheet", [[ -7700, -100, 0 ]] )

createPointTying( "p4", "Geometry tying set 2" )
setParameter( GEOMETRYTYING, "p4", "AXES", [ 1, 2 ] )
setParameter( GEOMETRYTYING, "p4", "TRANSL", [ 0, 1, 0 ] )
setParameter( GEOMETRYTYING, "p4", "ROTATI", [ 0, 0, 0 ] )
attachTo( GEOMETRYTYING, "p4", "SLAVE", "Timber sheet", [[ -6750, -100, 0 ],[ -6550, -100, 0 ]] )
attachTo( GEOMETRYTYING, "p4", "MASTER", "Timber sheet", [[ -6600, -100, 0 ]] )

createPointTying( "p5", "Geometry tying set 2" )
setParameter( GEOMETRYTYING, "p5", "AXES", [ 1, 2 ] )
setParameter( GEOMETRYTYING, "p5", "TRANSL", [ 0, 1, 0 ] )
setParameter( GEOMETRYTYING, "p5", "ROTATI", [ 0, 0, 0 ] )
attachTo( GEOMETRYTYING, "p5", "SLAVE", "Timber sheet", [[ -5650, -100, 0 ],[ -5450, -100, 0 ]] )
attachTo( GEOMETRYTYING, "p5", "MASTER", "Timber sheet", [[ -5500, -100, 0 ]] )

createPointTying( "p6", "Geometry tying set 2" )
setParameter( GEOMETRYTYING, "p6", "AXES", [ 1, 2 ] )
setParameter( GEOMETRYTYING, "p6", "TRANSL", [ 0, 1, 0 ] )
setParameter( GEOMETRYTYING, "p6", "ROTATI", [ 0, 0, 0 ] )
attachTo( GEOMETRYTYING, "p6", "SLAVE", "Timber sheet", [[ -4550, -100, 0 ],[ -4350, -100, 0 ]] )
attachTo( GEOMETRYTYING, "p6", "MASTER", "Timber sheet", [[ -4400, -100, 0 ]] )

createPointTying( "p7", "Geometry tying set 2" )
setParameter( GEOMETRYTYING, "p7", "AXES", [ 1, 2 ] )
setParameter( GEOMETRYTYING, "p7", "TRANSL", [ 0, 1, 0 ] )
setParameter( GEOMETRYTYING, "p7", "ROTATI", [ 0, 0, 0 ] )
attachTo( GEOMETRYTYING, "p7", "SLAVE", "Timber sheet", [[ -3450, -100, 0 ],[ -3250, -100, 0 ]] )
attachTo( GEOMETRYTYING, "p7", "MASTER", "Timber sheet", [[ -3300, -100, 0 ]] )

createPointTying( "p8", "Geometry tying set 2" )
setParameter( GEOMETRYTYING, "p8", "AXES", [ 1, 2 ] )
setParameter( GEOMETRYTYING, "p8", "TRANSL", [ 0, 1, 0 ] )
setParameter( GEOMETRYTYING, "p8", "ROTATI", [ 0, 0, 0 ] )
attachTo( GEOMETRYTYING, "p8", "SLAVE", "Timber sheet", [[ -2350, -100, 0 ],[ -2150, -100, 0 ]] )
attachTo( GEOMETRYTYING, "p8", "MASTER", "Timber sheet", [[ -2200, -100, 0 ]] )

createPointTying( "p9", "Geometry tying set 2" )
setParameter( GEOMETRYTYING, "p9", "AXES", [ 1, 2 ] )
setParameter( GEOMETRYTYING, "p9", "TRANSL", [ 0, 1, 0 ] )
setParameter( GEOMETRYTYING, "p9", "ROTATI", [ 0, 0, 0 ] )
attachTo( GEOMETRYTYING, "p9", "SLAVE", "Timber sheet", [[ -1250, -100, 0 ],[ -1050, -100, 0 ]] )
attachTo( GEOMETRYTYING, "p9", "MASTER", "Timber sheet", [[ -1100, -100, 0 ]] )

createPointTying( "p10", "Geometry tying set 2" )
setParameter( GEOMETRYTYING, "p10", "AXES", [ 1, 2 ] )
setParameter( GEOMETRYTYING, "p10", "TRANSL", [ 0, 1, 0 ] )
setParameter( GEOMETRYTYING, "p10", "ROTATI", [ 0, 0, 0 ] )
```

```
attachTo( GEOMETRYTYING, "p10", "SLAVE", "Timber sheet", [[ -150, -100, 0 ],[ 150, -100, 0 ]] )
attachTo( GEOMETRYTYING, "p10", "MASTER", "Timber sheet", [[ 0, -100, 0 ]] )

createPointTying( "p11", "Geometry tying set 2" )
setParameter( GEOMETRYTYING, "p11", "AXES", [ 1, 2 ] )
setParameter( GEOMETRYTYING, "p11", "TRANSL", [ 0, 1, 0 ] )
setParameter( GEOMETRYTYING, "p11", "ROTATI", [ 0, 0, 0 ] )
attachTo( GEOMETRYTYING, "p11", "SLAVE", "Timber sheet", [[ 1050, -100, 0 ],[ 1250, -100, 0 ]] )
attachTo( GEOMETRYTYING, "p11", "MASTER", "Timber sheet", [[ 1100, -100, 0 ]] )

createPointTying( "p12", "Geometry tying set 2" )
setParameter( GEOMETRYTYING, "p12", "AXES", [ 1, 2 ] )
setParameter( GEOMETRYTYING, "p12", "TRANSL", [ 0, 1, 0 ] )
setParameter( GEOMETRYTYING, "p12", "ROTATI", [ 0, 0, 0 ] )
attachTo( GEOMETRYTYING, "p12", "SLAVE", "Timber sheet", [[ 2150, -100, 0 ],[ 2350, -100, 0 ]] )
attachTo( GEOMETRYTYING, "p12", "MASTER", "Timber sheet", [[ 2200, -100, 0 ]] )

createPointTying( "p13", "Geometry tying set 2" )
setParameter( GEOMETRYTYING, "p13", "AXES", [ 1, 2 ] )
setParameter( GEOMETRYTYING, "p13", "TRANSL", [ 0, 1, 0 ] )
setParameter( GEOMETRYTYING, "p13", "ROTATI", [ 0, 0, 0 ] )
attachTo( GEOMETRYTYING, "p13", "SLAVE", "Timber sheet", [[ 3250, -100, 0 ],[ 3450, -100, 0 ]] )
attachTo( GEOMETRYTYING, "p13", "MASTER", "Timber sheet", [[ 3300, -100, 0 ]] )

createPointTying( "p14", "Geometry tying set 2" )
setParameter( GEOMETRYTYING, "p14", "AXES", [ 1, 2 ] )
setParameter( GEOMETRYTYING, "p14", "TRANSL", [ 0, 1, 0 ] )
setParameter( GEOMETRYTYING, "p14", "ROTATI", [ 0, 0, 0 ] )
attachTo( GEOMETRYTYING, "p14", "SLAVE", "Timber sheet", [[ 4350, -100, 0 ],[ 4550, -100, 0 ]] )
attachTo( GEOMETRYTYING, "p14", "MASTER", "Timber sheet", [[ 4400, -100, 0 ]] )

createPointTying( "p15", "Geometry tying set 2" )
setParameter( GEOMETRYTYING, "p15", "AXES", [ 1, 2 ] )
setParameter( GEOMETRYTYING, "p15", "TRANSL", [ 0, 1, 0 ] )
setParameter( GEOMETRYTYING, "p15", "ROTATI", [ 0, 0, 0 ] )
attachTo( GEOMETRYTYING, "p15", "SLAVE", "Timber sheet", [[ 5450, -100, 0 ],[ 5650, -100, 0 ]] )
attachTo( GEOMETRYTYING, "p15", "MASTER", "Timber sheet", [[ 5500, -100, 0 ]] )

createPointTying( "p16", "Geometry tying set 2" )
setParameter( GEOMETRYTYING, "p16", "AXES", [ 1, 2 ] )
setParameter( GEOMETRYTYING, "p16", "TRANSL", [ 0, 1, 0 ] )
setParameter( GEOMETRYTYING, "p16", "ROTATI", [ 0, 0, 0 ] )
attachTo( GEOMETRYTYING, "p16", "SLAVE", "Timber sheet", [[ 6550, -100, 0 ],[ 6750, -100, 0 ]] )
attachTo( GEOMETRYTYING, "p16", "MASTER", "Timber sheet", [[ 6600, -100, 0 ]] )

createPointTying( "p17", "Geometry tying set 2" )
setParameter( GEOMETRYTYING, "p17", "AXES", [ 1, 2 ] )
setParameter( GEOMETRYTYING, "p17", "TRANSL", [ 0, 1, 0 ] )
setParameter( GEOMETRYTYING, "p17", "ROTATI", [ 0, 0, 0 ] )
attachTo( GEOMETRYTYING, "p17", "SLAVE", "Timber sheet", [[ 7650, -100, 0 ],[ 7850, -100, 0 ]] )
attachTo( GEOMETRYTYING, "p17", "MASTER", "Timber sheet", [[ 7700, -100, 0 ]] )

createPointTying( "p18", "Geometry tying set 2" )
setParameter( GEOMETRYTYING, "p18", "AXES", [ 1, 2 ] )
setParameter( GEOMETRYTYING, "p18", "TRANSL", [ 0, 1, 0 ] )
setParameter( GEOMETRYTYING, "p18", "ROTATI", [ 0, 0, 0 ] )
```

```
attachTo( GEOMETRYTYING, "p18", "SLAVE", "Timber sheet", [[ 8750, -100, 0 ],[ 8950, -100, 0 ]] )
attachTo( GEOMETRYTYING, "p18", "MASTER", "Timber sheet", [[ 8800, -100, 0 ]] )

createPointTying( "p19", "Geometry tying set 2" )
setParameter( GEOMETRYTYING, "p19", "AXES", [ 1, 2 ] )
setParameter( GEOMETRYTYING, "p19", "TRANSL", [ 0, 1, 0 ] )
setParameter( GEOMETRYTYING, "p19", "ROTATI", [ 0, 0, 0 ] )
attachTo( GEOMETRYTYING, "p19", "SLAVE", "Timber sheet", [[ 9850, -100, 0 ],[ 9750, -100, 0 ]] )
attachTo( GEOMETRYTYING, "p19", "MASTER", "Timber sheet", [[ 9900, -100, 0 ]] )

addSet( GEOMETRYTYINGSET, "Geometry tying set 1" )
createLineTying( "p1", "Geometry tying set 1" )
setParameter( GEOMETRYTYING, "p1", "AXES", [ 1, 2 ] )
setParameter( GEOMETRYTYING, "p1", "TRANSL", [ 0, 1, 0 ] )
setParameter( GEOMETRYTYING, "p1", "ROTATI", [ 0, 0, 0 ] )
attachTo( GEOMETRYTYING, "p1", "SLAVE", "Timber sheet", [[ -10950, -100, 0 ]] )
attachTo( GEOMETRYTYING, "p1", "MASTER", "Timber sheet", [[ -11000, -100, 0 ]] )

addSet( GEOMETRYTYINGSET, "Geometry tying set 1" )
createLineTying( "p20", "Geometry tying set 1" )
setParameter( GEOMETRYTYING, "p20", "AXES", [ 1, 2 ] )
setParameter( GEOMETRYTYING, "p20", "TRANSL", [ 0, 1, 0 ] )
setParameter( GEOMETRYTYING, "p20", "ROTATI", [ 0, 0, 0 ] )
attachTo( GEOMETRYTYING, "p20", "SLAVE", "Timber sheet", [[ 10950, -100, 0 ]] )
attachTo( GEOMETRYTYING, "p20", "MASTER", "Timber sheet", [[ 11000, -100, 0 ]] )
```

GEOMETRY CROSS

```
createSheet( "Masonry sheet", [[ 0, 0, 0 ],[ 0, 2000, 0 ],[ 800, 2000, 0 ],[ 800, 0, 0 ]] )
createSheet( "Timber sheet", [[ 0, 0, 0 ],[ 0, -100, 0 ],[ 100, -100, 0 ],[ 200, -100, 0 ],[ 300, -100, 0 ],[ 400, -100, 0 ],[
500, -100, 0 ],[ 600, -100, 0 ],[ 700, -100, 0 ],[ 800, -100, 0 ],[ 900, -100, 0 ],[ 1000, -100, 0 ],[ 1100, -100, 0 ],[ 1200,
-100, 0 ],[ 1300, -100, 0 ],[ 1400, -100, 0 ],[ 1500, -100, 0 ],[ 1600, -100, 0 ],[ 1700, -100, 0 ],[ 1800, -100, 0 ],[ 1900,
-100, 0 ],[ 2000, -100, 0 ],[ 2100, -100, 0 ],[ 2200, -100, 0 ],[ 2300, -100, 0 ],[ 2400, -100, 0 ],[ 2500, -100, 0 ],[ 2600,
-100, 0 ],[ 2700, -100, 0 ],[ 2800, -100, 0 ],[ 2800, 0, 0 ]] )
```

TYINGS CROSS

```
addSet( GEOMETRYTYINGSET, "Geometry tying set 1" )

createPointTying( "p1", "Geometry tying set 1" )
setParameter( GEOMETRYTYING, "p1", "AXES", [ 1, 2 ] )
setParameter( GEOMETRYTYING, "p1", "TRANSL", [ 0, 1, 0 ] )
setParameter( GEOMETRYTYING, "p1", "ROTATI", [ 0, 0, 0 ] )
attachTo( GEOMETRYTYING, "p1", "SLAVE", "Timber sheet", [[ 50, -100, 0 ],[ 1750, -100, 0 ]] )
attachTo( GEOMETRYTYING, "p1", "MASTER", "Timber sheet", [[ 100, -100, 0 ]] )

createPointTying( "p2", "Geometry tying set 1" )
setParameter( GEOMETRYTYING, "p2", "AXES", [ 1, 2 ] )
setParameter( GEOMETRYTYING, "p2", "TRANSL", [ 0, 1, 0 ] )
setParameter( GEOMETRYTYING, "p2", "ROTATI", [ 0, 0, 0 ] )
attachTo( GEOMETRYTYING, "p2", "SLAVE", "Timber sheet", [[ 1150, -100, 0 ],[ 1250, -100, 0 ]] )
attachTo( GEOMETRYTYING, "p2", "MASTER", "Timber sheet", [[ 1200, -100, 0 ]] )

createPointTying( "p3", "Geometry tying set 1" )
setParameter( GEOMETRYTYING, "p3", "AXES", [ 1, 2 ] )
setParameter( GEOMETRYTYING, "p3", "TRANSL", [ 0, 1, 0 ] )
```

setParameter(GEOMETRYTYING, "p3", "ROTATI", [0, 0, 0])
attachTo(GEOMETRYTYING, "p3", "SLAVE", "Timber sheet", [[2650, -100, 0],[2750, -100, 0]])
attachTo(GEOMETRYTYING, "p3", "MASTER", "Timber sheet", [[2700, -100, 0]])

FUNCTIONS CROSS

setFunctionValues("Function 1", [ ], [0, 2000], [ ], [1, 0]) setFunctionValues("Function 2", [ ], [0, 1000, 2000], [ ], [1, 0, 0])
LOADS CROSS

addSet(GEOMETRYLOADSET, "Geometry load case 2")
addSet(GEOMETRYLOADSET, "Geometry load case 1")

createModelLoad("own", "Geometry load case 1")

createLineLoad("top", "Geometry load case 2")
setParameter(GEOMETRYLOAD, "top", "FORCE/VALUE", -500)
setParameter(GEOMETRYLOAD, "top", "FORCE/DIRECT", 2)
attach(GEOMETRYLOAD, "top", "Masonry sheet", [[400, 2000, 0]])

createLineLoad("sides", "Geometry load case 1")
setParameter(GEOMETRYLOAD, "sides", "FORCE/VALUE", -14.2)
setParameter(GEOMETRYLOAD, "sides", "FORCE/DIRECT", 1)
attach(GEOMETRYLOAD, "sides", "Masonry sheet", [[800, 1000, 0]])
setValueFunction(GEOMETRYLOAD, "sides", "Function 1")

createLineLoad("waters", "Geometry load case 1")
setParameter(GEOMETRYLOAD, "waters", "FORCE/VALUE", 6)
setParameter(GEOMETRYLOAD, "waters", "FORCE/DIRECT", 1)
attach(GEOMETRYLOAD, "waters", "Masonry sheet", [[0, 1000, 0]])
setValueFunction(GEOMETRYLOAD, "sides", "Function 2")

createLineLoad("sideextra", "Geometry load case 2")
setParameter(GEOMETRYLOAD, "sideextra", "FORCE/VALUE", -187)
setParameter(GEOMETRYLOAD, "sideextra", "FORCE/DIRECT", 1)
attach(GEOMETRYLOAD, "sideextra", "Masonry sheet", [[800, 1000, 0]])
setValueFunction(GEOMETRYLOAD, "sideextra", "Function 1")

createLineLoad("topextra", "Geometry load case 2") setParameter(GEOMETRYLOAD, "topextra", "FORCE/VALUE", -500) setParameter(GEOMETRYLOAD, "topextra", "FORCE/DIRECT", 2) attach(GEOMETRYLOAD, "topextra", "Timber sheet", [[1800, 0, 0]]) attach(GEOMETRYLOAD, "topextra", "Masonry sheet", [[400, 2000, 0]])
addGeometryLoadCombination("")
setGeometryLoadCombinationFactor("Geometry load combination 1", "Geometry load case 1", 1)
addGeometryLoadCombination("")
setGeometryLoadCombinationFactor("Geometry load combination 2", "Geometry load case 2", 1)

CONNECTIONS CROSS
createConnection("timber-masonry", "INTER", SHAPEEDGE)
setParameter(GEOMETRYCONNECTION, "timber-masonry", "MODE", "AUTO")
attachTo(GEOMETRYCONNECTION, "timber-masonry", "SOURCE", "Masonry sheet", [[0, 0, 0]])
setElementClassType(GEOMETRYCONNECTION, "timber-masonry", "STLIIF")
assignMaterial("Interface low", GEOMETRYCONNECTION, "timber-masonry")
assignGeometry("Line", GEOMETRYCONNECTION, "timber-masonry")
setParameter(GEOMETRYCONNECTION, "timber-masonry", "FLIP", False)
resetElementData(GEOMETRYCONNECTION, "timber-masonry")

```
createConnection( "slecht", "BNDSPR", SHAPEVERTEX )
attachTo( GEOMETRYCONNECTION, "slecht", "SOURCE", "Timber sheet", [[ 100, -100, 0 ]] )
setElementClassType( GEOMETRYCONNECTION, "slecht", "SPRING" )
assignMaterial( "Paal 25", GEOMETRYCONNECTION, "slecht" )
assignGeometry( "paalelement", GEOMETRYCONNECTION, "slecht" )
setParameter( GEOMETRYCONNECTION, "slecht", "FLIP", False )

createConnection( "goed", "BNDSPR", SHAPEVERTEX )
attachTo( GEOMETRYCONNECTION, "goed", "SOURCE", "Timber sheet", [[ 1200, -100, 0 ]] )
setElementClassType( GEOMETRYCONNECTION, "goed", "SPRING" )
assignMaterial( "Paal 100", GEOMETRYCONNECTION, "goed" )
assignGeometry( "paalelement", GEOMETRYCONNECTION, "goed" )
setParameter( GEOMETRYCONNECTION, "goed", "FLIP", False )

createConnection( "goed2", "BNDSPR", SHAPEVERTEX )
attachTo( GEOMETRYCONNECTION, "goed2", "SOURCE", "Timber sheet", [[ 2700, -100, 0 ]] )
setElementClassType( GEOMETRYCONNECTION, "goed2", "SPRING" )
assignMaterial( "Paal 100", GEOMETRYCONNECTION, "goed2" )
assignGeometry( "paalelement", GEOMETRYCONNECTION, "goed3l" )
setParameter( GEOMETRYCONNECTION, "goed2", "FLIP", False )
```

ANALYSIS BOTH

```
addAnalysis( "Analysis1" )
addAnalysisCommand( "Analysis1", "NONLIN", "Structural nonlinear" )
renameAnalysis( "Analysis1", "Analysis1" )
addAnalysisCommandDetail( "Analysis1", "Structural nonlinear", "EXECUT(1)/LOAD/LOADNR" )
setAnalysisCommandDetail( "Analysis1", "Structural nonlinear", "EXECUT(1)/LOAD/LOADNR", 1 )
setAnalysisCommandDetail( "Analysis1", "Structural nonlinear", "EXECUT(1)/ITERAT/MAXITE", 10 )
setAnalysisCommandDetail( "Analysis1", "Structural nonlinear", "EXECUT(1)/ITERAT/CONVER/DISPLA/NOCONV",
"CONTIN" )
setAnalysisCommandDetail( "Analysis1", "Structural nonlinear", "EXECUT(1)/ITERAT/CONVER/FORCE/NOCONV",
"CONTIN" )
setAnalysisCommandDetail( "Analysis1", "Structural nonlinear", "EXECUT(1)/ITERAT/MAXITE", 50 )
setAnalysisCommandDetail( "Analysis1", "Structural nonlinear", "EXECUT(1)/ITERAT/CONVER/SIMULT",
True )
setAnalysisCommandDetail( "Analysis1", "Structural nonlinear", "EXECUT/EXETYP", "LOAD" )
setAnalysisCommandDetail( "Analysis1", "Structural nonlinear", "EXECUT(2)/ITERAT/MAXITE", 50 )
setAnalysisCommandDetail( "Analysis1", "Structural nonlinear", "EXECUT(2)/ITERAT/CONVER/SIMULT",
True )
setAnalysisCommandDetail( "Analysis1", "Structural nonlinear", "EXECUT(2)/ITERAT/CONVER/FORCE", False
)
setAnalysisCommandDetail( "Analysis1", "Structural nonlinear", "EXECUT(2)/ITERAT/CONVER/DISPLA/NOCONV",
"TERMIN" )
setAnalysisCommandDetail( "Analysis1", "Structural nonlinear", "EXECUT(2)/ITERAT/CONVER/DISPLA/NOCONV",
"CONTIN" )
addAnalysisCommandDetail( "Analysis1", "Structural nonlinear", "EXECUT(2)/ITERAT/CONVER/ENERGY"
)
setAnalysisCommandDetail( "Analysis1", "Structural nonlinear", "EXECUT(2)/ITERAT/CONVER/ENERGY",
True )
setAnalysisCommandDetail( "Analysis1", "Structural nonlinear", "EXECUT(2)/ITERAT/CONVER/ENERGY/TOLCON",
0.01 )
setAnalysisCommandDetail( "Analysis1", "Structural nonlinear", "EXECUT(2)/ITERAT/CONVER/ENERGY/NOCONV",
"CONTIN" )
setAnalysisCommandDetail( "Analysis1", "Structural nonlinear", "EXECUT(1)/ITERAT/MAXITE", 50 )
```

```
setAnalysisCommandDetail( "Analysis1", "Structural nonlinear", "EXECUT(1)/ITERAT/CONVER/FORCE", False
)
addAnalysisCommandDetail( "Analysis1", "Structural nonlinear", "EXECUT(1)/ITERAT/CONVER/ENERGY"
)
setAnalysisCommandDetail( "Analysis1", "Structural nonlinear", "EXECUT(1)/ITERAT/CONVER/ENERGY",
True )
setAnalysisCommandDetail( "Analysis1", "Structural nonlinear", "EXECUT(1)/ITERAT/CONVER/ENERGY/TOLCON",
0.01 )
setAnalysisCommandDetail( "Analysis1", "Structural nonlinear", "EXECUT(1)/ITERAT/CONVER/ENERGY/NOCONV",
"CONTIN" )
```